Doctorate Program in Molecular Oncology and Endocrinology
Doctorate School in Molecular Medicine

XXVII cycle - 2011–2014
Coordinator: Prof. Massimo Santoro

"RET therapeutic targeting in medullary thyroid carcinoma: molecular mechanisms of resistance"

Preziosa Buonocore

University of Naples Federico II
Dipartimento di Medicina Molecolare e Biotecnologie Mediche

Administrative Location

Dipartimento di Medicina Molecolare e Biotecnologie Mediche
Università degli Studi di Napoli Federico II

Partner Institutions

Italian Institutions
Università degli Studi di Napoli "Federico II", Naples, Italy
Istituto di Endocrinologia ed Oncologia Sperimentale "G. Salvatore", CNR, Naples, Italy
Seconda Università di Napoli, Naples, Italy
Università degli Studi di Napoli "Parthenope", Naples, Italy

Foreign Institutions
Université Libre de Bruxelles, Bruxelles, Belgium
Universidade Federal de Sao Paulo, Brazil
University of Turku, Turku, Finland
University of Madras, Chennai, India
University Pavol Jozef Šafàrik, Kosice, Slovakia

Supporting Institutions
Dipartimento di Medicina Molecolare e Biotecnologie Mediche, Università degli Studi di Napoli "Federico II", Naples
Istituto di Endocrinologia ed Oncologia Sperimentale "G. Salvatore", CNR, Naples
Istituto Superiore di Oncologia
Regione Campania

Italian Faculty

Francesco Beguinot
Roberto Bianco
Bernadette Biondi
Francesca Carlomagno
Maria Domenica Castellone
Gabriella Castoria
Angela Celetti
Annamaria Cirafici
Annamaria Colao
Gerolama Condorelli
Valentina De Falco
Vittorio De Franciscis
Sabino De Placido
Gabriella De Vita
Monica Fedele
Pietro Formisano
Alfredo Fusco
Fabrizio Gentile
Domenico Grieco
Michele Grieco
Maddalena Illario
Paolo Laccetti
Antonio Leonardi
Paolo Emidio Macchia
Rosa Marina Melillo
Claudia Miele
Nunzia Montuori
Roberto Pacelli
Giuseppe Palumbo
Giovanna Maria Pierantoni
Rosario Pivonello
Giuseppe Portella
Maria Fiammetta Romano
Giuliana Salvatore
Massimo Santoro
Donatella Tramontano
Giancarlo Troncone
Giancarlo Vecchio
Mario Vitale

“RET therapeutic targeting in medullary thyroid carcinoma: molecular mechanisms of resistance”

TABLE OF CONTENTS

LIST OF PUBLICATIONS

This dissertation is based on the following publications:

I. Molecular mechanisms of resistance to RET inhibition (main body of the Dissertation)

II. De Falco V, Buonocore P, Muthu M, Torregrossa L, Basolo F, Billaud M, Gozgit JM, Carlomagno F, Santoro M. Ponatinib (AP24534) is a novel potent inhibitor of oncogenic RET mutants associated with thyroid cancer. J Clin Endocrinol Metab. 2013 May; 98(5):E811-9 (attached at the end of this Dissertation).

LIST OF ABBREVIATIONS

AKT	v-Akt murine Thymoma viral oncogene
ALK	Anaplastic Lymphoma Kinase
ATC	Anaplastic Thyroid carcinoma
ATP	Adenosine Triphosphate
BCR-ABL	Breakpoint Cluster Region-Abelson
BRAF	B-type RAF family kinase
CCDC6	Coiled Coin Domain Containing 6
CCH	C-cell hyperplasia
CDK5	Cyclin-Dependent Kinase 5
CHEK2	Checkpoint Kinase 2
CLA	Cutaneous Lichen Amyloidosis
CMML	Chronic Myelomonocytic Leukemia
CREB	cAMP Responsive Element Binding Protein
CTNNB1	β-catenin
DMEM	Dulbecco's modified Eagle's medium
DMSO	Dimethyl Sulfoxide
DOK	Docking Protein, 62kDa
EGFR	Epidermal growth factor receptor
EIF1AX	Eukaryotic Translation Initiation Factor 1A, X-Linked
ERK	Extracellular signal-Regulated Kinase
FBS	Fetal Bovine Serum
FDA	Food and Drug Administration
FGFR	Fibroblast Growth Factor Receptor
FGFR1OP	Fibroblast Growth Factor Receptor 1 Oncogenic Partner
FMTC	Familial Medullary Thyroid Carcinoma
FRS2	Fibroblast Growth Factor Receptor Substrate 2
FTA	Follicular Thyroid Adenoma
FTC	Follicular Thyroid carcinoma
FV-PTC	Follicular-variant PTC
GAB	GRB2-Associated Binding Protein
GDNF	Glial cell line-derived Neurotrophic Factor
GFL	Glial cell line-derived Neurotrophic Factor Family Ligands
GFRα	Glial cell line-derived Neurotrophic Factor Family Receptor α
GIST	Gastrointestinal Stromal Tumors
GRB	Growth Factor Receptor-Bound Protein
HMGA1	High-mobility group A1
IC50	Half maximal Inhibitory Concentration
IGF1R	Insulin-like Growth Factor 1 Receptor
INSR	Insulin Receptor
KI	Kinase Inhibitor
KIF5B	Kinesin Family Member 5B
LADC	Lung adenocarcinoma

MAPK	Mitogen-Activated Protein Kinases
MEN2	Multiple Endocrine Neoplasia type 2
MTC	Medullary Thyroid carcinoma
MYHI3	Myosin Heavy Chain 13 Skeletal Muscle
NCOA4	Nuclear Receptor Coactivator 4
NFKB	Nuclear Factor-Kappa B
NSCLC	Non Small Cell Lung Cancer
NTRK1	Neurotrophic Tyrosine Kinase Rceptor type 1
p70S6K	Ribosomal Protein S6 Kinase, 70kDa
p90RSK	Ribosomal Protein S6 Kinase, 90kDa
PAX8	Paired Box 8
PDAC	Pancreatic Ductal Adenocarcinoma
PDGFR	Platelet-derived Growth Factor Receptor
PDTC	Poorly differentiated Thyroid Carcinoma
PI3K	Phosphoinositide-3 (OH) kinase
PKI	Protein kinase inhibitors
PLCγ	Phospholipase-C gamma
PPARγ	Peroxisome-Proliferator Activated Receptor γ
PPM1D	Protein Phosphatase, Mg2+/Mn2+ Dependent, 1D
PTB	Phosphotyrosine Binding Domain
PTC	Papillary thyroid Carcinoma
RET	REarranged during Transfection
RET/PTC	RET/Papillary Thyroid Carcinoma
RTK	Receptor tyrosine kinase
S6	S6 ribosomal protein
SH2	Src-homology 2
SHC	Src homology 2 domain containing
TG	Thyroglobulin
TK	Tyrosine kinase
TKI	Tyrosine kinase inhibitor
TP53	Tumor protein p53
TRIMM33	Tripartite Motif Containing 33
TSH	Thyroid Stimulating Hormone
TSHR	Thyroid Stimulating Hormone Receptor
VEGFR	Vascular endothelial growth factor receptor
WDTC	Well differentiated thyroid carcinoma
WT	Wild type

ABSTRACT

Medullary Thyroid Carcinoma (MTC) is a rare C cell-derived thyroid tumor secreting calcitonin. MTC is sporadic in about 75% of cases and it is a component of the autosomal dominant "multiple endocrine neoplasia type 2" (MEN2) syndrome in about 25% of the cases. MTC represents a challenging clinical problem, as most MTC patients show distant metastases at time of diagnosis and chemotherapy and radiotherapy have limited efficacy. MTC is commonly associated to germline or somatic point mutations causing a gain-of-function of RET receptor tyrosine kinase. Given the oncogenic role of RET, it is feasible that specific targeting of this kinase could block tumor growth. Therefore, tyrosine kinase small molecule inhibitors (TKI) have been studied as potential novel agents for MTC treatment. The clinically most advanced RET TKIs are vandetanib (ZD6474) and cabozantinib (XL184), both recently registered for the treatment of locally advanced or metastatic MTC. However, cancer patients may be refractory to TKIs or develop secondary resistance after an initial response. Two major mechanisms have been envisaged to allow cancer cells to escape treatment with TKIs: 1) target up-regulation or mutations impairing drug binding; 2) activation of alternative pathways that bypass drug-mediated block. Thus, it is worth studying in preclinical models, molecular mechanisms of resistance to TKIs, since these informations can be thereafter clinically applied. In this dissertation, we have addressed molecular mechanisms of resistance to RET TKIs in cultured MTC cells. Our results show that MTC cells can develop resistance to chronic vandetanib treatment. Vandetanib-resistant cells show increased proliferation rate, anchorage-independent growth and *in vivo* tumorigenicity. Despite the absence of secondary RET genetic lesions, resistant cells escape RET inhibition and, differently from parental cells, they are able to grow even when RET is inhibited. Importantly, resistant cells feature hyper-activation of p90RSK kinase, a component of the MAPK (mitogen activated protein kinase) signaling cascade, a fact that mediates RET inhibition bypass. Accordingly, resistant cells are sensitive to p90RSK chemical blockade. In conclusion, gain of MAPK cascade signaling seems to be able to mediate escape from RET inibition *in vitro,* thus suggesting p90RSK as a promising molecular target to overcome resistance formation to RET TKIs.

1.0 BACKGROUND

1.1 Thyroid gland

The thyroid gland secretes thyroid hormones that control metabolism (Kondo et al. 2006). This gland is formed by two lobes connected by an isthmus (Santisteban 2012). Thyroid parenchima is composed of two types of cells: follicular cells, that are the most abundant and are responsible for iodine uptake and L-thyroxine (T4) and L-triiodothyronine (T3) hormones production, and parafollicular C cells that secrete the calcium-regulating hormone calcitonin (Kondo et al. 2006). Most of the thyroid follicular cells are derived from the endoderm. Instead, the C cells are of neural crest derivation and migrate from the ultimobranchial body to finally distribute in small clusters among the follicles in the intermediate part of the thyroid lobes (DeLellis et al. 2004; Santisteban 2012). Thyroid hormones production is controlled by the hypothalamic–pituitary axis, while calcitonin secretion is stimulated by elevated plasma calcium concentration (Kondo et al. 2006).

1.2 Thyroid carcinoma

Thyroid cancer is the most prevalent endocrine malignancy accounting for approximately 1% of cancers (DeLellis et al. 2004; Xing 2013; De Biase et al. 2014). Carcinomas derived from thyroid follicular cells are subdivided in well-differentiated thyroid carcinoma (WDTC), comprising follicular thyroid carcinoma (FTC) and papillary thyroid carcinoma (PTC), poorly differentiated thyroid carcinoma (PDTC), and anaplastic thyroid carcinoma (ATC). It is possible that in some cases, PDTC and ATC develop as a result of dedifferentiation of a pre-existing WDTC. However, the different types of thyroid cancer can also form starting from different types of thyroid stem or progenitor cells (Todaro et al. 2010). Thyroid cancers greatly differ in terms of biological, pathological and clinical aggressiveness. The 25-year cause-specific survival is 95% for patients with PTC and 66% for patients with FTC; the 10-year survival in patients with PDTC is approximately 40%, and ATC is virtually incurable (Wells et al. 2014).

Medullary thyroid carcinoma (MTC) accounts for about 5% of thyroid cancers. MTC occurs sporadically in about 3/4 of the cases, but in 25% of cases it is hereditary in the frame of multiple endocrine neoplasia (MEN) type 2A or 2B syndromes (Wells et al. 2013).

1.2.1 Follicular-cell derived thyroid carcinoma

PTC is the most common thyroid carcinoma, accounting for about 80% of cases (DeLellis et al. 2004). PTC is etiologically associated to radiation exposure as it is demonstrated by the strong PTC incidence increase in children after the Chernobyl accident of 1986 (Williams 2002; Kondo et al, 2006; Nikiforov et al. 2011; Xing 2013). The recently published systematic genetic analysis of PTCs by the Cancer Genome Atlas consortium has allowed to comprehensively describe PTC molecular features (Cancer Genome Atlas Research Network. 2014). **Table 1** summarizes the most common genetic lesions that have been so far associated to formation of PTC and other thyroid cancer types.

Table 1: Summary of most common genetic lesions associated to thyroid carcinoma

Genetic alteration	PTC	FTC	PDTC	ATC	Sporadic MTC	Familial MTC
RET/PTC rearrangement	~10%	—	uncommon	—	—	—
RET mutation	—	—	—	—	50%	95%
BRAF mutation	~60%	—	10-20%	10-35%	—	—
RAS mutation	~15%	30-45%	20-40%	20-30%	10-40%	—
PI3K/AKT pathway	~5%	5-15%	5-10%	15-25%	—	—
PPARγ rearrangement	—	30%	—	—	—	—
TP53	—	—	~25%	~70%	—	—

BRAF mutations (~60% of cases) are the most common genetic alterations found in PTC (Cancer Genome Atlas Research Network. 2014). BRAF (B-type RAF) codes for a component of the RAF family of serine-threonine kinases, involved in the RAS/ERK signaling cascade (Chong et al. 2003). Upon binding to RAS-GTP, RAF proteins dimerize and undergo phosphorylation in their regulatory region; this is followed by RAF-mediated phosphorylation of the MEK dual kinases (MEK1 and MEK2), which, in turn, dually (tyrosine and threonine) phosphorylate and activate p44 and p42 ERKs. In cancers such as melanoma and PTC, BRAF is oncogenically activated by

point mutations within its kinase domain; the most frequent (approximately 90%) BRAF mutation is represented by the substitution of a glutamic acid for a valine at position 600 (V600E) (Xing 2013). Mutations in HRAS, KRAS, or most commonly NRAS occur in ~15% of PTCs and are associated to follicular variant PTC (FV-PTC) (Garcia-Rostan et al. 2003; Nikiforov et al. 2011; Cancer Genome Atlas Research Network. 2014). The most common (~7%) PTC-associated chromosomal rearrangements are paracentric inversions, or less commonly balanced translocations, targeting the long arm of chromosome 10 and causing the formation of RET/PTC chimeric oncogenes. In these cases, the 3'-terminal portion of RET receptor tyrosine kinase (RTK), coding for its tyrosine kinase (TK) domain (see below for a RET description), is fused with the 5'-terminal sequence of unrelated genes, leading to constitutive activation of RET catalytic function (Cancer Genome Atlas Research Network. 2014). Several RET/PTCs rearrangements have been reported, the most common being RET/PTC1 (CCDC6-RET) and RET/PTC3 (NCOA4-RET) (Santoro et al. 2006, 2013). In PTCs, also other RTKs, such as NTRK1, can be targeted by chromosomal rearrangements leading to their oncogenic activation (Greco et al. 2010; Cancer Genome Atlas Research Network. 2014). NTRK1 rearrangements involve principally three fusion partners (TPR, TPM3 and TFG) (Greco et al. 2010). Other RTKs, such as ALK, NTRK3, MET, FGFR2 and LTK, have also been found to be rarely rearranged in PTC (Cancer Genome Atlas Research Network. 2014). Finally, in those PTC cases that lacked any known genetic lesions, mutations in EIF1AX (Eukaryotic Translation Initiation Factor 1A,X-linked) have been recently identified (Cancer Genome Atlas Research Network. 2014). Moreover, newly identified mutations in PPM1D, CHEK2 as other components of the DNA-damage response (DDR) pathway, can occur in PTC concomitantly with MAPK driver (RTKs, RAS, BRAF) mutations (Cancer Genome Atlas Research Network. 2014).

FTC is the second most common thyroid malignancy and accounts for less than 10 % of thyroid cancers (De Lellis et al. 2004). Prognosis of FTC is worse than PTC especially in patients with distant metastases. FTC can be hardly differentiated from FTA (Follicular Thyroid Adenoma) and possibly some FTC may have evolved from pre-existing FTA (Nikiforov et al. 2011). FTC develops through two different pathways, involving either RAS point mutations or PPARγ (Peroxisome Proliferator-Activated Receptor gamma, PPARγ) rearrangements. Approximately 50% of FTCs feature mutations in RAS. PPARγ is a member of the nuclear-hormone-receptor superfamily and functions through heterodimers with the retinoid X receptor (RXR). RAS-negative FTCs often (30%) harbour the t(2:3)(q12-13;p24-25) chromosomal translocation, which causes the PAX8-PPARγ fusion by joining the region encoding the DNA binding domain of the thyroid transcription factor PAX8 to the encoding domain A-F of PPARγ; this rearrangement can also be found in FV-PTC (Kroll et al. 2000; Castro et al. 2006). The PAX8-PPARγ chimeric

protein has a dominant negative activity on wild-type PPARγ and it has oncogenic properties in transgenic mice (Dobson et al. 2011) **(Table 1)**.

PDTC accounts for up to 10% of all thyroid cancers (Volante et al. 2010). PDTC is dominated by RAS (predominantly NRAS codon 61) mutations (Ricarte-Filho et al. 2009; Volante et al. 2010). BRAF V600E mutation has also been found in approximately 10-20% of PDTCs. Furthermore a significant fraction of PDTC cases shows point mutations of TP53 (Kondo et al. 2006). PDTC features in some cases mutations or gene copy number alterations in PI3K (phosphoinositide-3 (OH) kinase) (PIK3CA gene) and its downstream effector AKT (Xing 2013) **(Table 1)**.

ATC accounts for about 2% of all thyroid cancers. More than 25% of ATC patients have coincidentally detected WDTC (PTC or FTC) from which ATC possibly derives (DeLellis et al. 2004; Kondo et al. 2006; Smallridge and Copland 2010). ATC is associated with BRAF (10-35%) or RAS (20-30%) mutations. BRAF mutations are mainly found in samples containing a PTC component (Xing 2013). Additional mutations identified in ATC include those targeting the CTNNB1 gene encoding beta-catenin (Garcia-Rostan et al. 2001). TP53 loss-of-function mutations are common (67-88%) in ATC and likely critical for the establishment of such an aggressive cancer phenotype. Components of PI3K signaling cascade are also involved in ATC (15-25%) (Garcia-Rostan et al. 2005; Xing 2013) **(Table 1)**.

1.2.2 Parafollicular-cell derived thyroid carcinoma

MTC accounts for about 5% of all thyroid cancers (Schlumberger et al. 2008; Wells et al. 2013). MTC is sporadic in about 75% of cases and in the others it occurs as a component of the Multiple Endocrine Neoplasia type 2 (MEN2) syndrome. MEN2 is divided into two major variants: MEN2A (about 85% of cases) and MEN2B (15%), both inherited in an autosomal dominant fashion (de Groot et al. 2006; Wells et al. 2013; Mulligan 2014).

MEN2A is the most common MEN2 disease subtype and characterized by MTC associated with pheochromocytoma in about 50% of cases, parathyroid hyperplasia and, rarely, cutaneous lichen amyloidosis (CLA) and congenital megacolon (Hirschsprung's disease). MEN2B is the most severe phenotype featuring an earlier age of MTC onset associated with pheochromocytoma (about 50% of cases) and more rarely mucosal neuromas, intestinal ganglioneuromatosis, ocular (corneal nerve) and skeletal abnormalities (the so called marfanoid habitus) (Wells et al. 2013). A third MEN2 variant, initially recognized as FMTC and characterized by MTC as the only phenotype is currently regarded as a MEN2A subtype with reduced aggressiveness (Mulligan 2014).

MEN2-associated MTC is typically bilateral and multicentric and it is usually preceded by multifocal C-cell hyperplasia (CCH) (Wells et al. 2013).

Based on our current knowledge, MTC genetics is relatively simple. Genes commonly mutated in other types of cancer are not commonly mutated in MTC. Point mutations (single aminoacid substitutions or rarely small insertions/deletions -indels) in the RET proto-oncogene are present in about half of sporadic cases and virtually all familial cases. Thus, blood screening for RET mutations can be used to identify patients with familial form of MTC (Elisei et al. 2008; Romei et al. 2011) **(Table 1)** (see also below). RET mutations correlate with a more aggressive MTC phenotype in sporadic cases (Elisei et al. 2008; Romei et al. 2011). In some cases, RET gene amplification concurrent with RET mutation has been reported (Ciampi et al. 2012). Recently, a novel oncogenic RET fusion (MHY13/RET) has been found in one sporadic MTC sample negative for RET point mutations (Grubbs at al. 2015). Somatic mutations in HRAS, KRAS, and rarely NRAS, occur in 10–40% of sporadic MTCs and are almost always mutually exclusive with RET mutations (Ciampi et al. 2013; Moura et al. 2011). Thus, all together RET and RAS mutations account for about 80% driver mutations associated to MTC. A recent next generation sequencing screening did not reveal additional significantly mutated genes in MTCs (Agrawal et al. 2013). MTC can be however also associated to chromosome copy number alterations, including in particular deletions targeting the short arm of chromosome 1 (Mathew et al. 1987).

1.3 RET receptor tyrosine kinase

The RET (REarranged during Transfection) proto-oncogene was initially isolated secondary to activation occurred *in vitro* by a DNA rearrangement in NIH3T3 murine fibroblasts transfected with human lymphoma DNA (Takahashi et al. 1985). RET is normally expressed in the developing central, peripheral and enteric nervous systems (Pachnis et al. 1993). Gene targeting experiments in the mouse demonstrated that RET is essential for renal organogenesis and for spermatogenesis (Schuchardt et al. 1994; Meng et al. 2000). In adult tissues, high levels of RET are observed in brain, thymus, peripheral enteric, sympathetic and sensory neurons and testis. RET is normally expressed in C-cells, but not in follicular thyroid cells (De Groot et al. 2006).

RET protein is a single-pass transmembrane polypeptide featuring three major domains (**Fig. 1**):

1. An extracellular portion that contains four Ca^{2+}-dependent cadherin-like domains and a juxtamembrane cysteine-rich region (encoded by exons 10 and 11 of the RET gene).
2. A hydrophobic transmembrane peptide;
3. An intracellular region that comprises two kinase subdomains (TK1 and TK2) that are joined by a hinge region of 27 aminoacids.

RET is subject to alternative splicing of the 3' region generating three protein isoforms that contain 9 (RET9), 43 (RET43) and 51 (RET51) amino acids at their carboxyl-terminal tail downstream from glycine 1063 (**Fig. 1**). RET9 and RET51, consisting of 1072 and 1114 amino acids, respectively, are the main isoforms (de Groot et al 2006). These isoforms might have distinct signaling properties that could also result from their segregation in distinct cell membrane subdomains.

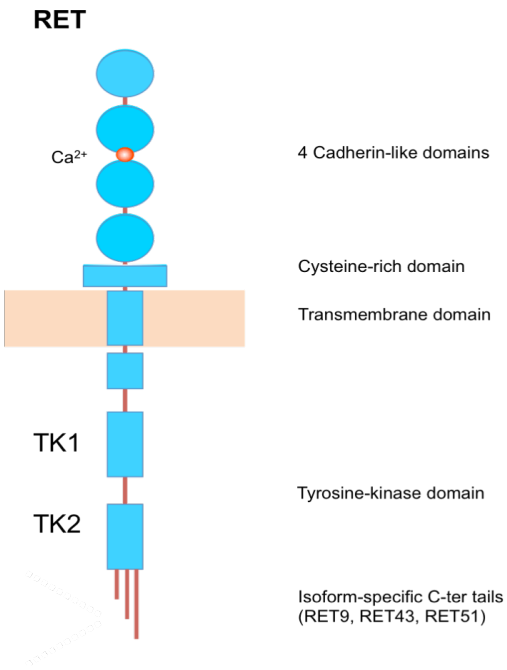

Figure 1. The RET receptor tyrosine kinase structure. The RET protein is composed of three regions: an extracellular domain that contains a cysteine rich region and a series of 4 cadherin-homology domains, a transmembrane domain and an intracellular tyrosine kinase domain splitted in 2 subdomains. Secondary to alternative splicing at the 3'-ter, RET gene codes for three different proteins differring at their C-tail of 1072 (RET9), 1106 (RET43) or 1114 (RET51) residues.

RET partecipates to a protein complex that binds membrane bound co-receptors and soluble ligands. Ligands are represented by the GDNF family of proteins (GFLs), including glial derived neurotrophic factor (GDNF), neurturin (NRTN), artemin (ARTN), and persephin (PSPN). Co-receptors are represented by the glycosylphosphatidylinositol (GPI)-anchored GDNF-family receptors (GFRα) (**Fig. 2**). Each one of the four GFLs binds to one GFRα to form a GFRα/GFL complex: GDNF binds to GFRα-1 as preferential receptor, NRTN to GFRα-2, ARTN to GFRα-3, and PSPN to GFRα-4, although there is some cross-specificity (Mulligan 2014). GFRαs also occur in a soluble form following enzymatic cleavage of their GPI anchor.

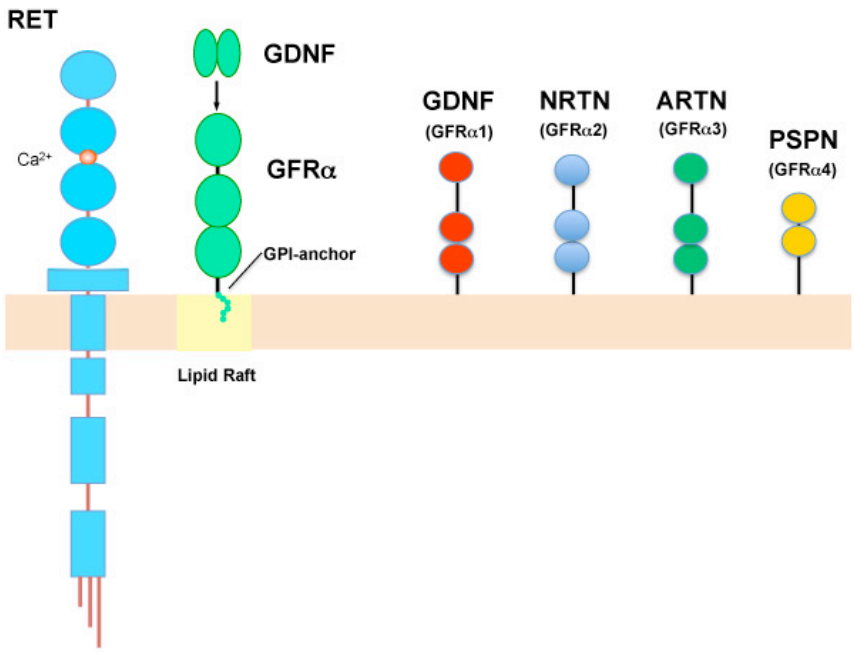

Figure 2. The RET protein complex. RET partecipates in a protein complex together with GDNF family receptors-α (GFRα) and GDNF family ligands (GFL).

RET activation can occur either in cis or in trans. In the cis model, RET and GFRαs are expressed on the same cell; the ligand binds to the membrane bound coreceptor and subsequently the complex brings together two RET molecules resulting in dimerization, TK activation and auto-phosphorylation of tyrosines required for intracellular signaling (De Groot et al. 2006). Membrane-bound GFRαs are distributed within lipid rafts, detergent-insoluble cholesterol-rich domains within the lipid bilayer of the cell membrane, which are enriched with signaling proteins. In its inactive form, RET is located outside the lipid rafts and upon cis-activation, RET is recruited to the lipid rafts by the complex (De Groot et al. 2006). In the trans model of RET activation, the ligand binds to a soluble (non membrane bound) form of the coreceptor (sGFRα). The complex, in turn, triggers RET activation via dimerization.

RET plays a central role in several intracellular signaling cascades that regulate multiple cellular processes including survival, differentiation, proliferation, and migration. Specific RET tyrosine residues are phosphorylated upon RET activation, which serve as docking sites for various adaptor proteins containing SRC-homology 2 (SH2) and phosphotyrosine binding (PTB) domain. These phosphorylation sites include tyrosine 687 (Y687) in the juxtamembrane domain, Y900, Y905 in the activation loop of the RET TK domain, Y981 in the TK domain and Y1015, Y1062, and Y1096 in the C-terminal tail (**Fig. 3**). Y1096 is present only in the long RET51 isoform (De Groot et al. 2006). Though Y905 corresponds to the autocatalytic residue in other kinases, whose phosphorylation is an early event and serves as a local switch to activate the kinase, its phosphorylation has been recently demonstrated to be delayed and to occur after than Y1062 in the C-tail is phosphorylated (Plaza-Menacho et al. 2014). Y905 is a binding site for Grb7/10 adaptors, Y981 is a docking site for c-Src, Y1015 for phospholipase Cγ and Y1096 for Grb2. Y1062 is embedded in a consensus sequence (NXXpY) for the binding to multiple PTB domain containing proteins and as such it is the binding site for diverse proteins including Shc, IRS1/2, FRS2, DOK1/4/5 and Enigma. Binding to Shc and FRS2 mediates recruitment of Grb2-SOS complexes leading to RAS pathway stimulation and of Grb2-GAB1/2 complexes leading to stimulation of the PI3K pathway (**Fig. 3)** (Santoro et al. 2013; De Groot et al. 2006; Wells et al. 2013; Mulligan 2014).

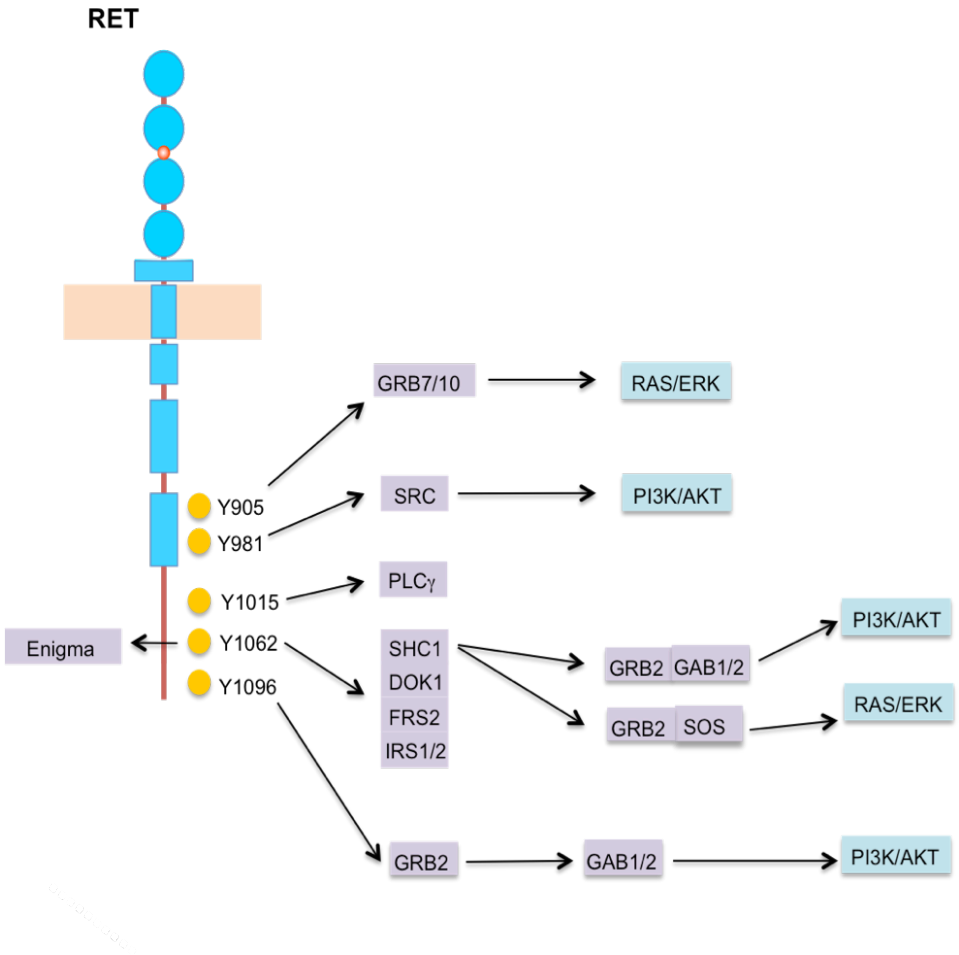

Figure 3. RET signaling pathways. Signaling network with RET docking sites and targets (see text for details).

1.3.1 RET activated signaling pathways

As mentioned above, RET Y1062 plays a central role in activating the two signaling pathways: RAS/ERK and PI3K/AKT (**Fig. 4**). Below, we summarize main features of these two signaling pathways (Mendoza et al. 2011).

ERKs belong to the Mitogen-activated protein kinases (MAPKs), Ser/Thr kinases that trigger a wide range of cellular responses (Widmann et al. 1999). The MAPK pathway is activated principally by cell surface receptors, such as receptor tyrosine kinases (RTKs) but also heterotrimeric G protein-coupled receptors (GPCRs) (Raman et al. 2007). Upon stimulation, ERKs (ERK1/2) phosphorylate a large number of cytosolic and nuclear substrates. Some of the ERK substrates are members of the AGC family proteins, one of the most evolutionary conserved group of kinases, containing 60 of the 518 human protein kinases (Pearce et al. 2010). AGC proteins consensus sequences for substrate phosphorylation display a marked preference for basic residues (Arginine and Lysine) N-terminal to the phosphorylatable Serine or Threonine. Because they have similar substrate preferences, several AGC kinases can phosphorylate the same proteins. ERK1/2 activate AGC kinases such as the 90-kDa ribosomal S6 kinases (p90RSKs). p90RSKs are a family of Ser/Thr kinases initially discovered for their ability of phsophorylating the S6 ribosomal protein (Erikson et al. 1985) (**Fig. 4**). p90RSK family includes four members (p90RSK1–4) and two homologues named RSK-like protein kinase (RLPK), also known as mitogen- and stress-activated kinase-1 (MSK1), and RSKB (also known as MSK2) (Anjum and Blenis. 2008).

The PI3K/AKT signaling pathway is involved in controlling cell growth, proliferation, motility and survival. Class I PI3K is activated by both RTKs and GPCRs. Its p110 catalytic subunit (PIK3CA) contains a binding site for the p85 regulatory subunit that mediates binding to membrane receptors. Catalytic PI3K subunit can also be activated directly by binding to RAS-GTP. Once activated, PI3K mediates phosphorylation of membrane lipid phosphatidylinositol-4,5-bisphosphate to produce phosphatidylinositol-3,4,5-trisphosphate (PIP3). PIP3 binds the PH domain of the AKT (PKB) protein kinase to localize it to the cell membrane, where finally AKT becomes phosphorylated and activated by the phosphoinositide-dependent kinases (PDK). PDK1 phosphorylates AKT at Thr308 while phosphorylation of a residue in the hydrophobic motif (Ser473) is required for maximal activity and mediated by mammalian target of rapamycin complex 2 (mTORC2). This system has remarkable similarities with the previously described ERK one; AKT is an AGC family kinase and its downstream substrates include mammalian target of rapamycin (mTOR), a member of the mTORC1 complex (mammalian target of rapamycin complex 1), that in turn phosphorylates another AGC family S6 kinase, named p70S6K (p70 ribosomal S6 kinase) (Pearce et al. 2010).

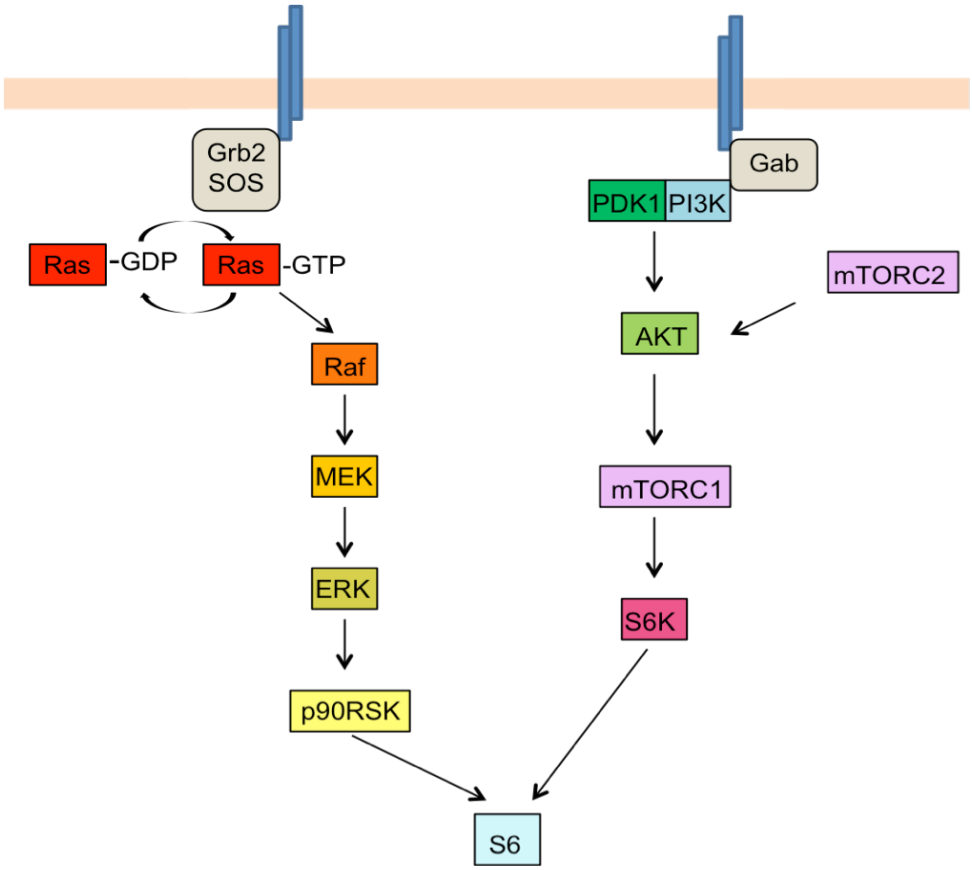

Figure 4. Similarities and cross-talk between RAS/ERK and PI3K/AKT pathways.
(Modified from Mendoza et al. 2011)

1.3.2 RET in medullary thyroid carcinoma

MEN2A and MEN2B are caused by germline mutations in RET, leading to its activation in the absence of ligands. Mutations are primarily aminoacid substitutions affecting a small number of RET codons in either the extracellular domain or kinase domain; rarely they consisted in small indels (Wells et al. 2013).

MEN2A mutations are substitutions of one of 6 cysteine residues in the RET extracellular domain (exons 10 or 11) (609, 611, 618, 620, 630, 634). C634 is the most frequently affected (85%), mainly by a C634R substitution. Mutations of residues 768, 790, or 804 (exons 13 and 14) of the RET TK domain have also been found in patients affected by isolated familial MTC (Wells et al. 2013; Mulligan 2014). Another recurrent mutation associated with MEN2A phenotype is the G533C substitution in the extracellular domain (**Fig. 5**).

Most MEN2B patients show the substitution of a methionine with a threonine at residue 918 (M918T) in the RET kinase domain (exon 16) whereas only a small fraction of them harbor the A883F substitution (exon 15). The M918T mutation occurs somatically in the vast majority of RET mutant sporadic MTCs, where it associates with more aggressive disease and poor prognosis (Wells et al. 2013; Mulligan 2014). MEN2B also associates to double mutations: V804M/E805K (Cranston et al. 2006), V804M/Y806C (Miyauchi et al. 1999), and V804M/S904C (Menko et al. 2002). It appears that the combination of two mild intracellular mutations can cooperate to produce a more severe mutant (**Fig. 5**).

Mechanisms leading to RET oncogenic conversion and constitutive kinase activation in familial or sporadic MTC depend on location of the amino acid change. Extracellular mutated cysteines normally form intramolecular disulfide bonds in the wild-type receptor; thus, cysteine ablation may render the partner cysteine free to form an activating intermolecular -S-S- bridge, thus leading to the formation of covalent RET dimers with constitutive kinase activity (Santoro et al. 1995). RET mutations affecting intracellular domain probably cause protein conformational changes that relax kinase autoinhibition, increase ATP binding and/or increase the ability of the kinase to transfer phosphate groups to substrates. M918T substitution lies in the substrate-binding pocket of the kinase; it appears to increase RET-ATP binding affinity and disturb the normally autoinhibited RET TK structure thereby making RET more active (Plaza-Menacho et al. 2014).

As previously mentioned, a novel oncogenic RET fusion has been recently found in MTC. Sequencing of RNA derived from a frozen tumor sample proved the existence of an in-frame fusion transcript joining MYH13 (myosin, heavy chain 13, skeletal muscle) exon 35 with RET exon 12. Consistent with other oncogenic RET fusions (RET/PTC rearrangements) overexpression of the kinase domain by the MYH13/RET exhibited *in vitro*

transforming activity. Thus, in MTC RET can rarely be activated secondary to gene rearrangements (Grubbs at al. 2015).

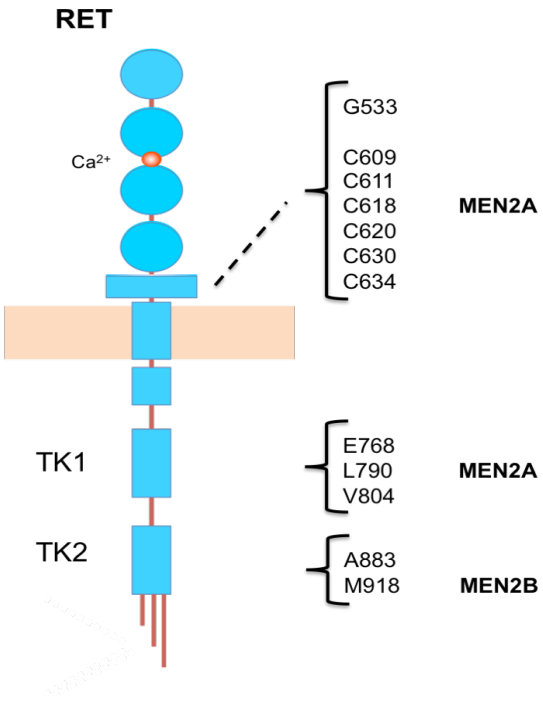

Figure 5. Schematic representation of most common RET point mutations associated to MTC. For a more complete list, see Ref. Wells et al. 2013.

1.3.3 RET in other types of cancer

Besides MTC, RET is targeted by gain-of-function genetic lesions in other cancer types (Santoro et al. 2013). As described above, somatic lesions of RET involve a rearrangement of the RET locus, at chromosome 10q11.2, in about 7.0% of PTCs (Cancer Genome Atlas Research Network. 2014). These rearrangements collectively named "RET/PTC" are significantly more prevalent in young age patients and in patients with a history of accidental or therapeutic radiation exposure, as demostrated by their increase in pediatric PTCs after the Chernobyl nuclear accident (Kondo et al. 2006; Williams 2008; Mulligan 2014). There are several types of RET/PTC fusions, as determined by the type of RET partner gene involved (**Fig. 6**). RET/PTCs form as the consequence of genetic recombination between the 3′ TK portion of RET and the 5′ portion of a partner gene, such as the coiled-coil domain-containing gene 6 (CCDC6; also known as H4) in RET/PTC1 and the nuclear receptor co-activator 4 (NCOA4; also known as ELE1) in RET/PTC3 (Santoro et al. 2006; Mulligan 2014). Virtually all the translocated amino-termini fused to RET are predicted to fold into coiled coils that are able to mediate protein dimerization; such protein-protein interaction, in turn, mediates ligand-independent RET kinase activation. The genomic mechanism that underlies the rearrangements might be explained by the specific subnuclear architecture found in thyroid cells. Loci that are involved in RET/PTC rearrangements lie in close proximity in the interphase nucleus, this favouring their illegitimate recombination (Nikiforova et al. 2000). Moreover, fragile DNA secondary structures in RET intron 11 might favour DNA breakage and subsequent recombination in response to radiation-induced DNA damage (Nikiforova et al. 2000). Consequently, RET/PTC acts as a classical oncoprotein that is able to activate the MAPK and PI3K/AKT pathways (Miyagi et al. 2004).

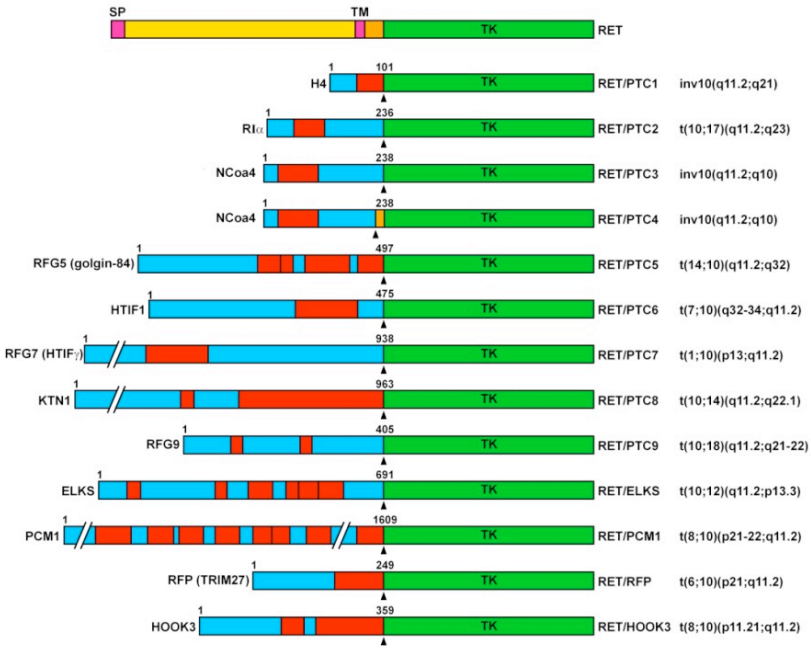

Figure 6. Schematic representation of RET/PTC rearrangements in PTC

Similarly to PTC, RET oncogenic conversion secondary to chromosomal rearrangements, has been identified in two chronic myelo-monocytic leukemia (CMML) and one primary myelofibrosis cases. In particular, BCR/RET and FGFR1OP/RET generated by two balanced translocations t(10;22)(q11;q11) and t(6;10)(q27;q11) respectively, were isolated from these hematopoietic neoplasms. Similarly to RET/PTC rearrangements, the 5' part of the leukemia-associated fusion genes encodes dimerization domains, thus mediating RET TK activation. These RET fusion genes are able to transform hematopoietic cells and impair the hematopoietic differentiation program (Ballerini et al. 2012; Bossi et al. 2014).

RET gene fusions have also been found in Non-Small Cell Lung Cancer (NSCLC). In particular, 1-2% of patients affected by lung adenocarcinoma (LADC) presented a pericentric inversion on chromosome 10 joining exons 1–15 of KIF5B (kinesin family member 5B) to exons 12–20 of RET. KIF5B exons 1–15 comprise the kinesin motor and coiled-coil domains that mediate homodimerization (Lipson et al. 2012). Different breakpoints leading to various KIF5B-RET fusions have been identified. The KIF5B-RET fusion leads to aberrant activation of RET kinase and it is considered a new driver mutation of LADC, because it is mutually exclusive with lesions of other LADC-associated oncogenes (EGFR, KRAS, HER2 and ALK) (Kohno et al. 2012). In LADC, less commonly, the RET TK was fused to the first exon of

CCDC6, NCOA4 or TRIMM33 genes, as it occurs in RET/PTC1, RET/PTC3 and RET/PTC7 respectively (Li et al. 2012; Wang et al. 2012; Drilon et al. 2013; Kohno et al. 2013; Gainor et al. 2013) Similar RET fusions, but with KIF5B or alternative partner genes (GOLGA5), have been recently isolated in patients affected by a particular melanocyte tumor subtype (Spitz melanoma) that is characterized by a rare association to BRAF mutations (Wiesner et al. 2014).

In the absence of structural genetic lesions, abnormal RET expression has been shown to occur in other tumour types. RET is expressed in 50–65% of pancreatic ductal adenocarcinomas, and associated to malignant transformation and perineural invasion (Sawai et al. 2005). RET is also up-regulated in 30–70% of invasive breast cancers particularly in estrogen receptor-positive tumours. In tamoxifen-resistant breast cancer cells, RET targeting was able to restore tamoxifen sensitivity (Plaza-Menacho et al. 2010).

In contrast, RET loss-of-function secondary to reduced expression or rare point mutations, has been found in colorectal carcinomas. Aberrant methylation of RET in colorectal cancer cell lines correlated with decreased RET expression, and the restoration of RET resulted in apoptosis of these cells (Luo et al. 2013).

1.4 Protein kinases in cancer

Over 500 protein kinases have been identified to date, several of them affecting pathways whose dysregulation is implicated in cancer (Manning et al. 2002; Krause et al. 2005). Point mutations, gene amplifications, chromosomal rearrangements or up-regulated expression target proto-oncogenic kinases providing them with transforming capacity. **Table 2** reports a list of most common lesions targeting kinases in human cancer.

Tumor cells commonly exhibit dependence on a single (often the initiating) activated oncogenic pathway or protein to maintain their malignant proliferation and survival, a phenomenon that is called "oncogene addiction" (Weinstein and Joe. 2008). According to this concept, protein kinases have been elected as promising molecular targets for cancer therapy. There are several possibilities to target these proteins in cancer, including monoclonal antibodies that can bind to the extracellular domain of the RTK, compounds able to favour the proteolytic degradation of the kinase and, finally, small molecule protein kinase inhibitors (PKI) (Baselga 2006). In this dissertation, we focus in particular on small molecule RET kinase inhibitors.

Table 2: Kinases implicated in human cancer

	Kinase	Tissue/Tumor Type	Oncogenic Alteration
RTK	**EGFR**	Cancers of breast and lung, glioma	Extracellular domain deletions & point mutations
	HER2/ErbB2	Cancers of breast, ovary, colon, lung, stomach	Overexpression
	IGF-IR	Cancers of colon, pancreas, breast, and ovary, MM	Overexpression
	PDGFR-a	Glioma, glioblastoma, HES	Overexpression & translocation
	PDGFR-b	CMML, glioma, DFSP	Translocation
	c-Kit	GIST, seminoma, mastocytosis	Point mutations
	Flt3	AML	Internal tandem duplication
	FGFR1	CML, myeloproliferative disorder	Translocations
	FGFR3	MM	Translocation & point mutations
	FGFR4	Cancers of breast and ovary	Overexpression
	MET	Glioblastoma, colorectal hepatocellular and renal carcinoma, HNSCC metastases	Overexpression, translocation ,point mutations
	RON	Colorectal and hepatocellular carcinoma	Overexpression
	VEGFR2	Renal cell carcinoma, breast carcinoma	Overexpression
	RET	Papillary thyroid carcinoma, MEN2A, MEN2B, and sporadic MTC. Lung adenocarcinoma, Siptz melanoma	Translocations and point mutations
	AXL	Lung, colon, and breast carcinoma, AML, CML	Overexpression, Translocations
	ALK	Anaplastic large cell lymphoma, NSCLC, neuroblastoma, anaplastic thyroid carcinoma	Translocations, point mutations, amplifications
CTK	**SRC**	Lung, colon, breast and prostate carcinoma	Overexpression, C-terminal truncation
	YES	Lung, colon, breast and prostate carcinoma	Overexpression
	ABL	CML, B-ALL	Translocation
	BTK	MCL, CLL, prostate cancer	Point mutations Overexpression
	JAK2	B-ALL, polycytemia and related myeloproliferative disorders	Translocation, point mutation
S/T Kinase	**AKT**	Multiple	Overexpression
	ATM	Ataxia telangectasia	Point mutations
	Aurora A & B	Multiple	Overexpression
	CDKs	Multiple	Overexpression
	mTOR	Multiple	Overexpression
	PKCi	Non-small cell lung, ovarian	Overexpression
	PLK	Multiple	Overexpression
	BRAF	Melanoma, thyroid, colon carcinoma, hairy cell leukemia, craniopharingioma	Point mutation
	S6K	Multiple	Overexpression
	STK11/LKB1	Peutz-Jeghers syndrome, sporadic cancers	Point mutations
LK	**PI3K**	Prostate, colorectal, breast, thyroid carcinomas	Overexpression, point mutations

Table 2: Summary of kinases mutated in cancer (modified from Zhang et al. 2009). RTK: receptor tyrosine kinase, CTK: cytoplasmic tyrosine kinase, S/T Kinase: serine/threonine kinase, LK: lipid kinase. MM: Multiple Myeloma; HES: Hypereosinophilic Syndrome; CMML: Chronic Myelomonocytic Leukemia; DFSP: Dermatofibrosarcoma Protuberans; AML: Acute Myelogenous Leukemia; GIST: Gastrointestinal Stromal tumor; HNSCC: Head and neck squamous cell carcinoma; MEN2: Multiple Endocrine Neoplasia; MTC: Medullary Thyroid Carcinoma; CML: Chronic Myelogenous Leukemia; ALL: Acute Lymphoblastic Leukemia; NSCLC: Non Small Cell Lung Cancer; MCL: Mantle Cell Lymphoma; CLL: Chronic Lymphocytic leukaemia.

1.5 Small molecule protein kinase inhibitors

Protein kinases are defined by their ability to catalyze the transfer of the terminal γ-phosphate of ATP to substrates that usually contain a serine, threonine or tyrosine residue. Kinase domains are typically arranged into 12 subdomains that fold into a bi-lobed (N-terminal and C-terminal) catalytic core with ATP binding site mapping between the 2 lobes (Manning et al. 2002). Into the ATP pocket there is a residue called the "gatekeeper" (for instance T315 in ABL, T790 in EGFR and V804 in RET), whose mutation mediates kinase resistance to PKIs. In addition, kinases have a conserved activation loop (A-loop, AL), which is important in regulating opening of the ATP and substrate binding pockets. Conserved DFG (Asp-Phe-Gly) and APE (Ala-Pro-Glu) motifs are present at the start and end of the AL, respectively (Manning et al. 2002; Liu and Gray. 2006) (**Fig. 7**).

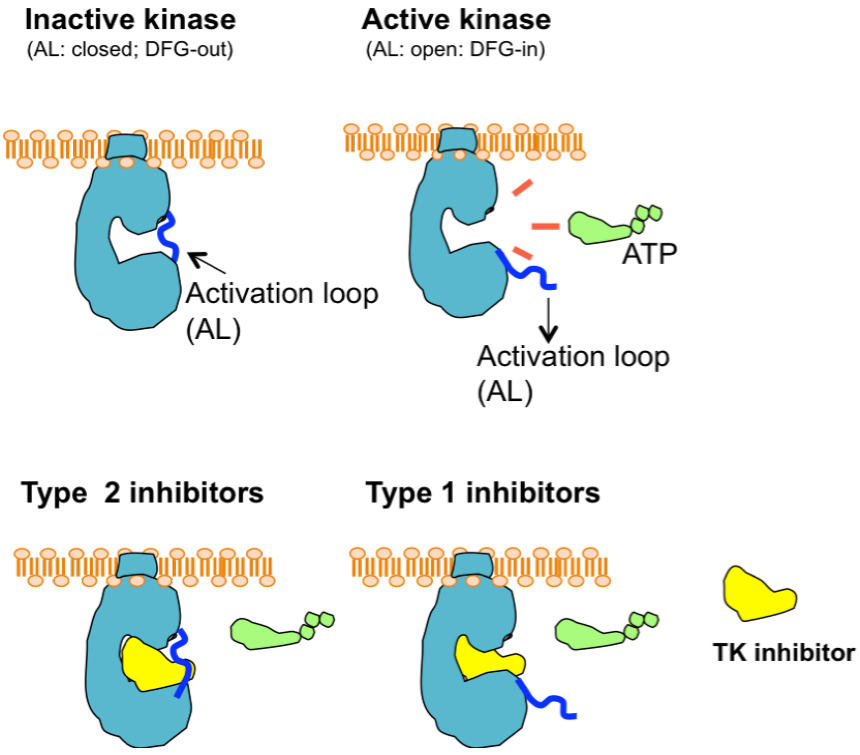

Figure 7. Top: schematic representation of the kinase domain structure and the role of the activation loop (AL). Bottom: kinase inhibitors are divided into 2 classes (type 1 and 2) depending on structural constraints (AL open/closed, DFG in/out) dictating their binding to cognate kinase.

PKIs (or TKIs for tyrosine kinases) are small organic compounds that have been designed to fit within the kinase domain and block the function of the kinase (**Fig. 7**). Covalent PKIs bind covalently to the ATP-site thus preventing ATP binding (Liu and Gray. 2006). Non-covalent PKIs can be further classified into type 1 and type 2 reversible inhibitors (Zhang et al. 2009). Type 1 inhibitors, such as gefitinib, erlotinib, vandetanib, dasatinib and sunitinb, are pure competitive ATP-mimetics; they bind to the active (AL open) conformation of the kinase (referred to as DFG-in). Instead, the type 2 PKIs, such as imatinib, nilotinib, ponatinib or sorafenib bind to the inactive (AL closed), called "DFG-out conformation" taking contacts not only with the ATP site but also with an additional hydrophobic pocket, referred as the "allosteric site", adjacent to the ATP one (Zhang et al. 2009).

1.6 Kinase inhibitors in thyroid cancer: RET inhibitors

Based on the common presence of oncogenic conversion in proto-oncogenic kinases (BRAF, RET, NTRK1, AKT), thyroid cancer is felt to be an attractive candidate whereby to explore the efficacy of PKIs. While WDTC patients can take advantage of capability of their tumors to concentrate radioactive iodine to treat local and metastatic disease, the same does not apply to undifferentiated follicular-cell derived thyroid carcinomas as well as to MTC (Wells et al. 2014). Total thyroidectomy, with or without resection of lymph nodes in the neck, is the primary treatment for patients with MTC. Treatment of MTC at an early stage is associated with a 25-year cause-specific survival of 80%, but 10-year survival is less than 50% in patients with distant metastases. Family members with hereditary MTC who are diagnosed by direct DNA analysis can be treated by early thyroidectomy (Wells et al. 2013). Cytotoxic chemotherapy and radioterapy have limited efficacy in patients with unresectable or metastatic MTC (Schlumberger et al. 2008; Wells et al. 2013).

The role of RET in MTC, as well as its contribution to other cancer types (PTC, LADC, CMML, Spitz melanoma), makes it an important target for therapeutic intervention in multiple diseases (Santoro et al. 2014). To date, two TKIs, vandetanib and cabozantinib have been approved for the treatment of locally advanced and metastatic MTC. Trials of additional multi-kinase inhibitors in thyroid cancer are in progress (**Table 3**). Some of these inhibitors target RET and therefore might be useful in MTC. These agents are multitargeted and able to inhibit several kinases besides RET, most commonly VEGFRs (**Table 3**). It is feasible, that combined action on several targets (polypharmacology) may have the advantage of blocking simultaneously multiple pathways active in both tumor parenchyma and stroma (Knight et al. 2010).

Table 3. Tyrosine kinase inhibitors in current trials for thyroid carcinoma.

Drug	Targeted tyrosine kinases	Clinical trials
Axitinib	VEGFR1-3, PDGFR, c-Kit	Phase I-II
Cabozantinib	VEGFR-2, RET, MET	**FDA approved**
Imatinib	RET, c-KIT, PDGFR	Phase I-II
Lenvatinib	VEGFR1-3, FGFR1-4, KIT, PDGFRβ, RET	Phase III
Motesanib	VEGFR1-3, PDGFR, c-Kit, RET	Phase I-II
Nintedanib	FGFR1-3, PDGFR, VEGFR1-3, RET	Phase II
Pazopanib	VEGFR, PDGFR, c-Kit	Phase II
Ponatinib	ABL, FLT-3, KIT, FGFR, PDGFR, VEGFR, RET	Phase II
Sorafenib	VEGFR1-3, PDGFR, RET, RAF, c-Kit	Phase I-II
Sunitinib	PDGFR, VEGFR1-3, c-Kit, RET, CSF1R, FLT3	Phase I-II
Vandetanib	VEGFR2-3, RET, EGFR	**FDA approved**

Abbreviations: CSF1R, macrophage colony-stimulating factor 1 receptor; EGFR, Epidermal growth factor receptor; FGFR, Fibroblast growth factor receptor; FLT3, FL cytokine receptor 3; PDGFR, Platelet-derived growth factor receptor; VEGFR, Vascular endothelial growth factor receptor. (Mulligan 2014; Wells et al. 2013)

Vandetanib (ZD6474) is a type 1 TKI (Wedge et al. 2002; Herbst et al. 2007). X-ray diffraction has shown that it binds to the ATP-binding pocket of the RET kinase (Knowles et al. 2006). The compound inhibits RET with an inhibitory concentration 50 (IC_{50}) of 100-130 nM (Carlomagno et al. 2002; Herbst et al. 2007). Its activity was initially demonstrated in RET/PTC3, RET C634R and RET M918T transfected NIH3T3 cells (Carlomagno et al. 2002), in a transplanted mouse model of human MTC (Johanson et al. 2007) and in a Drosophila model of RET-mediated tumorigenesis (Vidal et al. 2005). Vandetanib shares with other RET TKIs (sorafenib, sunitinib, cabozantinib) the capability of targeting vascular endothelial growth factor receptor type 2 (VEGFR2/KDR) (IC_{50} = 38-40 nM), VEGFR3 (Flt-4) (IC_{50} = 110-260 nM) and VEGFR1 (Flt-1) (150-1000 nM) (Wedge et al. 2002; Bianco et al. 2008). In addition, vandetanib targets also the epidermal growth factor receptor (EGFR) (Wedge et al. 2002; Ciardiello et al. 2003; Bianco et al. 2008). Vandetanib was studied in a Phase III clinical trial in MTC and found to be able to prolong progression free survival of MTC patients with respect to placebo. Based on these data, it has been approved by US Food and Drug Administration for the treatment of locally advanced or metastatic MTC (Wells et al. 2012; Thornton et al. 2012).

Cabozantinib (XL184) is another type 1 oral tyrosine kinase inhibitor,

also known as a multikinase inhibitor (Viola et al. 2013). Cabozantinib is a potent inhibitor of MET and VEGFR2 with IC50 values of 1.3 and 0.035 nM, respectively and displayed strong inhibition of several other kinases that have also been implicated in tumorigenesis, including KIT, RET, AXL, TIE2 and FLT3 (Grüllich et al. 2014; Mologni et al. 2013; Bentzien et al. 2013). A phase III clinical study was conducted in 330 patients with locally advanced or metastatic MTC with documented RECIST progression. Cabozantinib treatment resulted in prolongation-free survival respect to placebo treated patients and has been registered by FDA for MTC treatment (Elisei et al. 2013).

Recently, we and others reported that ponatinib (AP24534), a type 2 TKI, inhibited purified RET kinase with the IC50 of 2 digit nM (De Falco et al. 2013- Attached at the end of this Dissertation; Mologni et al 2013). Ponatinib is a BCR/ABL kinase inhibitor that was derived from a structure-guided strategy targeting the inactive, DFG-out conformation of ABL. It is a multi-targeted, broad-spectrum tyrosine kinase inhibitor, which has shown inhibitory activities also against SRC, FLT3, FGFR, VEGFR, PDFGR and others. Ponatinib was FDA approved in 2012 for patients with chronic myeloid leukemia (CML) and Philadelphia chromosome–positive acute lymphoblastic leukemia (Ph+ ALL). Ponatinib was able to inhibit both wild-type and mutant (T315I) BCR-ABL kinases with low nM IC50 values. We could show that this drug was active against both of point-mutant and rearranged RET-derived oncoproteins, including RET/V804M, a RET mutant in the gatekeeper residue that displayed resistance to other tyrosine kinase inhibitors. Moreover, the drug was strongly active against xenografts induced in nude mice by the injection of TT cell (a medullary thyroid carcinoma harboring C634W RET mutation) (De Falco et al. 2013 - Attached at the end of this Dissertation).

1.7 Mechanisms of resistance to protein kinase inhibitors

Despite promising results in cancer treatment with PKIs, clinical experience has shown that only a fraction of patients respond to targeted therapies, even if their tumor expresses the altered target. This kind of resistance is known as primary resistance. Moreover, secondary or acquired resistance to the treatment arises almost invariably when tumors are treated with PKIs (Sierra et al. 2010). Acquired resistance mechanisms can be divided into two main categories: 1) target-dependent and 2) target-independent mechanisms.

Target-dependent resistance typically occurs through genetic modifications of the target. Such genetic modifications may include: point mutations and copy number amplifications (Sierra et al. 2010). The acquisition of mutations conferring drug resistance has been documented for several inhibitors, such as for example drugs against BCR/ABL, EGFR, FLT3, KIT and PDGFR (Kobayashi et al. 2005; Roumiantsev et al. 2002; Fletcher and Rubin. 2007; Cools et al. 2004). A prevalent mechanism is the occurrence of point mutations within the kinase domain, which decrease the binding of the PKI either directly or allosterically by making conformational changes that in turn impede PKI binding. The most extensive characterization of such a type of resistance-causing mutations has been performed for BCR/ABL in the context of treatment with imatinib. Typically, mutation at the gatekeeper residue (T315I) confers imatinib resistance to BCR/ABL. Indeed, although the gatekeeper residue comes in close contact with ATP binding site, it does not interact with ATP and therefore its mutation is able to cause resistance without impeding ATP binding and therefore kinase activity (Gorre et al. 2001; Liu and Gray. 2006). Likewise, mutation of the EGFR T790 residue to methionine induces resistance to gefitinib and erlotinib (Pao et al. 2005). The gatekeeper mutation in KIT (T670I) induces resistance to imatinib (Fletcher and Rubin. 2007), G697R in FLT3 induces resistance to PKC412 (Cools et al. 2004) and the gatekeeper mutation in RET (V804M/L) induces resistance to vandetanib (Carlomagno et al. 2004). Evidences suggest the mutation may pre-exist in a minority of cancer cells, and it is then selected upon PKI treatment. This suggests that secondary PKIs that can bind also the mutated kinase can be used to overcome resistance.

Gene amplification is another major mechanism of target-dependent resistance. The selective pressure of the drug can drive amplification of the target gene, thus leading to additional overexpression of the encoded protein (Sierra et al. 2010). This event has been observed in CML relapsed patients treated with imatinib, who displayed an increase in the BCR/ABL gene copy number (Gorre et al. 2001).

Instead, target-independent mechanisms occur through activation of alternative pathways that allow the bypass of the drug-mediated block. In other words, cancer cells escape treatment by switching to an alternative-signaling pathway that is not inhibited by the PKI. For instance, despite blocking MAPK

signaling, MEK inhibitors engage feedback loops that promote hyper activation of the PI3K/AKT pathway through the activation of diverse RTKs. Similarly, feedback circuits cause mTORC1-mediated recruitment of insulin like growth factor I receptor kinase and resistance to PI3K inhibitors (Pettazzoni et al. 2015). Moreover, overexpression of the MET receptor or of its ligand hepatocyte growth factor (HGF) accounts for EGFR acquired resistance (Mueller et al. 2010). A study of gefitinib-resistant cell lines and human lung adenocarcinoma specimens showed that HGF overexpression (coupled with MET activation) leads to PI3K/AKT pathway restoration in the absence of MET amplification (Yano et al. 2008). Signaling bypass is the typical mechanism of resistance to BRAF PKIs. Melanoma cells chronically treated with BRAF inhibitors acquire drug resistance via upregulated expression of a number of RTKs (Nazarian et al. 2010) or genomic amplification of COT in turn able to restore RAS/ERK pathway (Johannessen et al. 2010). Under these circumstances, co-inhibition of both pathways can be exploited to reduce tumor growth (Mendoza et al. 2011).

Other mechanisms of resistance can exploit the enormous genome plasticity of cancer cells by modulating miRNA expression or remodeling chromatin. Finally, though not as commonly as with classical cytotoxic drugs other resistance mechanisms can cause a decrease of the effective intracellular concentration of the PKI (Sierra et al. 2010). Overexpression of certain ATP-binding cassette (ABC) transporter proteins such as P-glycoprotein (MDR1/P-gp/ABCB1) and the breast cancer resistance protein (BCRP/ABCG2) confer resistance to imatinib in CML or gefitinib in NSCLC (Vasconcelos et al. 2011).

2.0 AIM OF THE STUDY

Preclinical and clinical studies have demonstrated that targeted therapy based on RET inhibition may be a promising strategy for the treatment of cancers in which this oncogene is involved (Santoro et al. 2014). Clinical experience with RET TKIs is very limited since the first drugs inhibiting RET have been registered less than 5 years ago (Wells et al. 2014). However, lessons learned from other tumor types have thought that cancer patients commonly develop resistance to TKIs. Resistance can be mediated by mutations in the target kinase that impair drug binding or other mechanisms that allow cancer cells bypassing signaling block exerted by the used TKI. In principle, the first mechanism can be overcome by second line inhibitors able to bind the mutated kinase, while the second one can be challenged by additional inhibitors able to intercept the escape pathway. Thus, it is of great relevance to understand molecular mechanisms of resistance to devise strategies to overcome it.

In this framework, aim of this study has been to explore secondary resistance mechanisms to vandetanib in RET mutant human MTC cells.

We pursued this goal by:

1) Generating *in vitro* and characterizing MTC cells resistant to vandetanib;
2) Analyzing the molecular mechanism involved in such resistance.

3.0 MATERIALS & METHODS

3.1 Compounds

For *in vitro* experiments, vandetanib was dissolved in DMSO at a concentration of 50 mM and stored at –80°C. BI-D1870 and PF-4708671 were provided by Selleckchem (Houston, TX, USA). They were dissolved in dimethyl sulfoxide (DMSO) at a concentration of 10 mM and stored at -80°C. U0126 was provided by Cell Signaling (Danvers, MA, United States); it was dissolved in DMSO at a concentration of 10 mM and stored at –20°C.

3.2 Cell culture

TT cells were from American Type Culture Collection (ATCC) and authenticated by RET genotyping. TT was derived from the primary tumor of an apparently sporadic MTC (Berger et al. 1984). TT harbor a cysteine 634 to tryptophan (C634W) exon 11 RET mutation (Carlomagno et al. 1995) as well as a tandem duplication of the mutated RET allele (Huang et al. 2003). TT cells were grown in RPMI 1640 supplemented with 16% fetal calf serum (GIBCO, Paisley, PA) (complete medium). Media was supplemented with 2 mM L-glutamine and 100 units/ml penicillin-streptomycin (GIBCO).

3.3 Cell proliferation assay

$2x10^5$ cells were plated in 60-mm dishes. Cells were kept in RPMI 1640 supplemented with 16% fetal calf serum. The day after plating, compounds or vehicle were added. Cells were counted in triplicate every 3-4 days. To estimate IC50 value, cells were counted after 14 days.

3.4 RNA silencing

For RNA silencing, the small inhibitor duplex RNA (siRNA) (ON-target plus SMARTpool) siRET (#L-003170-00) from Dharmacon (Lafayette, CO, USA) was used. The siCONTROL Non-targeting Pool (siCTR) (#D-001810-10-20) was used as a negative control. Cells were transfected with 100 nM siRNAs using Dharmafect reagent following manufacturer's instructions. The day before transfection, cells were plated in 35-mm dishes at 40% of

confluence in RPMI 1640 supplemented with 16% FBS without antibiotics. Cells were harvested 48 hours after transfection.

3.5 BrdU assay

DNA synthesis rate was measured by 5′-bromo-3′-deoxyuridine (BrdU) incorporation assay performed by using 5-Bromo-2′-deoxy-uridine Labeling and Detection Kit I from Roche Applied Science (Penzberg, BY, Germany). Cells transfected with siRET and siCTR, previously seeded onto glass coverslips, were incubated in complete medium supplemented with 10 μM of BrdU for 1 h, fixed and permealized. Cells were than stained with anti-BrdU mouse monoclonal and with rodamine-conjugated secondary antibodies. Hoechst 33258 (final concentration 1 μg/mL; Sigma Chemicals Co) was used to counterstain cell nuclei. The fluorescent signal was visualized with an epifluorescent microscope (Axiovert 2, Ziess) (equipped with a 100X lens) interfaced with the image analyzer software KS300 (Zeiss). The percentage of BrdU incorporation was quantified in 10 randomly photographed fields in a blinded fashion.

3.6 Soft agar assay

Petri dishes of 60 mm diameter were prepared by adding 7 ml of complete medium containing 0.5% soft agar. TT cells cultured in standard conditions were trypsinized, centrifuged and resuspended in a single-cell suspension of $1x10^5$ viable cells/ml ($5x10^4$/well). The cell suspension was mixed with complete medium containing 0.5% soft agar at a ratio 1:2 and then divided in two aliquots, one of which was supplemented with 500 nM vandetanib. These suspensions were seeded onto the Petri dishes containing the solidified agar medium (1.5 ml/dish) and incubated at 37°C and 5% CO_2. Control and treated cultures were observed under microscope just after plating, to verify the absence of cell aggregates, and next periodically checked for colonies formation. After four weeks, colonies were counted with an optical microscope at a 10X magnification.

3.7 Tumorigenicity in nude mice

Animals were housed in barrier facilities at the Dipartimento di Medicina Molecolare e Biotecnologie Mediche Animal Facility. Animal studies were carried out according to Institutional-approved protocols in compliance with

the Italian Ministry of Health guide for the care and use of Laboratory Animals.

TT and TT ZD/R cells ($5x10^7$/mouse) were injected subcutaneously into the right dorsal portion of 4-week-old female BALB/c nu/nu mice (n. 28 mice) from Charles River Laboratories International (Lecco, LC, Italy). Tumor size was assessed by caliper at regular intervals and tumor volume was calculated according to the formula: (LxW2)/2 (were L = length and W = width of tumor).

3.8 Immunoblotting

Protein lysates were prepared according to standard procedures. Briefly, cells were harvested in lysis buffer (50 mM Hepes, pH 7.5, 150 mM NaCl, 10% glycerol, 1% Triton X-100, 1 mM EGTA, 1.5 mM $MgCl_2$, 10 mM NaF, 10 mM sodium pyrophosphate, 1 mM Na_3VO_4, 10 μg of aprotinin/ml, 10 μg of leupeptin/ml) and clarified by centrifugation at 10,000 x*g*. Protein concentration was estimated with a modified Bradford assay (Bio-Rad) and lysates were subjected to western blot. Membranes were probed with the indicated antibodies. Immune complexes were revealed by an enhanced chemiluminescence detection kit (ECL, Amersham Pharmacia Biotech). Signal intensity was quantified with the Phosphorimager (Typhoon 8600, Amersham Pharmacia Biotech) interfaced with the ImageQuant software.

3.9 Antibodies

Anti-RET is a polyclonal antibody raised against the tyrosine kinase protein fragment of human RET (Santoro et al. 2005). Anti-phospho-Y905 and anti-phospho-Y1062 are phospho-specific affinity-purified polyclonal antibodies that recognize RET proteins phosphorylated at Y905 and Y1062, respectively (Carlomagno et al. 2002). Anti-phospho-SHC (#Y317), which recognizes SHC proteins when phosphorylated at Y317, was from Upstate Biotechnology Inc. Anti-phospho-PLCγ (#2821) recognizing PLCγ phosphorylated at Y783, anti-phospho-MAPK (#9102) specific for p44/42MAPK (ERK1/2) phosphorylated at Thr202/Tyr204, anti-phospho-MEK1/2 (#9121), anti-phospho-CRAF phosphorylated at Ser338 (#9427), anti-phospho AKT specific for phosphorylated Ser473 (#9271) or Thr308 (#9275), anti-phospho p90RSK specific for phosphorylated Ser380 (#9341), Thr573 (#9346) or Thr359/Ser363 (#9344), and anti-p90RSK (#9355) antibodies were from Cell Signaling Technology. Antibodies recognizing BAD phosphorylated at Ser112 (#5284), S6 Ribosomal Protein when phosphorylated at Ser235/236 (#2211) or when phosphorylated at Ser240/244 (#2215), YB1 phosphorylated at Ser102 (#2900) and p70S6 Kinase phosphorylated at Ser389 (#9234), were

from Cell Signaling Technology. Anti-phospho p90RSK1(S221)/ p90RSK2(S227) (#AF892) specific for p90RSK1 when phosphorylated at Ser221 and p90RSK2 when phosphorylated at Ser227, was from R&D Systems. Anti phospho-p27/Kip1 (#AF3994), which recognizes p27/Kip1 when phosphorylated at Thr198, was from R&D Systems. Anti-p27/Kip1 (#71-9600) was from Invitrogen. Monoclonal anti-α-tubulin (#T9026) was from Sigma Aldrich (St Louis, MO, USA). Secondary antibodies coupled to horseradish peroxidase were from Amersham Pharmacia Biotech (Piscataway, NJ, USA).

3.10 Statistical analysis

Unpaired Student's t tests using the Instat software program (Graphpad Software Inc) were performed to compare cell growth. All P values were two-sided, and differences were considered statistically significant at $P < 0.01$. IC50 doses were calculated through a curve fitting analysis from last day values using the PRISM software program (Graphpad Software Inc). To compare tumour growth we used an unpaired t-student test (InStat program, GraphPad software). P values were statistically significant at $P < 0.01$.

4.0 RESULTS

4.1 Selection of MTC cells resistant to vandetanib

In order to generate MTC cells resistant to vandetanib, we chronically exposed TT cells (a human MTC cell line carrying the RET-C634W mutation) to the drug. We started from a dose (50 nM) that was lower than the IC50 of the drug for RET (100 nM) (Carlomagno et al. 2002), and stepwise scaled-up drug concentration (by increasing the dose of 50 nM at each step) up to 500 nM. In this way we isolated a mass population of TT cells (named TT ZD/R) adapted to proliferate at this vandetanib dose. The process took about 24 months.

To measure vandetanib (ZD6474)-inibitory concentration 50 (IC50) in TT ZD/R cells compared to parental ones, cells were exposed for 14 days to different doses of the inhibitor (**Fig. 8**). Treatment of parental cells (TT) with vandetanib reduced proliferation with an IC50 of about 100 nM, confirming previous results. Noteworthy, significantly higher doses of vandetanib were required to achieve 50% growth inhibition in ZD/R cells (IC50 of about 400 nM) confirming their resistance (**Fig. 8**).

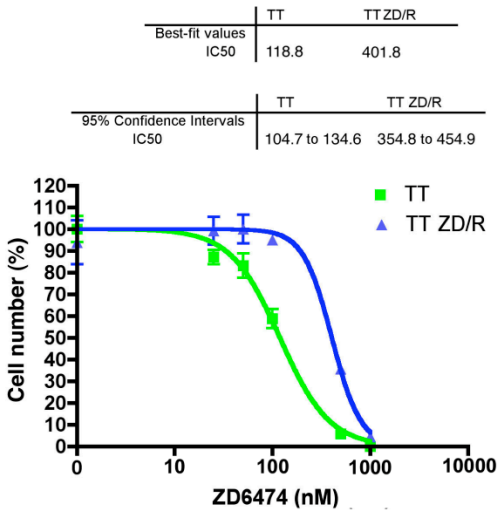

Figure 8. TT cells chronically treated with ZD6474 develop drug resistance. Sensitivity of parental (TT) and corresponding resistant cells (TT ZD/R) to vandetanib (ZD6474) was assessed by proliferation assay. $2x10^5$ cells were plated in RPMI 1640 supplemented with 16% Fetal Bovine Serum (FBS) (complete medium) in presence of different doses of ZD6474 and refreshed every 3-4 days. After 14 days cells were counted in triplicate: data are reported as percentage of cell number. Top: IC50 values with their respective 95% confidence intervals are reported. Sensitivity of parental and resistant cells was significantly different ($p<0.001$) at dose 250 nM.

We asked whether TT ZD/R resistance to vandetanib was irreversible or depended on continous exposure to the drug. To this aim, we cultured TT ZD/R cells in the absence of vandetanib (wash-out) for about 3 months. Vandetanib-IC50 in washed-out TT ZD/R cells (TT ZD/R wash-out) compared to that of TT ZD/R cells continuously kept in vandetanib was measured by a 14 days proliferation assay with different doses of the inhibitor (**Fig. 9**). TT ZD/R wash-out cells did not change significantly vandetanib-IC50 that remained of about 400 nM (**Fig. 9**). Thus, TT ZD/R cells were irrereversibly resistant to vandetanib.

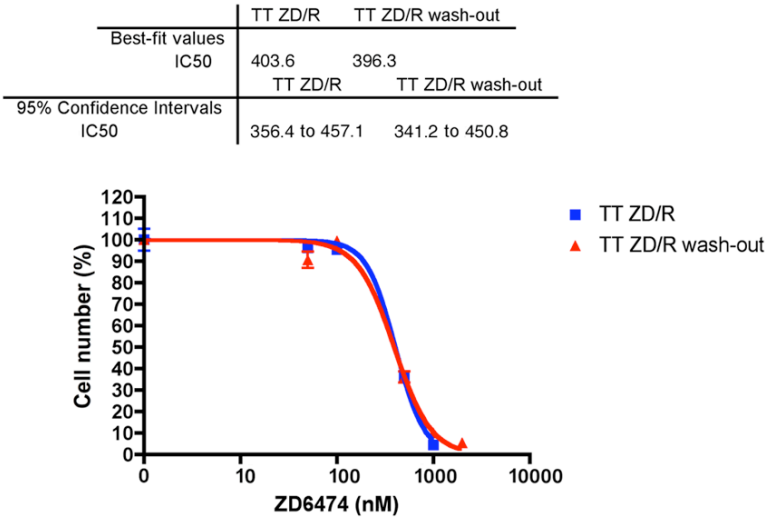

Figure 9. Resistance of TT ZD/R cells was irreversible. Sensitivity to vandetanib (ZD6474) of TT ZD/R and washed-out TT ZD/R (TT ZD/R wash-out) cells was assessed by proliferation assay as described in Fig. 8. Sensitivity of the two cell lines was not significantly different ($p>0.1$) at every analyzed dose.

4.1.1 Cloning of resistant cells

In order to obtain pure populations of vandetanib-resistant cells, TT ZD/R cells were subjected to limiting dilution cloning and individual colonies picking. Cell cloning was carried out from mass population both in the presence and in the absence of vandetanib for about two months. Then, to test if the isolated clones were vandetanib-resistant, proliferation assays were performed with 500 nM vandetanib (ZD6474) for 14 days (**Fig. 10A**). All the isolated clones were resistant to the treatment. Indeed while at 500 nM vandetanib, parental cells growth was arrested, vandetanib-resistant clones (TT ZD/R CL1-11) proliferation rate was only modestly slowed down (**Fig. 10A**). To measure vandetanib-IC50, six representative vandetanib-resistant clones (TT ZD/R CL1, TT ZD/R CL2, TT ZD/R CL4, TT ZD/R CL9, TT ZD/R CL10 and TT ZD/R CL11) were exposed to different doses of vandetanib for 14 days (**Fig. 10B**). All the analyzed clones, irrespectively of their previous selection in the presence or not of vandetanib, featured a significant vandetanib resistant phenotype. These data confirmed the irreversible nature of mechanism of resistance.

A

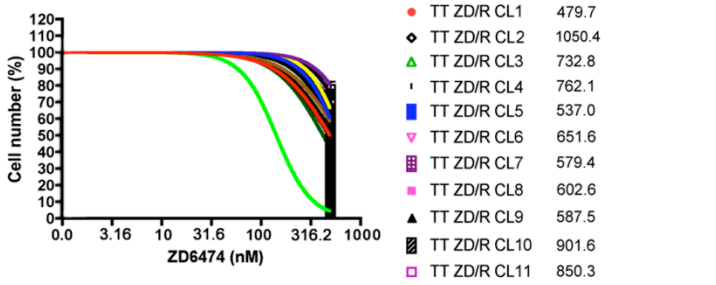

B

	TT ZD/R CL11	TT ZD/R CL9	TT ZD/R CL1	TT ZD/R CL 2	TT ZD/R CL4	TT ZD/R CL10
Best-fit values IC50	865.0 TT ZD/R CL11	537.0 TT ZD/R CL9	464.5 TT ZD/R CL1	1114.2 TT ZD/R CL 2	781.6 TT ZD/R CL4	1007.0 TT ZD/R CL10
95% Confidence Intervals IC50	826.0 to 905.7	468.8 to 615.2	354.0 to 609.5	1025.6 to 1210.6	734.5 to 833.7	841.4 to 1202.3

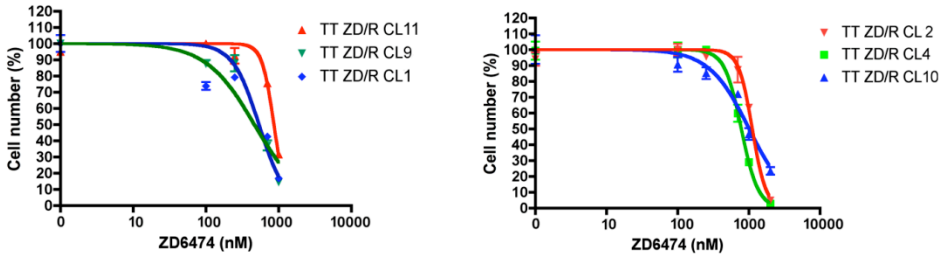

Figure 10. TT ZD/R cell clones are resistant to vandetanib. **A)** Sensitivity of parental (TT) and isolated TT ZD/R clones (TT ZD/R CL) to vandetanib (ZD6474) was assessed by proliferation assay. $2x10^5$ cells were plated in complete medium in the presence of 500 nM ZD6474 and refreshed every 3-4 days. After 14 days cells were counted in triplicate: data are reported as percentage of cell number. On the right, are reported the approximate IC50 values extrapolated by a single dose curve. **B)** Sensitivity to ZD6474 of six representative TT ZD/R clones (TT ZD/R CL11, TT ZD/R CL9, TT ZD/R CL1 isolated in the absence of vandetanib; TT ZD/R CL2, TT ZD/R CL4, TT ZD/R CL10 isolated in the presence of vandetanib) was assessed by proliferation assay as described in Fig. 8. IC50 values and the relative 95% confidence intervals are reported.

4.1.2 Resistant cells feature increased proliferation rate

Morphologically vandetanib-resistant cells were more refractile and spindle shaped than parental cells; moreover, they grew in clusters and were less adherent to the culture dish (**Fig. 11**).

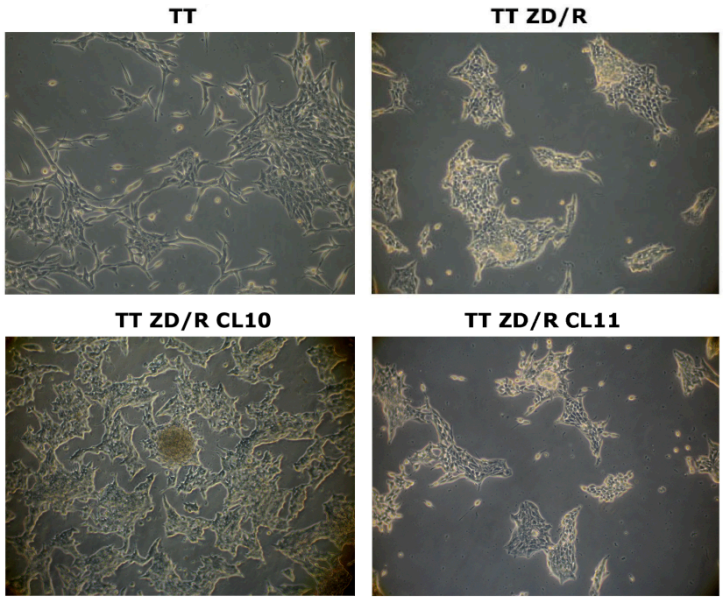

Figure 11. Resistant cells display an increase of the transformed phenotype. Cells (TT, TT ZD/R, TT ZD/R CL10, TT ZD/R CL11) were grown in complete medium. Cells were photographed at 50-70% of confluence with an optical microscope at 10X magnification.

Thus, growth curves at 15 days of resistant compared to parental cells were performed. At 15 days TT ZD/R cells had increased their number by almost 36 fold (from 109000 to 3900000 cells) whereas TT cells only by 21 fold (from 85500 to 1830000 cells) (**Fig 12**).

To confirm these findings, we performed a 5′-bromodeoxyuridine (BrdU) incorporation assay able to measure DNA synthesis rate. Cells were incubated in complete medium for 1 h supplemented with 10 μM BrdU. Cells were fixed and than stained with an anti-BrdU and secondary fluorescein-conjugated antibodies. Hoechst was used to counterstain cell nuclei. TT ZD/R showed increased DNA synthesis rate (30% incorporation) compared to parental TT cells (20% incorporation) (**Fig. 12**). Error bars represent standard deviations.

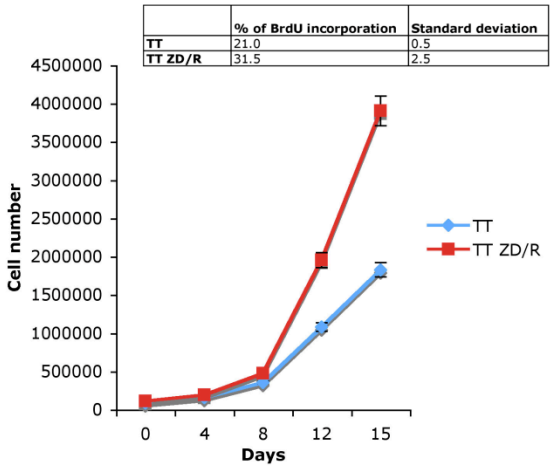

Figure 12. Resistant cells display increased growth rate. $2x10^5$ TT and TT ZD/R cells were plated, in the absence of vandetanib (ZD6474), in complete medium and counted at different time points. Error bars represent standard deviation derived from experimental triplicates. BrdU incorporation assay was performed to assess TT and TT ZD/R cells DNA synthesis rate (inset). Cells were plated in complete medium and incubated with 10 μM 5′-bromodeoxyuridine for 1 h. The percentage of cells in active DNA synthesis (anti-BrdU antibody positive) was calculated with respect to total cells (Hoechst 33258 positive). Standard deviations were calculated from experimental triplicates.

4.1.3 Resistant cells display increased capability to form colonies in soft agar

In order to evaluate anchorage-independent growth, $5x10^4$ TT cells, pool TT ZD/R and three representative resistant cell clones (TT ZD/R CL9, TT ZD/R CL10 and TT ZD/R CL11) were seeded in soft agar in a 60 mm dish in the presence or not of 500 nM vandetanib (ZD6474). Colonies were counted after 28 days and photographed with an optical microscope at a 10X magnification (**Fig. 13**). Resistant cells feature increased size (**Fig. 13, upper**) and number (**Fig. 13, lower**) of colonies with respect to parental TT cells.

Moreover while parental TT cells were unable to form colonies in the presence of vandetanib, resistant cells featured partial anchorage-independent growth even in the presence of vandetanib. At 500 nM vandetanib, resistant cells only featured a partial reduction (about 50%) in size and number of the colonies (**Fig. 13**).

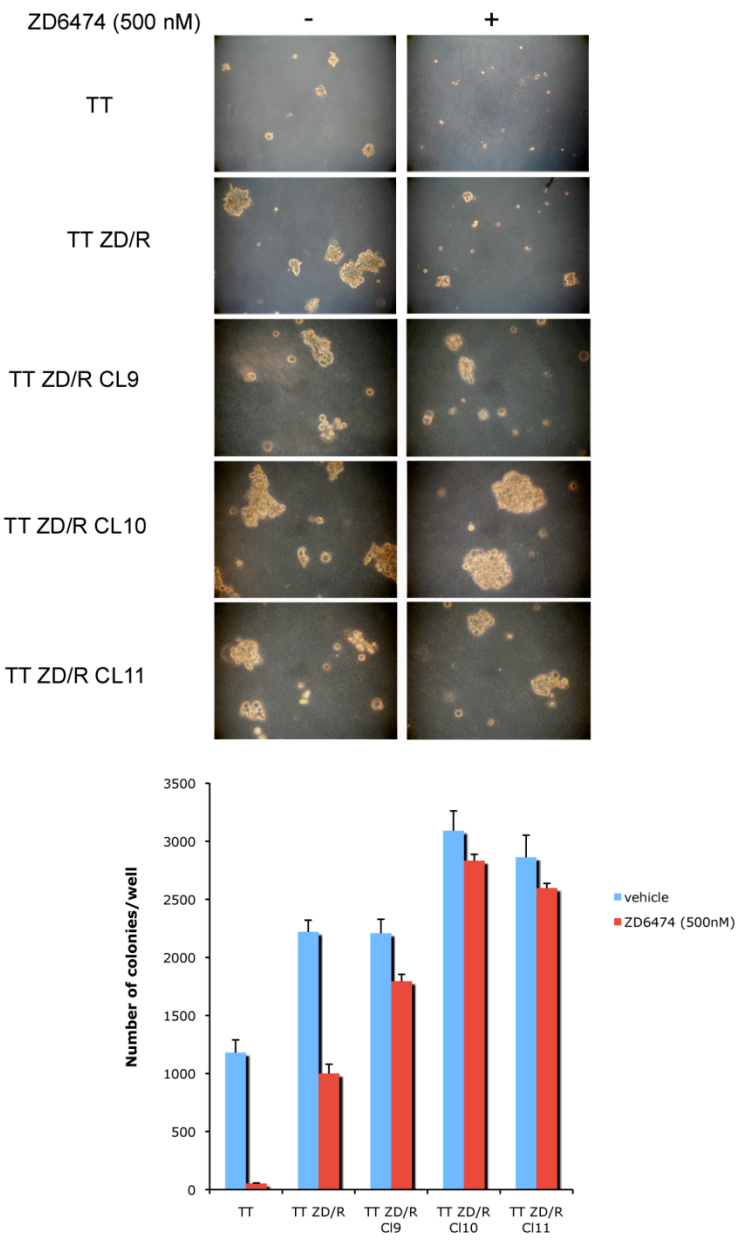

Figure 13. Resistant cells feature increased anchorage-independent growth in soft-agar assay. Petri dishes of 60 mm were prepared by adding 7 ml of complete medium to 0.5% soft agar. $5x10^4$ parental (TT) or resistant cells (TT ZD/R, TT ZD/R CL 9, TT ZD/R CL 10, TT ZD/R CL 11) were resuspended in complete medium containing 0.25% soft agar and then divided in two aliquots, one of which was supplemented with 500 nM vandetanib (ZD6474). Cell suspensions were seeded onto the Petri dishes containing the solidified agar medium. After four weeks the colonies larger than about 50 µm in diameter were photographed and counted with an optical microscope at 10X magnification. Error bars represent standard deviations from experimental triplicates.

4.1.4 Resistant cells display increased capability to form tumors in nude mice

An *in vivo* tumorigenicity assay was performed. TT and TT ZD/R cells ($5x10^7$/mouse) were injected subcutaneously into the right dorsal portion of BALB/c nude mice (20 for each group). Three weeks after injection tumor volumes were assessed; xenografts induced by TT ZD/R cells displayed increased tumor incidence than those induced by TT cells (**Fig. 14**). Indeed, after three weeks only 15% of TT injected mice and more than 90% of TT ZD/R injected mice showed measurable tumors (>40 mm^3). Moreover the mean volume of tumors derived from TT cells was 32.9 mm^3 whereas that of tumors derived from TT ZD/R cells was 327.5 mm^3 (P<0.001).

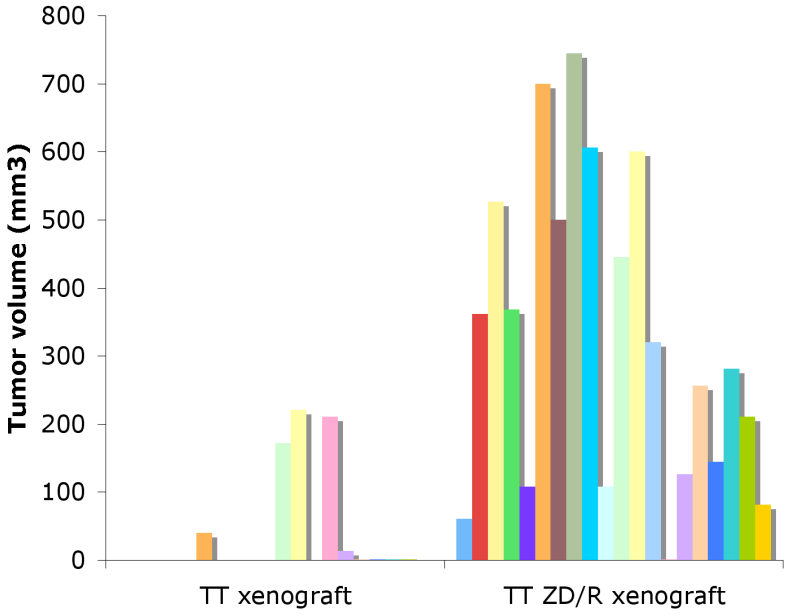

Figure 14. TT ZD/R cells feature increased *in vivo* tumorigenicity. TT or TT ZD/R cells ($5x10^7$/mouse) were injected subcutaneously into the right dorsal portion of 4-week-old female BALB/c nu/nu mice. After three weeks, tumor size was assessed by caliper and tumor volume was calculated according to the formula: (LxW2)/2 (were L = length and W = width of tumor). Tumors derived from TT cells measured on average 32.9 mm^3 (relative standard deviation=73.5). Tumors derived from TT ZD/R cells measured on average 327.5 mm^3 (relative standard deviation=227.2). Statistical significance was determined by unpaired Student's T test (P<0.001).

4.1.5 Resistant cells have no secondary genetic RET alterations

Target-dependent resistance can be mediated by secondary kinase lesions imparing drug binding or kinase copy number gains altering drug-kinase stoichiometry. In the case of RET, V804 and Y806 mutations have been previously shown to impair vandetanib binding (Carlomagno et al. 2004; Carlomagno et al. 2009). Thus, we asked whether resistant cells kept the C634W RET mutation carried by parental cells and whether they have developed novel mutations possibly mediating vandetanib resistance. To this aim, RET cDNA was subjected to DNA sequencing in TT ZD/R pool and two representative resistant clones. Resistant cells kept the C634W RET mutation and did not feature any additional RET mutation or rearrangement (data not shown).

In order to verify if resistant cells developed RET gene amplifications, we analyzed RET gene copy number comparing TT ZD/R to TT cells by quantitative PCR. It was already known that TT cells have three copy of RET gene (Huang et al. 2003). We found that there was no further RET amplification in TT ZD/R cells (data not shown).

Finally to check if RET was over-expressed in resistant cells, we analyzed RET expression levels in resistant clones compared to parental cells by immunoblotting. In parallel, we checked RET phosphorylation at the major RET signaling docking site, Y1062 (**Fig. 15**). RET levels and RET phosphorylation were comparable in resistant clones with respect to parental cells (**Fig. 15**).

All together, these results allowed to exclude that changes in RET contributed to vandetanib-resistance.

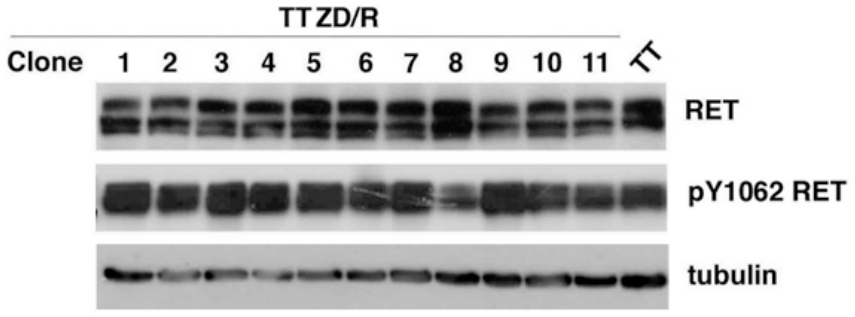

Figure 15. RET expression and phosphorylation levels were not changed in resistant with respect to parental cells. Total cell lysates (50 μg) from parental cells (TT) and resistant clones were analyzed with anti-RET and anti-pY1062 antibodies by immunoblotting. Total tubulin levels were used for normalization.

4.1.6 Resistant cells are still RET-addicted

In order to clarify whether the resistant cells retained RET-addicted proliferation as parental TT cells, we transiently silenced RET expression by RNA interference in parental TT cells, TT ZD/R pool and in two representative resistant clones (TT ZD/R CL6 and TT ZD/R CL8) (**Fig. 16**). The efficacy of small RNA interference against RET (siRET) was proved by immunoblotting; siRNA transfection reduced by more than 70% RET protein levels (**Fig. 16**). In resistant such as in parental cells RET silencing reduced by about 6-fold DNA synthesis rate measured as percentage of BrdU incorporation (**Fig. 16**). These findings indicated that resistant cells were still dependent on RET for their proliferation.

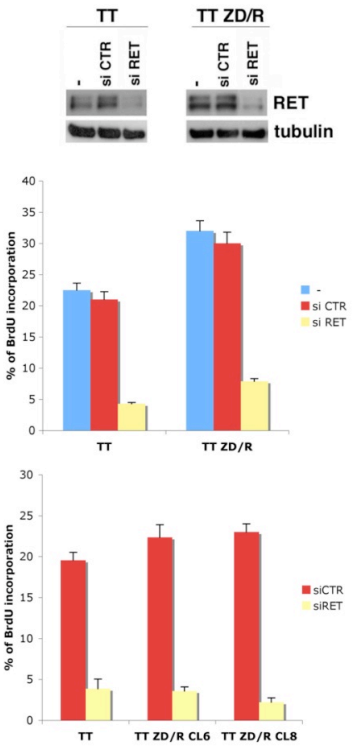

Figure 16. Resistant cells display a RET-addicted DNA synthesis rate. RET silencing was performed in parental (TT) and resistant cells (TT ZD/R, TT ZD/R CL6, TT ZD/R CL8). Cells were plated in 35-mm dishes at 40% confluency in complete medium without antibiotics. The following day, cells were transfected with 100 nM small interference against RET (siRET) or negative control (siCTR) using Dharmafect reagent following manufacturer's instructions. 48 hours after transfection, cells were incubated in complete medium supplemented with 10 μM 5′-bromodeoxyuridine for 1 h. Total cell lysates (50 μg) were analyzed with anti-RET antibody by immunoblotting. Total tubulin level was used for normalization. The percentage of cells in DNA synthesis measured by BrdU incorporation was calculated with respect to total cell number. Error bars represent standard deviations derived from experimental triplicates.

4.1.7 RET is effectively inhibited by vandetanib in resistant cells

In order to verify whether vandetanib was still able to inhibit RET in resistant cells, RET phosphorylation was assessed upon one-hour treatment with different doses of vandetanib. We compared RET response to vandetanib (ZD6474) of TT ZD/R cells and two representative resistant clones (TT ZD/R CL7 and TT ZD/R CL11) with respect to parental TT cells by immunoblotting. RET phosphorylation was evaluated at Y1062 and Y905 sites. Consistent with lack of acquired secondary RET alterations, resistant cells did not show different RET response to vandetanib with respect to parental cells. Indeed, as expected for parental cells, at 100 nM vandetanib RET was approximately 50% inhibited in both cell types (**Fig. 17**). However, about 700 nM vandetanib was required to blunt RET phosphorylation to less than 20% in both cell types.

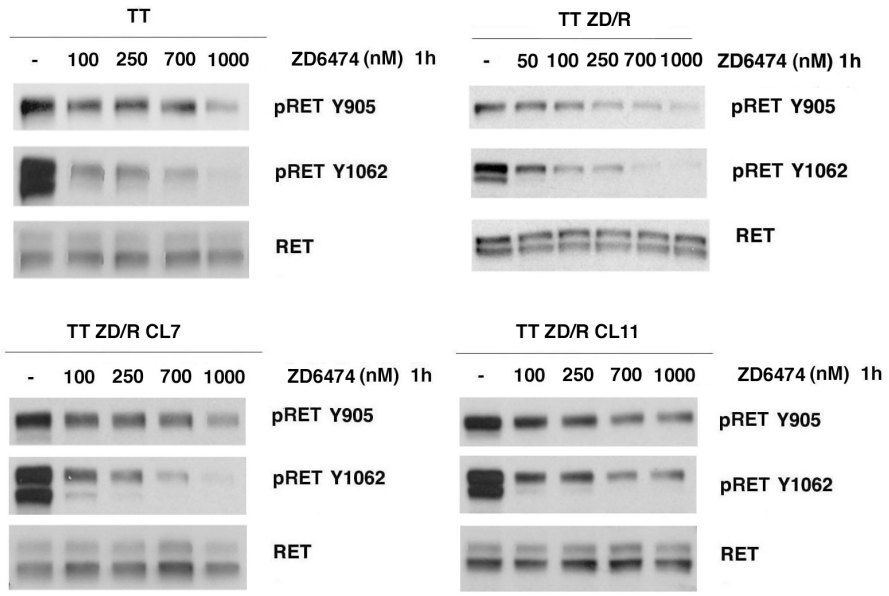

Figure 17. Vandetanib was able to inhibit RET in both parental and resistant cells. TT cells, TT ZD/R pool and two representative resistant clones (TT ZD/R CL7, TT ZD/R CL11) were treated for 1 hr with indicated concentrations of vandetanib (ZD6474). Total cell lysates (50 μg) were subjected to immunoblotting; RET phosphorylation was assessed with anti-phosho Y1062 (pRET Y1062) and anti-phosho Y905 (pRET Y905) antibodies. Total RET level was used for normalization.

In order to verify the duration of RET inhibition upon vandetanib treatment, parental cells and two representative resistant clones (TT ZD/R CL9 and TT ZD/R CL11) were treated with 500 nM vandetanib (ZD6474) at different time points and RET phosphorylation at Y1062 and at Y905 residues was analysed (**Fig. 18**). Comparable kinetics of RET inhibition and phosphorylation recovery were detected in resistant and parental cells, confirming the notion that altered RET activation levels were not directly involved in the mechanism of resistance (**Fig. 18**).

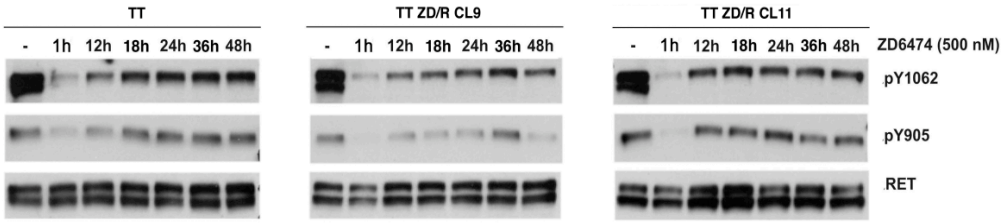

Figure 18. Vandetanib-mediated RET inhibition was comparable in parental and resistant cells. Parental cells (TT) and two representative resistant clones (TT ZD/R CL9, TT ZD/R CL11) were treated at the indicated time points with 500 nM vandetanib (ZD6474). Total cell lysates (50 μg) were analyzed for RET phosphorylation with anti-phosho Y1062 (pY1062) and anti-phosho Y905 (pY905) antibodies. Total RET level was used for normalization.

All together, these findings indicated that functional or genetic RET alterations were not involved in vandetanib resistance of TT ZD/R cells, thus pointing to a target-independent mechanism of resistance. However, resistant cells remained addicted to RET, as shown by siRNA experiments, though threshold of sensitivity to RET inhibition was increased in resistant with respect to parental cells. Indeed, growth of ZD/R cells was still arrested by vandetanib but only when RET phosphorylation was reduced to less than 20% at drug doses higher than 500 nM. These findings suggested that signaling perturbations may have been selected in ZD/R cells to be able to compensate effects of RET inhibition on cell proliferation and allow cells to escape drug treatment effects.

4.2 Resistant cells show p90RSK hyper-activation

To find out whether intracellular signaling was altered in resistant cells, initially the phosphorylation of two direct RET substrates, SHC protein, recruited by Y1062 phosphorylation, and PLCγ protein, recruited by Y1015 phosphorylation was analyzed in a time-course experiment (**Fig. 19A**). No significant changes over time in these RET substrates were observed in resistant versus parental cells (**Fig. 19A**).

Then, we studied activation of other known members of the two principal RET signaling pathways: PI3K/AKT and RAS/ERK signaling cascades. In particular, we explored PI3K/AKT pathway by studying AKT activation at the two main phosphorylation residues, T308, phosphorylated by PDK1, and S473, phosphorylated by mTORC2 (PDK2). RAS/ERK pathway was explored by studying CRAF, MEK and ERK (MAPK) phosphorylation (**Fig. 19B**). Again, comparable changes at each time points in phosphorylation levels of analyzed proteins upon vandetanib (ZD6474) treatment were noted in parental and resistant cells (**Fig. 19B**).

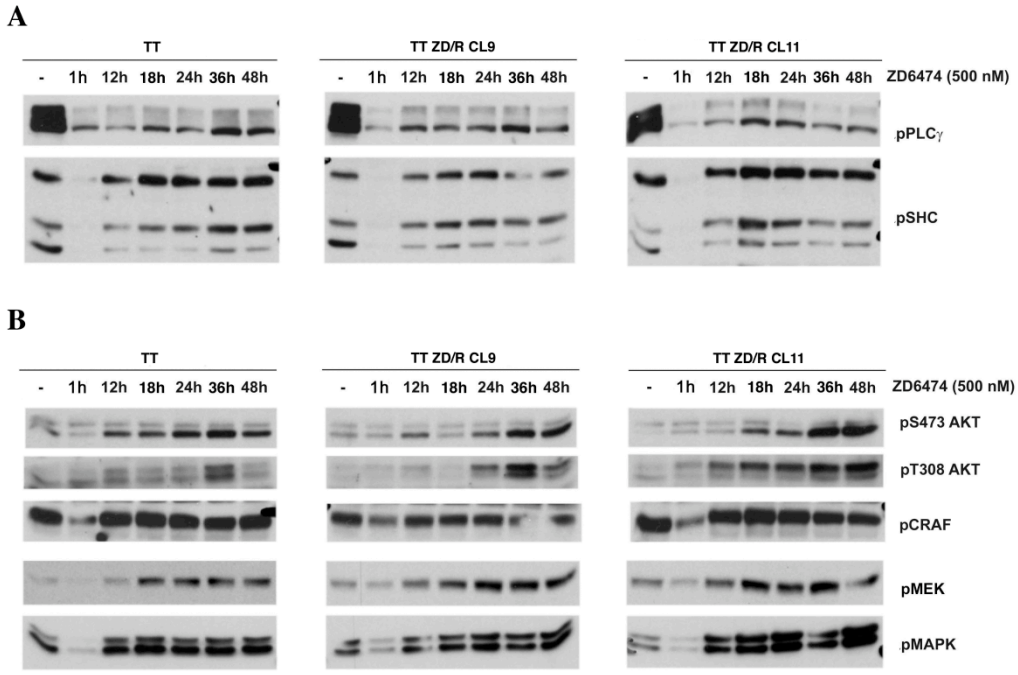

Figure 19. Time-course of vandetanib-mediated PI3K/AKT and RAS/ERK pathways inhibition is comparable in parental and resistant cells. Parental cells (TT) and two representative resistant clones (TT ZD/R CL9, TT ZD/R CL11) were treated as in Fig. 18. **A)** Total cell lysates (50 μg) were analyzed with phospho-PLCγ (pPLCγ) and phospho-SHC (pSHC) antibodies. **B)** Total cell lysates (50 μg) were analyzed with anti-phospho AKT (pS473 AKT and pT308 AKT), anti-phospho CRAF (pCRAF), anti-phospho MEK (pMEK) and anti-phospho MAPK (pMAPK) antibodies.

To investigate more in depth the possible involvement of PI3K/AKT and RAS/ERK pathways in vandetanib-resistance, we checked phosphorylation levels of additional downstream proteins. No phosphorylation changes at each time points in resistant compared to parental cells were noted in the analyzed proteins with the exception of a hyper-activation (see below) of p90RSK, a serine-threonine kinase effector of RAS/ERK pathway.

p90RSK is directly activated by MAPK and it comprises two functionally distinct kinase domains (NTKD: N-terminal and CTKD: C-terminal), a linker region, and N- and C-terminal tails (**Fig. 20**).

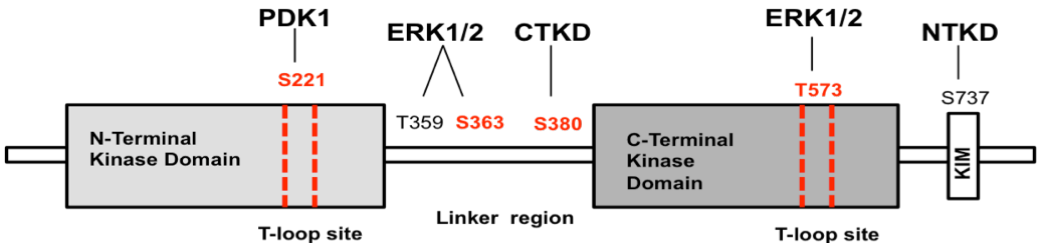

Figure 20. The p90RSK structure. p90RSK is characterized by the presence of two functional kinase domains, the NTKD and the CTKD, which are connected by a linker region of approximately 100 aa. Activation of p90RSK is associated with increased phosphorylation at six sites. These phosphorylation sites were shown to be either essential (221, 363, 380, 573) or accessory (359, 737) for p90RSK activation. The C-terminal end of the protein contains an ERK1/2-docking domain resembling a KIM region (kinase interaction motif), and the extreme C-terminus comprises a PDZ-binding motif. Activation loop (T-loop site) of each kinase domain is indicated. Aminoacid numbering refers to human p90RSK1 (modified from Romeo et al. 2012).

The N-terminal p90RSK kinase domain (NTKD) belongs to the AGC family (Romeo et al. 2012; Frodin and Gammeltoft. 1999) and is responsible for phosphorylating p90RSK substrates recognizing the basophilic consensus motif: Arg/Lys-X-Arg-X-X-Ser/Thr or Arg-Arg-X-Ser/Thr (Frodin and Gammeltoft. 1999). The C-terminal kinase domain (CTKD) of p90RSK belongs to the CaMK (Ca2+ /calmodulin-dependent protein kinase) family (Romeo et al. 2012). The only known function of the CTKD is to activate the NTKD via autophosphorylation of the hydrophobic motif within the linker region and no heterologous substrate has as yet been ascribed to this kinase domain (Romeo et al. 2012). NTKD and CTKD are connected by a linker region of approximately 100 aa (amino acids) containing essential regulatory domains, including hydrophobic and turn motifs, involved in activation of the NTKD (Romeo et al. 2012). The C-terminal tail contains an ERK1/2 docking site, which differs from classical D-type ERK1/2 docking domains. Indeed,

ERK docking domain found in p90RSK appears to fit the KIM consensus sequence (Romeo et al. 2012). Finally, the N-terminal tail contains a potential nuclear localization sequence. Based on this structure, p90RSK is sequentially activated via coordinated phosphorylation by MAPK (ERK1/2), autophosphorylation, and PDK1 (Romeo et al. 2012) (**Fig. 21**). Briefly, upon mitogenic stimulation, ERK cooperatively phosphorylates p90RSK at Thr573 (p90RSK1 numbering) located within the T loop of the C-terminal kinase domain and at Thr359/Ser363 in the linker region between the two kinase domains. Phosphorylation at Thr573 promotes activation and phosphorylation of Ser380 within the linker region by the C-terminal kinase domain. When phosphorylated, Ser380 acts as a docking site for the constitutively active Ser/Thr kinase PDK1, which in turn phosphorylates p90RSK at Ser221 (p90RSK1 numbering) within the T loop of N-terminal kinase domain. Once PDK1 dissociates from p90RSK allowing phosphorylated Ser380 to bind a phosphate-binding site in the NTKD, resulting in a stable association between the hydrophobic motif of the linker and a proximal hydrophobic pocket within the NTKD. The αC-helix then collaborates with phosphorylated Ser221 to stabilize NTKD in an active conformation, resulting in synergistic full activation of NTKD. Ser221 can be also autophosphorylated by the NTKD. Finally, autophosphorylation at the C-terminal Ser737 by NTKD results in dissociation of ERK1/2 from the KIM motif and thereby allows active p90RSK to associate to many cytoplasmic and nuclear substrates and mediate their phosphorylation (Romeo et al. 1012) (**Fig. 21**).

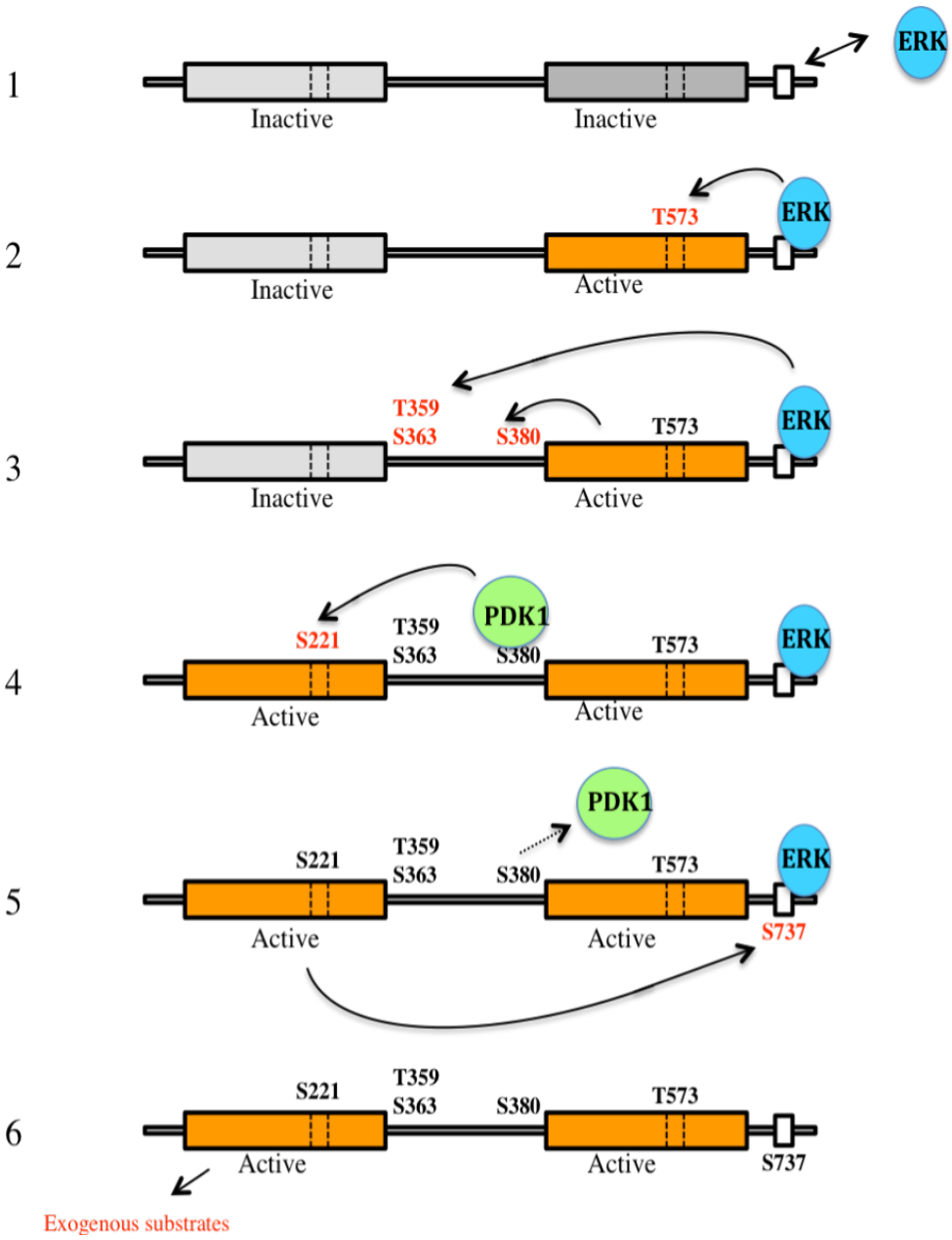

Figure 21. Model of p90RSK activation by sequential phosphorylation. Phosphorylated sites are coloured in red and kinases mediating these events are indicated close to them. Active kinase domains are coloured in orange. See text for details (Romeo et al. 2012).

In order to evaluate p90RSK activation level in a time-course upon vandetanib treatment, its phosphorylation was analyzed. p90RSK phosphorylation at S380 and Thr359/Ser363 residues was up-regulated in resistant compared to parental cells. Then, at 1 hour time point, vandetanib (ZD6474) was able to de-phosphorylate p90RSK both in parental and resistant cells (**Fig. 22**). However, 12 hours after treatment, p90RSK phosphorylation was completely restored only in resistant cells (**Fig. 22**). Instead, no difference in response to the treatment in parental and resistant cells was noted at T573 residue (**Fig. 22**).

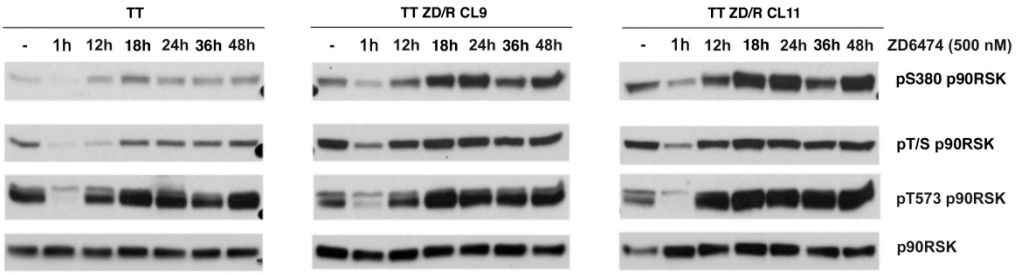

Figure 22. p90RSK is hyper-activated in resistant cells. Parental cells (TT) and two representative resistant clones (TT ZD/R CL9, TT ZD/R CL11) were treated as in Fig. 18. Total cell lysates (50 μg) were analyzed with anti-phospho p90RSK (pS380, pT/S 359/363 and pT573 p90RSK) antibodies. Total p90RSK level was used for normalization.

4.2.1 Resistant cells display phosphorylation signature of p90RSK hyper-activation

To characterize p90RSK function in resistant cells, we checked basal levels of phosphorylation, and in response to vandetanib, of bona fide p90RSK substrates (Mendoza et al. 2011). p90RSK is a member of AGC protein kinases. Because AGC have similar consensus phosphorylation preferences, several of them phosphorylate common substrates (**Fig. 23**).

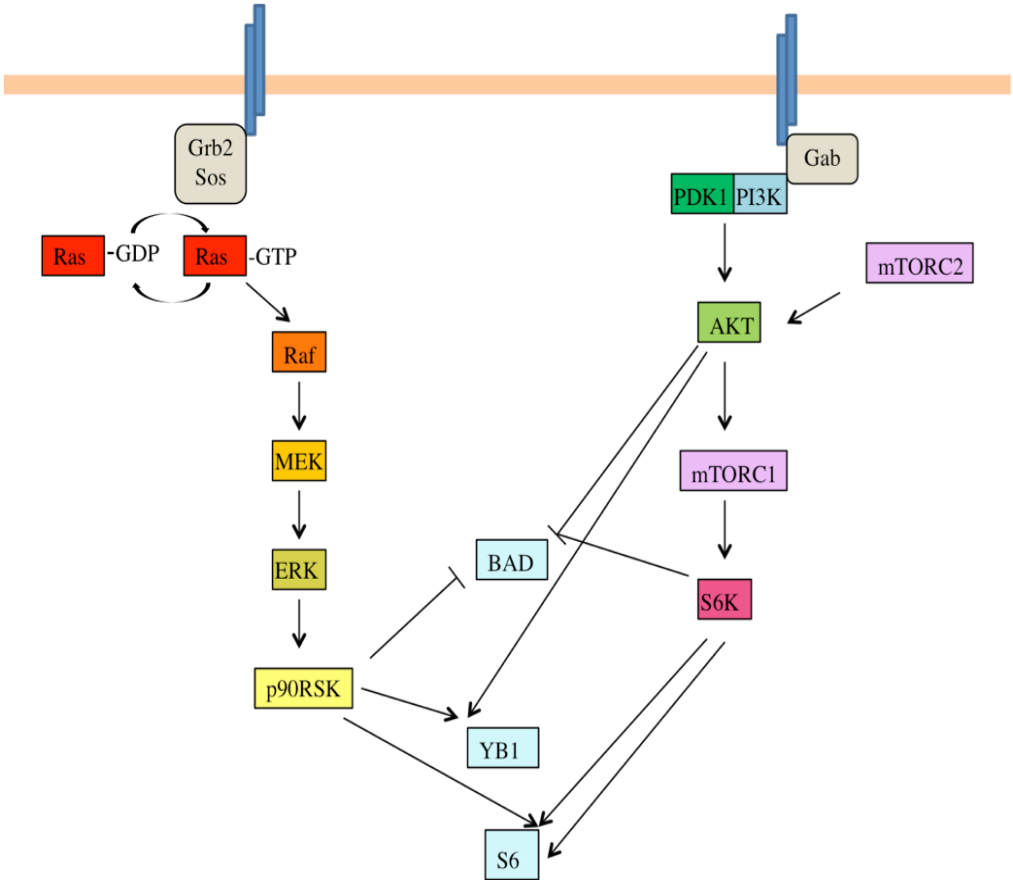

Figure 23. Pathway convergence and AGC kinase promiscuity. Situations in which the same residue is phosphorylated by multiple AGC kinases are indicated. Representative substrates of AGC kinase inputs are in light blue. (Modified from Mendoza et al. 2011)

Thus, parental and two representative resistant clones (TT ZD/R CL10 and TT ZD/R CL11) were treated or not with 500 nM vandetanib (ZD6474) (**Fig. 24**). Important S6 ribosomal protein phosphorylation sites include residues (Ser235/Ser236, and Ser240/Ser244) located within a small, carboxy-terminal region (Ferrari et al. 1991; Romeo et al. 2012). S6 ribosomal protein is

activated by both p70 S6 kinase (p70S6K) and p90RSK (Mendoza et al. 2011) (**Fig. 23**). Its phosphorylation was analyzed at the residues above mentioned by immunoblotting. We found that S6 ribosomal protein was basally hyper-phosphorylated in resistant compared to parental cells. Moreover it was able to rapidly rescue (24 hours time points) its phosphorylation upon vandetanib-treatment only in resistant cells (**Fig. 24A**). To discriminate p70S6K and p90RSK contribution on S6 phosphorylation we compared changes in phosphorylation levels of both kinases in response to vandetanib. Kinetics of S6 ribosomal protein phosphorylation perfectly paralleled with p90RSK one (**Fig. 24A and B**).

We also analyzed phosphorylation of another AGC kinase substrate, YB1 and its response to vandetanib. p90RSK and AKT are both able to directly phosphorylate YB1 at Ser102 (Sutherland et al. 2005). To test if the hyper-activation of p90RSK resulted also in hyper-phosphorylation of YB1, we checked Ser102 YB1 phosphorylation in resistant with respect to parental cells. Resistant cells displayed a high basal level of Ser102 phosphorylation and showed more rapid rescue upon vandetanib treatment (**Fig. 24A**). At 24 hours from treatment, while in parental cells Ser102 of YB1 was still dephosphorylated, resistant cells completely rescued Ser102 phosphorylation (**Fig. 24A**). To discriminate the contribution of AKT from p90RSK on YB1 phosphorylation we followed changes in Ser473 AKT phosphorylation under vandetanib treatment. AKT, differently from p90RSK, was not significantly changed in parental versus resistant cells and therefore seemed not to be involved in sustaining YB1 phosphorylation.

Then, we compared BAD phosphorylation levels in resistant with respect to parental cells. p90RSK is able to phosphorylate BAD at Ser112 (Bonni et al. 1999; Tan et al. 1999). Phosphorylation kinetics of BAD Ser112 perfectly correlated with vandetanib-mediated p90RSK changes (**Fig. 24A and B**).

Finally, we wondered whether also the cell-cycle inhibitor p27 Kip1 (p27), another known p90RSK substrate (Larrea et al. 2009), had increased phosphorylation level in resistant cells. p90RSK and AKT are both able to directly phosphorylate p27 at T198 (Larrea et al. 2009). Resistant cells displayed high levels of p27 T198 phosphorylation; additionally this phosphorylation was virtually unaffected by vandetanib treatment. AKT was not involved in sustaining p27 phosphorylation; indeed changes in phosphorylation of AKT and p27 did not correlate each other under vandetanib-treatment (**Fig. 24B**). Conversely, high levels of p27 phosphorylation in resistant cells paralleled p90RSK hyper-activation (**Fig. 24A and B**). We also analyzed total level of p27. While in parental cells, at 24 hours from treatment, vandetanib strongly increased the amount of p27, the same increment did not occur in resistant cells (**Fig. 24A**). This was strongly suggestive of a potentiated mechanism of p27 degradation through T198 phosphorylation in resistant versus parental cells.

All together, these data show that resistant cells feature a phosphorylation signature of p90RSK hyper-activation.

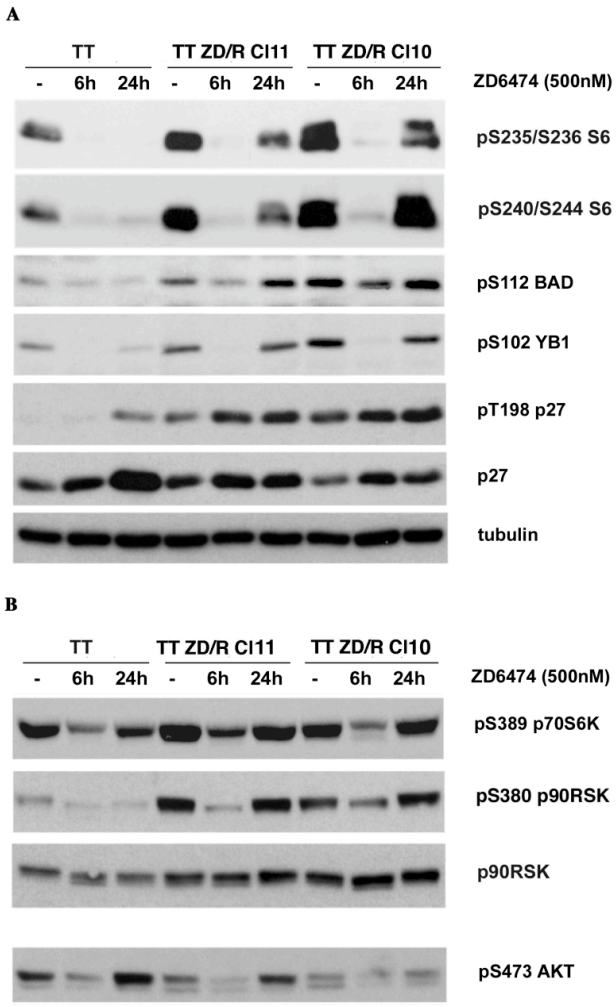

Figure 24. p90RSK substrates are persistently hyper-phosphorylated in resistant cells. Parental (TT) cells and two representative resistant clones (TT ZD/R CL10, TT ZD/R CL11) were treated at indicated time points with 500 nM vandetanib (ZD6474). **A)** Total cell lysates (50 μg) were analyzed with anti-phospho S6 (pS235/S236 and pS240/S244), anti-phospho BAD (pS112 BAD), anti-phospho YB1 (pS102 YB1), anti-phospho p27 (pT198 p27) and anti p27 antibodies. Total tubulin level was used for normalization. **B)** Total cell lysates (50 mg) were analyzed with anti-phospho p70S6K (pS389 p70S6K), anti-phospho p90RSK (pS380 p90RSK) and anti-phospho AKT (pS473 AKT) antibodies. Total p90RSK level was used for normalization.

4.2.2 Resistant cells are sensitive to BI-D1870-mediated p90RSK inhibition

We wondered whether inhibition of p90RSK was biologically effective in resistant cells. To this aim an inhibitor of p90RSK, the dihydropteridinone BI-D1870, was tested. BI-D1870 is a reversible inhibitor that competes with ATP by binding to the NTKD ATP-binding site. BI-D1870 is a highly specific p90RSK inhibitor; treatment of cells with 10 μM BI-D1870 did not significantly inhibit other AGC kinases (Sapkota et al. 2007).

Thus, parental and resistant cells were exposed for 14 days to different doses of BI-D1870. Treatment of parental cells with BI-D1870 reduced proliferation with an IC50 of about 2 μM. Consistent with p90RSK activation, higher doses of BI-D1870 were required to achieve 50% growth inhibition in resistant cells (IC50 of about 4 μM) (**Fig. 25A**).

We performed a 1-hour dose-response treatment with BI-D1870 in parental and two representative resistant clones (TT ZD/R CL11 and TT ZD7R CL 10). As expected, BI-D1870 was able to reduce phosphorylation of p90RSK at S221; in parallel we showed a compensatory hyperphosphorylation of S380 possibly related to a released feedback mechanism (Dalby et al. 1998) (**Fig. 25B**).

Thus, we checked phosphorylation events in response to BI-D1870. S6 ribosomal protein (S6), BAD and YB1 phosphorylations were all sensitive to BI-D1870 treatment both in parental and resistant cells. However, while in parental cells the phosphorylation of these proteins was strongly inhibited at 4 μM, consistent with p90RSK hyperactivation, it was necessary 10 μM BI-D1870 to reach their complete inhibition in resistant cells (**Fig. 25B**).

Overall these results show that resistant cells are sensitive to BI-D1870-mediated p90RSK inhibition. Therefore we hypotize that p90RSK inhibition could be really able to trigger vandetanib sensitization in resistant cells.

A

	TT	TT ZD/R CL11	TT ZD/R CL10
Best-fit values IC50	1.78	3.16	5.62
95% Confidence Intervals IC50	TT: 1.85 to 1.99	TT ZD/R CL12A: 3.87 to 4.17	TT ZD/R CL2B: 3.17 to 3.79

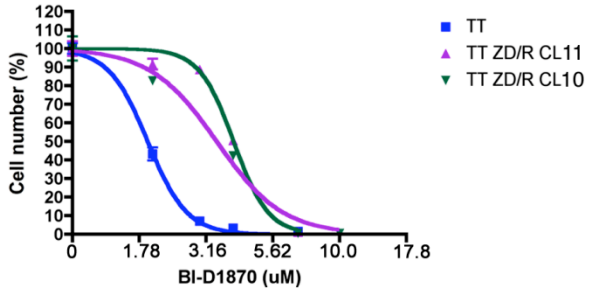

B

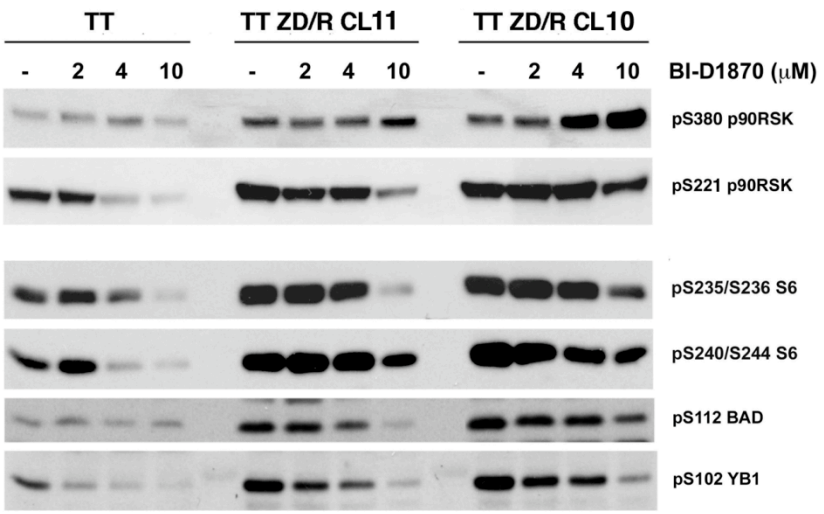

Figure 25. BI-D1870 was effective at inhibiting resistant cells proliferation. A) Cell sensitivity to BI-D1820 was assessed by proliferation assay. $2x10^5$ parental (TT) cells and two representative resistant clones (TT ZD/R CL10, TT ZD/R CL11) were plated in complete medium in the presence of different doses of BI-D1820 and refreshed every 3-4 days. After 14 days, cells were counted in triplicate: data are reported as % of cell number. In the table are reported IC50 values with their respective 95% confidence intervals (CI). **B)** Parental (TT) cells and two representative resistant clones (TT ZD/R CL10, TT ZD/R CL11) were treated for 1 hr with indicated concentrations of BI-D1820. Total cell lysates (50 μg) were analyzed with anti-phospho p90RSK (pS380 and pS221 p90RSK), anti-phospho S6 (pS235/S236 and pS240/S244 S6), anti-phospho BAD (pS112 BAD) and anti-phospho YB1 (pS102 YB1) antibodies.

5.0 DISCUSSION

RET RTK plays a role as a driver oncogene in diverse human cancer types, such as medullary (MTC) and papillary (PTC) thyroid carcinoma, lung adenocarcinoma (LADC), chronic myelomonocytic leukemia (CMML) and other myeloproliferative disorders, and Spitz melanoma (Wells et al. 2013; Lipson et al. 2012; Ballerini et al. 2012; Wiesner et al. 2014). RET has been therefore considered a suitable protein for molecular targeting of these diseases (Santoro et al. 2014). Unresectable locally advanced or metastatic MTC, in particular, is a challenging clinical problem, and it is very commonly associated to genetic lesions causing RET activation (Wells et al. 2013). Therefore, among the RET-driven cancers, it has been the first one whereby RET TKIs have been exploited. Vandetanib and cabozantinib are two multi-kinase inhibitors with potent RET activity; both have been tested clinically in MTC patients and finally registered for the treatment of advanced disease (Wells et al. 2012; Elisei et al. 2013). Both drugs are also being tested in patients affected by other RET-driven cancers, such as LADC (Gautschi et al. 2013; Drilon et al. 2013). Both vandetanib and cabozantinib are type 1 TKI, thus binding to the active conformation of the kinase; other type 1 and type 2 RET TKIs are currently being developed and characterized preclinically (Mulligan 2014)

Targeted cancer therapy has several limitations with resistance to the treatment being one of the most challenging ones. Some patients (or preclinical model systems) do not respond to therapy (primary resistance) and others develop resistance after an initial response (secondary resistance). Both types of resistance can be mediated by the drug target itself or by alternative non-target-mediated mechanisms. Prospective studies in preclinical models have the potentiality of anticipating molecular mechanisms that cause resistance *in vivo* and therefore could be useful to devise strategies that can be clinically applicable.

Target-dependent resistance mechanism is illustrated by mutations at the gatekeeper residue that is essential for proper TKI binding to the target kinase. This is a common mechanism of resistance for a variety of kinases, as paradigmatically illustrated by T315I gatekeeper mutation in BCR/ABL CML (Gorre et al. 2001; Radich 2014). In principle, this type of resistance can be overcome by the use of second line TKIs able to bind the target kinase even when modified by the resistance-causing mutation. Again, this concept is well illustrated by the use of second and third line ABL inhibitors in CML; even the T315I mutation, that has been proved to be recalcitrant to most drugs tested, at the end was found to be responsive to ponatinib a recently developed type 2 TKI (Cortes et al. 2013). Importantly, this concept can be extended to other kinase-drug interactions. For instance, we and others have shown that ponatinib is a potent RET TKI and able to inhibit the RET-V804M gatekeeper mutant (De Falco et al. 2013-Attached at the end of this Dissertation; Mologni et al.

2013).

Non-target dependent resistance mechanisms represent another challenging problem and commonly mediate treatment failure. This is typically mediated by the activation of alternative pathways that bypass the drug-mediated block (Sierra et al. 2010). Perhaps, the most stringent example of this type of mechanism is that involved in resistance to BRAF kinase inhibitors. Instead, melanomas, colon and thyroid cancers escape treatment with BRAF inhibitors because they activate RTKs (such as PDGFR, EGFR, HER3) or other kinases (such as COT) that overcome drug-mediated block (Lito et al. 2013; Solit et al. 2014). In the case of RTK activation, MAPK signaling is restored parallel to BRAF, because RTK-mediated triggering of RAS drives the signal through CRAF, thus bypassing BRAF that remains drug inhibited; in the case of COT activation, instead, MAPK signaling is rescued downstream from BRAF, due to its COT-mediated activation. Importantly, these resistance mechanisms can occur slowly when mutational and therefore requiring the time necessary for mutation occurrence and then clonal selection. However, they can also occur rapidly because not mediated by DNA lesions but only by functional signaling rewiring (adaptation). This is nicely illustrated again by lessons learned with BRAF inhibitors, where resistance can be rapidly put in place due to drug-induced release from feedback mechanisms. For instance melanoma cells can escape BRAF PKIs because they not only results in MAPK inhibition but also in inibition of feedback mediators (such as MAPK phosphatases or negative signaling adaptors), this in turn rescuing the pathway (Lito et al. 2012; Lito et al. 2014). Similarly, in thyroid cancer cells, the use of BRAF PKIs results in the suppression of the transcriptional repressors C-terminal binding protein 1 and 2 which in turn causes upregulated HER3 RTK expression (Montero-Conde et al. 2014). Importantly, these studies are being rapidly translated into clinical experimentations with drug combinations designed to block the resistance driving mechanism (Chapman et al. 2014).

In this Dissertation, we have addressed molecular mechanisms of acquired resistance to vandetanib in cultured MTC cells. We used a RET mutant MTC cell line (TT) and selected TT cells able to proliferate also in the presence of a vandetanib dose approximately 5-fold higher than that normally required to affect proliferation of parental cells. We isolated a mass population and several cell clones. The striking similarity of the various isolated resistance cells makes it unlikely that their resistance depends on the occurrence of independent events and perhaps more likely that vandetanib-resistant sub-populations already exist within parental cells and be selected during the treatment.

Vandetanib-resistant cells did not display secondary genetic RET alterations neither altered RET gene copy number, RNA or protein expression levels. However, resistant cells remained addicted to RET as shown by RET interference and TKI treatment experiments, though threshold of sensitivity to RET inhibition was increased in resistant with respect to parental cells. All together, these findings suggested that some altered signaling mechanisms may

have been selected in resistant cells able to attenuate effects of RET inhibition on cell proliferation, thus allowing cells to escape drug treatment effects.

We have explored this possibility by analyzing activation state of components of the two principal RET signaling pathways PI3K/AKT and RAS/ERK, and found that resistant cells featured a persistent hyper-activation of p90RSK, a serine/threonine kinase of the RAS/ERK pathway.

Functional studies have implicated p90RSK in the regulation of diverse cellular processes, including transcription, translation, survival, cell-cycle progression and migration. p90RSK has been linked to tumorigenesis. p90RSK1 and p90RSK2 are overexpressed in breast and prostate cancer (Serra et al. 2013). Moreover p90RSK3 and p90RSK4 can mediate resistance to PI3K inhibitors in breast cancer cells (Serra et al. 2013). Interestingly, p90RSK4 has been implicated in sunitinib resistance (Bender and Ullrich. 2011). p90RSK functions through phosphorylation of targets including S6 ribosomal protein, BAD, YB1 and p27Kip1, among others (Serra et al. 2013; Aronchik et al. 2014). Accordingly, vandetanib-resistant cells displayed a phosphorylation signature compatible with p90RSK hyper-activation and this signature was consistent with the increase in the transformed phenotype (aggressive morphology, increased proliferation and tumorigenicity and capability of proliferating in semisolid medium) featured by vandetanib-resistant cells. Increased phosphorylation of S6 ribosomal protein correlates with an increase in translation of mRNA transcripts encoding proteins involved in cell cycle progression, as well as ribosomal proteins and elongation factors necessary for protein translation (Peterson et al. 1998). Interestingly, it has been previously demonstrated the involvement of S6 phosphorylation in primary MTC and lymph node metastases (Tamburrino et al. 2012). BAD is a proapoptotic member of the Bcl-2 family that promotes cell death by displacing BAX from binding to Bcl-2 and Bcl-xL (Yang et al. 1995). Survival factors inhibit the pro-apoptotic activity of BAD by activating intracellular signaling pathways that result in its phosphorylation at Ser112 and Ser136 (Zha et al. 1998). Thus, increased BAD phosphorylation may allow vandetanib-resistant cells to escape apoptosis. Phosphorylation-mediated activation of YB1 transcription factor activates genes associated with proliferation and cancer, such as cyclin A, cyclin B1, matrix metalloproteinase-2 (MMP-2), and the multi-drug resistance 1 (MDR1) gene (Jurchott et al. 2003) while repressing genes associated with cell death, including the cell death-associated receptor FAS and the p53 tumor suppressor gene (Lasham et al. 2000). Finally, p27 is a member of the Cip/Kip family of cyclin-dependent kinase inhibitors. Expression levels of p27 are upregulated in quiescent cells and in cells treated with negative cell cycle regulators. Downregulation of p27 can be induced by treatment with mitogens; this involves phosphorylation of p27 at residues such as T157 and T198 followed by nuclear export and degradation by the ubiquitin-proteasome pathway (Lloyd et al. 1999; Larrea et al 2009). Thus, increased phosphorylation of p27 may mediate evasion by cell growth arrest exerted by vandetanib-resistant cells.

To validate p90RSK role in vandetanib-resistance, we tested efficacy of BI-D1870, an ATP-competitive inhibitor of p90RSK NTKD. Our results showed that resistant cells are sensitive to BI-D1870-mediated p90RSK inhibition. Based on these results we want to test whether BI-D1870 in combination with vandetanib, is able to revert resistance in resistant cells. We hypotize that BI-D1870 treatment could restore vandetanib-IC50 value of resistant cells to a vandetanib-IC50 value similar to that of parental cells. Consistently we hypotize that p90RSK downstream signaling could be affected by vandetanib and BI-D1870 combined treatment.

The molecular mechanism driving p90RSK upregulation in vandetanib-resistant cells is still unknown. No point mutation was found by next generation sequencing in the four p90RSK family members (data not shown). Moreover, no significant increase in p90RSK family members expression was seen in vandetanib-resistant cells at both protein and RNA level (data not shown). Rather, we observed increased basal phosphorylation levels of p90RSK at CTKD-dependent Ser380 (in the linker region) and at PDK1-dependent Ser221 (in the NTKD) in resistant cells, whereas the MAPK-dependent Thr573 (in the CTKD) phosphorylation level was unchanged with respect to parental cells.

These findings suggest the possibility that some altered signaling mechanisms may have occurred in vandetanib-resistant cells to mediate p90RSK upregulation and consequently attenuate response to RET TKI. Possible mechanisms are depicted in **Fig. 26**.

One possibility is that an unidentified kinase phosphorylates p90RSK on Ser380 in vandetanib-resistant cells bypassing canonical MAPK-mediated activation of the CTKD (**Fig. 26**). In favor of our hypothesis, Cohen et al. (2007) showed that in certain cellular contexts (for example, LPS-stimulated macrophages) an unidentified kinase bypassed the CTKD requirement and phosphorylated p90RSK at Ser380, thus driving activation of the NTKD. According to this possibility, saturating concentrations of FMK (an inhibitor of CTKD) failed to inhibit Ser380 phosphorylation in vandetanib-resistant cells (data not shown), supporting the possibility that Ser380 phosphorylation occurs in a CTKD-independent manner. Consistently, Zaru et al. (2007) demonstrated that in dendritic cells (DCs), phosphorylation of Ser380 was incompletely suppressed by PD184352 (MEK inhibitor), which suggested that the ERK-activated CTKD of p90RSK could be bypassed. Ser380 phosphorylation was completely blunted, however, in the presence of inhibitors of ERK and p38. Notably, Ser380 phosphorylation persisted in the presence of FMK, consistent with the possibility that a second pathway of p90RSK activation may exist (Zaru et al. 2007). Similarly, preliminary data show that in vandetanib-resistant cells a MEK inhibitor (U0126) was not able to completely inhibit p90RSK, still pointing to a partially MAPK-independent mechanism of p90RSK activation (data not shown).

However, we would favor a second possibility, e.g. that p90RSK upregulation is sustained by the downregulation of some negative feedback

mechanisms normally in place to restrain p90RSK signaling. Indeed, we observed that upon 1 hour treatment vandetanib was able to mediate p90RSK dephosphorylation in both parental and resistant cells; however, at 12 hours treatment p90RSK phosphorylation was promptly restored only in resistant cells, a phenotype that suggests the release from some feedback mechanisms. Inactivation of p90RSK involves NTKD-catalyzed phosphorylation Ser737. This event decreases the affinity of ERK for p90RSK, preventing reactivation of p90RSK after that phosphatases have dephosphorylated the activating sites. One of the phosphatases involved in p90RSK inactivation is PP2Cδ, a member of the PP2C family protein of metal-dependent phosphatases. PP2Cδ is recruited to the activated p90RSK and forms a complex with its NTKD. The binding of p90RSK to PP2Cδ then induces a conformational change in the latter, allowing ERK to phosphorylate PP2Cδ, leading to dissociation of the p90RSK–PP2Cδ complex. However, no difference in response to the treatment between parental and resistant cells was noted at the level of MAPK-dependent T573 residue. Therefore, if a perturbed negative feedback mechanism is involved, this should occur at the level of S380 phosphorylation or the NTKD (**Fig. 26**).

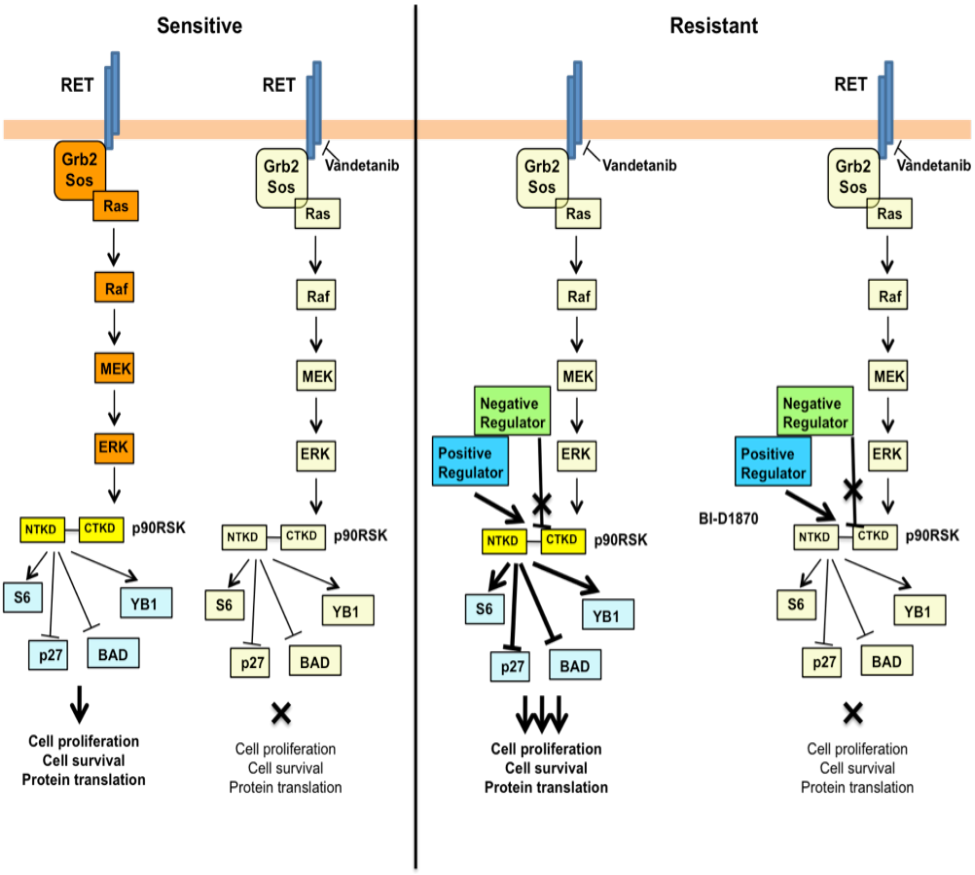

Figure 26. Schematic representation of adaptive mechanism of secondary resistance of MTC cells to RET TKI involving p90RSK hyper-activation.

Whatever the mechanism, increase of a positive regulator or decrease of a negative one, this should be fixed at the genomic or epigenomic level in resistant cells since resistance was irreversible and maintained also upon several months (and therefore cell duplications) of vandetanib deprivation.

In conclusion, our data demonstrate that vandetanib-resistant cells were sensitive to BI-D1870 inhibitor, thereby suggesting the use of p90RSK inhibitors in combination with RET TKIs as a possible strategy to overcome resistance and possibly prevent resistance in MTC cells. This study also suggests a number of possible read-outs, including p90RSK, BAD, YB1, S6 and p27 phosphorylation levels, to verify whether the mechanism identified *in vitro* in TT cell line is also involved in clinical samples in MTC patients who develop resistance to RET TKI treatment.

6.0 CONCLUSIONS

In conclusion, here we show that MTC cells develop *in vitro* irreversible resistance to chronic RET TKI treatment. Resistant cells featured a more agressive phenotype with respect to parental cells. We excluded that genetic changes in RET contributed to resistance. Instead, resistant cells featured hyper-activation of p90RSK, a kinase of the MAPK signaling pathway, and a phosphorylation protein signature typical of p90RSK hyper-activation. Finally resistant cells are sensitive to p90RSK blockade suggesting that p90RSK targeting may represent a strategy to overcome resistance to RET TKIs.

7.0 ACKNOWLEDGMENTS

All my work has been conducted at the dipartimento di Medicina Molecolare e Biotecnologie Mediche (DMMBM), Università degli studi di Napoli "Federico II''.

I am extremely grateful to Prof. Massimo Santoro for giving me the opportunity to participate in very interesting projects in his lab, for always being helpful and supportive.

I wish to express my thanks to Prof. Giancarlo Vecchio who every day continues to devote his life to the research…he is for me a great model to follow!

Above all I want to thank my direct supervisor Dr. Valentina De Falco. I'm grateful to her for teaching me everything I know about good-bench-work practice and for her meticulous and loving guidance. Her passion and enthusiasm that have been for me a fundamental example in every satisfying and disappointing day!

I am thankful to our collaborators: Prof. Francesca Carlomagno and Dr. Donatella Vitagliano for their previous work with vandetanib (ZD6474); Dr. Paolo Salerno for his contribution in DNA sequencing; and Prof. Sergio Cocozza for his support in data analysis. I finally want to thank Astra Zeneca Pharmaceuticals (Macclesfield, United Kingdom) for providing us vandetanib.

I wish to express my gratitude to Salvatore, Massimo and Antonella for animal care.

My whole hearted thanks go to all my Present and former colleagues Mariolina, Annamaria, Paolo, Gennaro, Simona, Roberto and Valentina, for their kind co-operation and instructive scientific discussions.

Among my collegues, in particular I feel the necessity to thank Francesca, Alessia, Chiara and Fede…not just my lab-angels but friends of every day! In difficult moment they have let me feel not so far from home!!!

My special thanks are for my friends Mari, Claudia and Ale! In particular I need to express my gratitude to Annetta and Laura…for their presence, great support and for believing in me even when I did not anymore. I want to apologize for my absence and for my silence that only them can understand and accept!!!

Finally, but first of all, I want to thank my family… for patience and comprehension! I thank Raffaele and Marco to make me feel with a single loving glance, the perfect sister! Claudia and Cori to be the bigger sisters I

never had! I thank my little Marta for her adult sensibility, unconditionally love and for all the comforting cuddles!!! Then I thank the most important people of my very short life, my parents… examples of honesty, determination and kindness. I thank them for having always been close to me, despite the distance and the difficulty in communicating with me. To them who are the perfect idols to imitate, I dedicate my work!
If fate had given me the chance to choose my family… I would choose always and only you!!!

8.0 REFERENCES

- Agrawal N, Jiao Y, Sausen M, Leary R, Bettegowda C, Roberts NJ, Bhan S, Ho AS, Khan Z, Bishop J, Westra WH, Wood LD, Hruban RH, Tufano RP, Robinson B, Dralle H, Toledo SP, Toledo RA, Morris LG, Ghossein RA, Fagin JA, Chan TA, Velculescu VE, Vogelstein B, Kinzler KW, Papadopoulos N, Nelkin BD, Ball DW. Exomic sequencing of medullary thyroid cancer reveals dominant and mutually exclusive oncogenic mutations in RET and RAS. J Clin Endocrinol Metab. 2013 Feb;98(2):E364-9.
- Anjum R, Blenis J. The RSK family of kinases: emerging roles in cellular signalling. Nat Rev Mol Cell Biol 2008;9(10):747-58.
- Aronchik I, Appleton BA, Basham SE, Crawford K, Del Rosario M, Doyle LV, Estacio WF, Lan J, Lindvall MK, Luu CA, Ornelas E, Venetsanakos E, Shafer CM, Jefferson AB. Novel potent and selective inhibitors of p90 ribosomal S6 kinase reveal the heterogeneity of RSK function in MAPK-driven cancers. Mol Cancer Res. 2014 May;12(5):803-12.
- Ballerini P, Struski S, Cresson C, Prade N, Toujani S, Deswarte C, et al. RET fusion genes are associated with chronic myelomonocytic leukemia and enhance monocytic differentiation. Leukemia 2012;26:2384-9.
- Baselga J. Targeting tyrosine kinases in cancer: the second wave. Science 2006;312:1175–1178.
- Bender C, Ullrich A. PRKX, TTBK2 and RSK4 expression causes Sunitinib resistance in kidney carcinoma- and melanoma-cell lines. Int J Cancer. 2012 Jul 15;131(2):E45-55.
- Bentzien F, Zuzow M, Heald N, Gibson A, Shi Y, Goon L, Yu P, Engst S, Zhang W, Huang D, Zhao L, Vysotskaia V, Chu F, Bautista R, Cancilla B, Lamb P, Joly AH, Yakes FM. In vitro and in vivo activity of cabozantinib (XL184), an inhibitor of RET, MET, and VEGFR2, in a model of medullary thyroid cancer. Thyroid. 2013 Dec;23(12):1569-77.
- Berger CL, de Bustros A, Roos BA, Leong SS, Mendelsohn G, Gesell MS, Baylin SB. Human medullary thyroid carcinoma in culture provides a model relating growth dynamics, endocrine cell differentiation, and tumor progression. J Clin Endocrinol Metab. 1984 Aug;59(2):338-43.
- Bianco R, Rosa R, Damiano V, Daniele G, Gelardi T, Garofalo S, Tarallo V, De Falco S, Melisi D, Benelli R, Albini A, Ryan A, Ciardiello F & Tortora G. Vascular endothelial growth factor receptor-1 contributes to resistance to anti-epidermal growth factor receptor drugs in human cancer cells. Clinical Cancer Research 2008;14:5069–5080.

- Bonni A, Brunet A, West AE, Datta SR, Takasu MA, Greenberg ME. Cell survival promoted by the Ras-MAPK signaling pathway by transcription-dependent and-independent mechanisms. Science. 1999 Nov 12;286(5443):1358-62.
- Bossi D, Carlomagno F, Pallavicini I, Pruneri G, Trubia M, Raviele PR, Marinelli A, Anaganti S, Cox MC, Viale G, Santoro M, Di Fiore PP, Minucci S. Functional characterization of a novel FGFR1OP-RET rearrangement in hematopoietic malignancies. Mol Oncol 2014;8(2):221-31.
- Cancer Genome Atlas Research Network. Integrated genomic characterization of papillary thyroid carcinoma. Cell 2014;159(3):676-90.
- Carlomagno F, Guida T, Anaganti S, Provitera L, Kjaer S, McDonald NQ, Ryan AJ, Santoro M. Identification of tyrosine 806 as a molecular determinant of RET kinase sensitivity to ZD6474. Endocr Relat Cancer. 2009 Mar;16(1):233-41.
- Carlomagno F, Salvatore D, Santoro M, de Franciscis V, Quadro L, Panariello L, Colantuoni V, Fusco A. Point mutation of the RET proto-oncogene in the TT human medullary thyroid carcinoma cell line. Biochem Biophys Res Commun. 1995 Feb 27;207(3):1022-8.
- Carlomagno F, Vitagliano D, Guida T, Ciardiello F, Tortora G, Vecchio G, Ryan AJ, Fontanini G, Fusco A, Santoro M. ZD6474, an orally available inhibitor of KDR tyrosine kinase activity, efficiently blocks oncogenic RET kinases. Cancer Res. 2002 Dec 15;62(24):7284-90.
- Carlomagno F., Guida T., Anaganti S., et al. Disease associated mutations at valine 804 in the RET receptor tyrosine kinase confer resistance to selective kinase inhibitors. Oncogene 2004;23: 6056-63.
- Castro P, Rebocho AP, Soares RJ, Magalhaes J, Roque L, Trovisco V, Viera de castro I, Cardoso-de-Oliveira M, Fonseca E, Soares P, Sobrinho-Simoes M. PAX8-PPARgamma rearrangement is frequently detected in the follicular variant of papillary thyroid carcinoma. J Clin Endocrinol Metab 2006;91(1):213-20.
- Chapman PB, Solit DB, Rosen N. Combination of RAF and MEK inhibition for the treatment of BRAF-mutated melanoma: feedback is not encouraged. Cancer Cell. 2014 Nov 10;26(5):603-4.
- Chong H, Vikis HG, Guan KL. Mechanism of regulating the RAF kinase family. Cell signaling 2003;15(5):463–469.
- Ciampi R, Mian C, Fugazzola L, et al. Evidence of a low prevalence of RAS mutations in a large medullary thyroid cancer series. Thyroid 2013;23:50–57.
- Ciampi R, Romei C, Cosci B, Vivaldi A, Bottici V, Renzini G, Ugolini C, Tacito A, Basolo F, Pinchera A, Elisei R. Chromosome 10 and RET gene copy number alterations in hereditary and sporadic Medullary Thyroid Carcinoma. Molecular and Cellular Endocrinology 2012;348(1):176–182.

- Ciardiello F, Caputo R, Damiano V, Caputo R, Troiani T, Vitagliano D, Carlomagno F, Veneziani BM, Fontanini G, Bianco AR & Tortora G. Antitumor effects of ZD6474, a small molecule vascular endothelial growth factor receptor tyrosine kinase inhibitor, with additional activity against epidermal growth factor receptor tyrosine kinase. Clinical Cancer Research 2003;9:1546–1556.
- Cohen MS, Hadjivassiliou H, Taunton J. A clickable inhibitor reveals context-dependent autoactivation of p90 RSK. Nat Chem Biol. 2007 Mar;3(3):156-60.
- Cools J, Mentens N, Furet P, Fabbro D, Clark JJ, Griffin JD, Marynen P, Gilliland DG. Prediction of resistance to small molecule FLT3 inhibitors: implications for molecularly targeted therapy of acute leukemia. Cancer Res. 2004 Sep 15;64(18):6385-9.
- Cortes J, Goldman JM, Hughes T. Current issues in chronic myeloid leukemia: monitoring, resistance, and functional cure. J Natl Compr Canc Netw. 2012 Oct 1;10
- Cortes JE, Kim DW, Pinilla-Ibarz J, le Coutre P, Paquette R, Chuah C, Nicolini FE, Apperley JF, Khoury HJ, Talpaz M, DiPersio J, DeAngelo DJ, Abruzzese E, Rea D, Baccarani M, Müller MC, Gambacorti-Passerini C, Wong S, Lustgarten S, Rivera VM, Clackson T, Turner CD, Haluska FG, Guilhot F, Deininger MW, Hochhaus A, Hughes T, Goldman JM, Shah NP, Kantarjian H; PACE Investigators. A phase 2 trial of ponatinib in Philadelphia chromosome-positive leukemias. N Engl J Med. 2013 Nov 7;369(19):1783-96.
- Cranston AN, Carniti C, Oakhill K, Radzio-Andzelm E, Stone EA, McCallion AS, Hodgson S, Clarke S, Mondellini P, Leyland J, Pierotti MA, Whittaker J, Taylor SS, Bongarzone I, Ponder BA. RET is constitutively activated by novel tandem mutations that alter the active site resulting in multiple endocrine neoplasia type 2B. Cancer Res 2006;66(20):10179-87.
- Dalby KN, Morrice N, Caudwell FB, Avruch J, Cohen P. Identification of regulatory phosphorylation sites in mitogen-activated protein kinase (MAPK)-activated protein kinase-1a/p90rsk that are inducible by MAPK. J BiolChem 1998;273(3):1496-505.
- de Biase D, Visani M, Pession A, Tallini G. Molecular diagnosis of carcinomas of the thyroid gland. Front Biosci (Elite Ed). 2014 Jan 1;6:1-14.
- De Falco V, Buonocore P, Muthu M, Torregrossa L, Basolo F, Billaud M, Gozgit JM, Carlomagno F, Santoro M. Ponatinib (AP24534) is a novel potent inhibitor of oncogenic RET mutants associated with thyroid cancer. J Clin Endocrinol Metab. 2013 May;98(5):E811-9.
- de Groot JW, Links TP, Plukker JT, Lips CJ, Hofstra RM. RET as a diagnostic and therapeutic target in sporadic and hereditary endocrine tumors. Endocr Rev 2006;27(5):535-60.

- DeLellis RA, Williams ED. Thyroid and parathyroid tumors. In Tumours of Endocrine Organs, World Health Organization Classification of Tumors. In: DeLellis RA, Lloyd RV, Heitz PU and Eng C editors. 2004 (eds):51-56.
- Dobson ME, Diallo-Krou E, Grachtchouk V, Yu J, Colby LA, Wilkinson JE, Giordano TJ, Koenig RJ. Pioglitazone induces a proadipogenic antitumor response in mice with PAX8-PPARgamma fusion protein thyroid carcinoma. Endocrinology. 2011 Nov;152(11):4455-65.
- Drilon A, Wang L, Hasanovic A, Suehara Y, Lipson D, Stephens P, Ross J, Miller V, Ginsberg M, Zakowski MF, Kris MG, Ladanyi M, Rizvi N. Response to Cabozantinib in patients with RET fusion-positive lung adenocarcinomas. Cancer Discov 2013;3(6):630-5.
- Elisei R, Agate L, Viola D, Matrone A, Biagini A, Molinaro E. How to manage patients with differentiated thyroid cancer and a rising serum thyroglobulin level. Endocrinol Metab Clin North Am. 2014 Jun;43(2):331-44.
- Elisei R, Cosci B, Romei C, Bottici V, Renzini G, Molinaro E, Agate L, Vivaldi A, Faviana P, Basolo F, Miccoli P, Berti P, Pacini F, Pinchera A. Prognostic significance of somatic RET oncogene mutations in sporadic medullary thyroid cancer: a 10-year follow-up study. Journal of Clinical Endocrinology & Metabolism 2008;93(3):682–687.
- Elisei R, Schlumberger MJ, Müller SP, Schöffski P, Brose MS, Shah MH, Licitra L, Jarzab B, Medvedev V, Kreissl MC, Niederle B, Cohen EE, Wirth LJ, Ali H, Hessel C, Yaron Y, Ball D, Nelkin B, Sherman SI. Cabozantinib in progressive medullary thyroid cancer. J Clin Oncol. 2013 Oct 10;31(29):3639-46.
- Erikson E, Maller JL. A protein kinase from Xenopus eggs specific for ribosomal protein S6. Proc Natl Acad Sci U S A.1985;82(3):742-6.
- Ferrari S, Bandi HR, Hofsteenge J, Bussian BM, Thomas G. Mitogen-activated 70K S6 kinase. Identification of in vitro 40 S ribosomal S6 phosphorylation sites. J Biol Chem. 1991 Nov 25;266(33):22770-5.
- Fletcher JA, Rubin BP. KIT mutations in GIST. Curr Opin Genet Dev 2007; 17**:** 3-7.
- Frödin M, Gammeltoft S. Role and regulation of 90 kDa ribosomal S6 kinase (RSK) in signal transduction. Mol Cell Endocrinol 1999;151(1-2):65-77.
- Gainor JF, Shaw AT. The new kid on the block: RET in lung cancer. Cancer Discov. 2013 Jun;3(6):604-6.
- Garcia-Rostan G, Camp RL, Herrero A, Carcangiu ML, Rimm DL, Tallini G. Beta-catenin dysregulation in thyroid neoplasms: down-regulation, aberrant nuclear expression, and CTNNB1 exon 3 mutations are markers for aggressive tumor phenotypes and poor prognosis. Am J Pathol. 2001 Mar;158(3):987-96.

- García-Rostán G, Costa AM, Pereira-Castro I, Salvatore G, Hernandez R, Hermsem MJ, Herrero A, Fusco A, Cameselle-Teijeiro J, Santoro M. Mutation of the PIK3CA gene in anaplastic thyroid cancer. Cancer Res. 2005 Nov 15;65(22):10199-207.
- Garcia-Rostan G, Zhao H, Camp RL, Pollan M, Herrero A, Pardo J, Wu R, Carcangiu ML, Costa J, Tallini G. ras mutations are associated with aggressive tumor phenotypes and poor prognosis in thyroid cancer. J Clin Oncol. 2003 Sep 1;21(17):3226-35.
- Gautschi O, Zander T, Keller FA, Strobel K, Hirschmann A, Aebi S, Diebold J. A patient with lung adenocarcinoma and RET fusion treated with vandetanib. J Thorac Oncol. 2013 May;8(5):e43-4.
- Gorre ME, Mohammed M, Ellwood K, Hsu N, Paquette R, Rao PN, Sawyers CL. Clinical resistance to STI-571 cancer therapy caused by BCR-ABL gene mutation or amplification. Science. 2001 Aug 3;293(5531):876-80.
- Greco A, Miranda C, Pierotti MA. Rearrangements of NTRK1 gene in papillary thyroid carcinoma. Mol Cell Endocrinol. 2010;321(1):44-9.
- Grubbs EG, Ng PK, Bui J, Busaidy NL, Chen K, Lee JE, Lu X, Lu H, Meric-Bernstam F, Mills GB, Palmer G, Perrier ND, Scott KL, Shaw KR, Waguespack SG, Williams MD, Yelensky R, Cote GJ. RET Fusion as a Novel Driver of Medullary Thyroid Carcinoma. J Clin Endocrinol Metab 2015;100(3):788-93.
- Grüllich C. Cabozantinib: a MET, RET, and VEGFR2 tyrosine kinase inhibitor. Recent Results Cancer Res. 2014;201:207-14.
- Herbst RS, Heymach JV, O'Reilly MS, Onn A and Ryan AJ. Vandetanib (ZD6474): an orally available receptor tyrosine kinase inhibitor that selectively targets pathways critical for tumor growth and angiogenesis. Expert Opinion on Investigational Drugs 2007;16:239–249.
- Huang S.C., Torres-Cruz J., Pack S.D., Kock C.A., Vortmeyer A.O., Mannan P., Lubensky I.A., Gagel R.F., Zhuang Z. Amplification and overexpression of mutant RET in multiple endocrine neoplasia type 2-associated medullary thyroid carcinoma. Journal of Clinical Endocrinology & Metabolism. 2003 88(1):459-463.
- Johannessen CM, Boehm JS, Kim SY, Thomas SR, Wardwell L, Johnson LA, Emery CM, Stransky N, Cogdill AP, Barretina J, Caponigro G, Hieronymus H, Murray RR, Salehi-Ashtiani K, Hill DE, Vidal M, Zhao JJ, Yang X, Alkan O, Kim S, Harris JL, Wilson CJ, Myer VE, Finan PM, Root DE, Roberts TM, Golub T, Flaherty KT, Dummer R, Weber BL, Sellers WR, Schlegel R, Wargo JA, Hahn WC, Garraway LA. COT drives resistance to RAF inhibition through MAP kinase pathway reactivation. Nature. 2010 Dec 16;468(7326):968-72.
- Johanson V, Ahlman H, Bernhardt P, Jansson S, Kölby L, Persson F, Stenman G, Swärd C, Wängberg B, Stridsberg M & Nilsson O. A transplantable human medullary thyroid carcinoma as a model for RET

tyrosine kinase-driven tumorigenesis. Endocrine Related Cancer 2007;14:433–444.

- Jurchott K, Bergmann S, Stein U, Walther W, Janz M, Manni I, Piaggio G, Fietze E, Dietel M, Royer HD. YB-1 as a cell cycle-regulated transcription factor facilitating cyclin A and cyclin B1 gene expression. J Biol Chem. 2003 Jul 25;278(30):27988-96.
- Knight ZA, Lin H & Shokat KM. Targeting the cancer kinome through polypharmacology. Nature Reviews Cancer 2010;10:130–137.
- Knowles PP, Murray-Rust J, Kjaer S, Scott RP, Hanrahan S, Santoro M, Ibáñez CF, McDonald NQ. Structure and chemical inhibition of the RET tyrosine kinase domain. J Biol Chem. 2006 Nov 3;281(44):33577-87.
- Kobayashi S, Boggon TJ, Dayaram T, Janne PA, Kocher O, Meyerson M, et al. (2005). EGFR mutation and resistance of non-small-cell lung cancer to gefitinib. N Engl J Med 352**:** 786-792.
- Kohno T, Ichikawa H, Totoki Y, Yasuda K, Hiramoto M, Nammo T, Sakamoto H, Tsuta K, Furuta K, Shimada Y, Iwakawa R, Ogiwara H, Oike T, Enari M,Schetter AJ, Okayama H, Haugen A, Skaug V, Chiku S, Yamanaka I, Arai Y, Watanabe S, Sekine I, Ogawa S, Harris CC, Tsuda H, Yoshida T, Yokota J, Shibata T. KIF5B-RET fusions in lung adenocarcinoma. Nat Med 2012;18(3):375-7
- Kohno T, Tsuta K, Tsuchihara K, Nakaoku T, Yoh K, Goto K. RET fusion gene: translation to personalized lung cancer therapy. Cancer Sci. 2013 Nov;104(11):1396-400.
- Kondo T, Ezzat S, Asa SL. Pathogenetic mechanisms in thyroid follicular-cell neoplasia. Nat Rev Cancer 2006; 6:292-306.
- Krause DS, Van Etten RA. Tyrosine Kinases as Targets for Cancer Therapy. New England Journal of Medicine 2005;353:172–187.
- Kroll TG, Sarraf P, Pecciarini L, Chen CJ, Mueller E, Spiegelman BM, Fletcher JA. PAX8-PPARgamma1 fusion oncogene in human thyroid carcinoma. Science 2000;289:1357-60.
- Larrea MD, Hong F, Wander SA, da Silva TG, Helfman D, Lannigan D, Smith JA, Slingerland JM. RSK1 drives p27Kip1 phosphorylation at T198 to promote RhoA inhibition and increase cell motility. Proc Natl Acad Sci U S A. 2009 Jun 9;106(23):9268-73.
- Lasham A, Lindridge E, Rudert F, Onrust R, Watson J. Regulation of the human fas promoter by YB-1, Puralpha and AP-1 transcription factors. Gene. 2000 Jul 11;252(1-2):1-13.
- Li F, Feng Y, Fang R, Fang Z, Xia J, Han X, et al. Identification of RET gene fusion by exon array analyses in "pan-negative" lung cancer from never smokers. Cell Res 2012;22:928-31.
- Lipson D, Capelletti M, Yelensky R, Otto G, Parker A, Jarosz M, et al. Identification of new ALK and RET gene fusions from colorectal and lung cancer biopsies. Nat Med 2012;18:382-4.

- Lito P, Pratilas CA, Joseph EW, Tadi M, Halilovic E, Zubrowski M, Huang A, Wong WL, Callahan MK, Merghoub T, Wolchok JD, de Stanchina E, Chandarlapaty S, Poulikakos PI, Fagin JA, Rosen N. Relief of profound feedback inhibition of mitogenic signaling by RAF inhibitors attenuates their activity in BRAFV600E melanomas. Cancer Cell. 2012 Nov 13;22(5):668-82.
- Lito P, Rosen N, Solit DB. Tumor adaptation and resistance to RAF inhibitors. Nat Med. 2013 Nov;19(11):1401-9.
- Lito P, Saborowski A, Yue J, Solomon M, Joseph E, Gadal S, Saborowski M, Kastenhuber E, Fellmann C, Ohara K, Morikami K, Miura T, Lukacs C, Ishii N, Lowe S, Rosen N. Disruption of CRAF-mediated MEK activation is required for effective MEK inhibition in KRAS mutant tumors. Cancer Cell. 2014 May 12;25(5):697-710.
- Liu Y, Gray NS. Rational design of inhibitors that bind to inactive kinase conformations. Nat Chem Biol 2006;2(7):358-64.
- Lloyd RV, Erickson LA, Jin L, Kulig E, Qian X, Cheville JC, Scheithauer BW. p27kip1: a multifunctional cyclin-dependent kinase inhibitor with prognostic significance in human cancers. Am J Pathol. 1999 Feb;154(2):313-23.
- Luo Y, Tsuchiya KD, Il Park D, Fausel R, Kanngurn S, Welcsh P, Dzieciatkowski S, Wang J, Grady WM. RET is a potential tumor suppressor gene in colorectal cancer. Oncogene 2013;32(16):2037-47.
- Manning G, Whyte DB, Martinez R, Hunter T, Sudarsanam S. The protein kinase complement of the human genome. Science 2002;298(5600):1912-34.
- Mathew CG, Smith BA, Thorpe K, Wong Z, Royle NJ, Jeffreys AJ, Ponder BA. Deletion of genes on chromosome 1 in endocrine neoplasia. Nature. 1987 Aug 6-12;328(6130):524-6.
- Mendoza MC, Er EE, Blenis J. The Ras-ERK and PI3K-mTOR pathways: cross-talk and compensation. Trends Biochem Sci 2011;36**:** 320-328.
- Meng X, Lindahl M, Hyvönen ME, Parvinen M, de Rooij DG, Hess MW, Raatikainen-Ahokas A, Sainio K, Rauvala H, Lakso M, Pichel JG, Westphal H, Saarma M, Sariola H. Regulation of cell fate decision of undifferentiated spermatogonia by GDNF. Science. 2000 Feb 25;287(5457):1489-93.
- Menko FH, van der Luijt RB, de Valk IA, Toorians AW, Sepers JM, van Diest PJ, et al. Atypical MEN type 2B associated with two germline RETmutations on the same allele not involving codon 918. J Clin Endocrinol Metab 2002;87(1):393-7.
- Miyagi E, Braga-Basaria M, Hardy E, Vasko V, Burman KD, Jhiang S, Saji M, Ringel MD. Chronic expression of RET/PTC 3 enhances basal and insulin-stimulated PI3 kinase/AKT signaling and increases IRS-2 expression in FRTL-5 thyroid cells. Mol Carcinog 2004;41(2):98-107.

- Miyauchi A, Futami H, Hai N, Yokozawa T, Kuma K, Aoki N, et al. Two germline missense mutations at codons 804 and 806 of the RET proto oncogene in the same allele in a patient with multiple endocrine neoplasia type 2B without codon 918 mutation. Jpn J Cancer Res 1999;90(1):1-5.
- Mologni L, Redaelli S, Morandi A, Plaza-Menacho I, Gambacorti-Passerini C. Ponatinib is a potent inhibitor of wild-type and drug-resistant gatekeeper mutant RET kinase. Mol Cell Endocrinol. 2013 Sep 5;377(1-2):1-6.
- Moura MM, Cavaco BM, Pinto AE, Leite V. High prevalence of RAS mutations in RET-negative sporadic medullary thyroid carcinomas. J Clin Endocrinol Metab. 2011;96(5):E863-8.
- Mueller KL, Yang ZQ, Haddad R, Ethier SP, Boerner JL. EGFR/Met association regulates EGFR TKI resistance in breast cancer. J Mol Signal. 2010 Jul 12;5:8.
- Mulligan LM. RET revisited: expanding the oncogenic portfolio. Nat Rev Cancer 2014;14(3):173-86.
- Nazarian R, Shi H, Wang Q, Kong X, Koya RC, Lee H, Chen Z, Lee MK, Attar N, Sazegar H, Chodon T, Nelson SF, McArthur G, Sosman JA, Ribas A, Lo RS. Melanomas acquire resistance to B-RAF(V600E) inhibition by RTK or N-RAS upregulation. Nature. 2010 Dec 16;468(7326):973-7.
- Nikiforov YE, Nikiforova MN. Molecular genetics and diagnosis of thyroid cancer. Nature Reviews Endocrinology 2011;7(10):569–580
- Nikiforova MN, Stringer JR, Blough R, Medvedovic M, Fagin JA, Nikiforov YE. Proximity of chromosomal loci that participate in radiation-induced rearrangements in human cells. Science 2000;290(5489):138-41.
- Pachnis V, Mankoo B, Costantini F. Expression of the c-ret proto-oncogene during mouse embryogenesis. Development. 1993 Dec;119(4):1005-17.
- Pao W, Miller VA, Politi KA, Riely GJ, Somwar R, Zakowski MF, Kris MG, Varmus H. Acquired resistance of lung adenocarcinomas to gefitinib or erlotinib is associated with a second mutation in the EGFR kinase domain. PLoS Med. 2005 Mar;2(3):e73.
- Pearce LR, Komander D, Alessi DR. The nuts and bolts of AGC protein kinases. Nat Rev Mol Cell Biol 2010;11(1):9-22.
- Peterson RT, Schreiber SL. Translation control: connecting mitogens and the ribosome. Curr Biol. 1998 Mar 26;8(7):R248-50.
- Pettazzoni P, Viale A, Shah P, Carugo A, Ying H, Wang H, Genovese G, Seth S, Minelli R, Green T, Huang-Hobbs E, Corti D, Sanchez N, Nezi L, Marchesini M, Kapoor A, Yao W, Francesco ME, Petrocchi A, Deem AK, Scott K, Colla S, Mills GB, Fleming JB, Heffernan TP, Jones P, Toniatti C, DePinho RA, Draetta GF. Genetic Events That Limit the Efficacy of MEK and RTK Inhibitor Therapies in a Mouse

Model of KRAS-Driven Pancreatic Cancer. Cancer Res. 2015 Mar 15;75(6):1091-101.

- Plaza-Menacho I, Barnouin K, Goodman K, Martínez-Torres RJ, Borg A, Murray-Rust J, Mouilleron S, Knowles P, McDonald NQ. Oncogenic RET kinase domain mutations perturb the autophosphorylation trajectory by enhancing substrate presentation in trans. Mol Cell. 2014 Mar 6;53(5):738-51.
- Plaza-Menacho I, Morandi A, Robertson D, Pancholi S, Drury S, Dowsett M, Martin LA, Isacke CM. Targeting the receptor tyrosine kinase RET sensitizes breast cancer cells to tamoxifen treatment and reveals a role for RET in endocrine resistance. Oncogene 2010;29(33):4648-57.
- Radich JP. Monitoring of TKI-Resistant Chronic Myeloid Leukemia. Clin Adv Hematol Oncol. 2014 Jul;12(7 Suppl 13):3-6.
- Raman M, Chen W and Cobb MH. Differential regulation and properties of MAPKs. Oncogene 2007;26:3100–3112.
- Ricarte-Filho JC, Ryder M, Chitale DA, Rivera M, Heguy A, Ladanyi M, Janakiraman M, Solit D, Knauf JA, Tuttle RM, Ghossein RA, Fagin JA. Mutational profile of advanced primary and metastatic radioactive iodine-refractory thyroid cancers reveals distinct pathogenetic roles for BRAF, PIK3CA, and AKT1. Cancer Res. 2009 Jun 1;69(11):4885-93.
- Romei C, Cosci B, Renzini G, Bottici V, Molinaro E, Agate L, Passannanti P, Viola D, Biagini A, Basolo F, Ugolini C, Materazzi G, Pinchera A, Vitti P, Elisei R. RET genetic screening of sporadic medullary thyroid cancer (MTC) allows the preclinical diagnosis of unsuspected gene carriers and the identification of a relevant percentage of hidden familial MTC (FMTC). Clinical Endocrinology (Oxf) 2011;74(2):241–247.
- Romeo Y, Zhang X, Roux PP. Regulation and function of the RSK family of protein kinases. Biochem J.2012;441(2):553-69.
- Roumiantsev S, Shah NP, Gorre ME, Nicoll J, Brasher BB, Sawyers CL, Van Etten RA. Clinical resistance to the kinase inhibitor STI-571 in chronic myeloid leukemia by mutation of Tyr-253 in the Abl kinase domain P-loop. Proc Natl Acad Sci U S A. 2002 Aug 6;99(16):10700-5.
- Santisteban P. Development of the hypothalamic-pituitary-thyroid axis. In: Braverman LE and Cooper D. Werner & Ingbar's The Thyroid: A Fundamental and Clinical Text. 10th ed. Philadelphia: Lippincott Williams & Wilkins; 2012. p. 1-31.
- Santoro M, Carlomagno F, Romano A, Bottaro DP, Dathan NA, Grieco M, Fusco A, Vecchio G, Matoskova B, Kraus MH, et al. Activation of RET as a dominant transforming gene by germline mutations of MEN2A and MEN2B. Science. 1995 Jan 20;267(5196):381-3. PubMed PMID: 7824936.
- Santoro M, Carlomagno F. Central role of RET in thyroid cancer. Cold Spring Harb Perspect Biol. 2013 Dec 1;5(12):a009233.

- Santoro M, Carlomagno F. Drug insight: Small-molecule inhibitors of protein kinases in the treatment of thyroid cancer. Nature Clinical Practice Endocrinology & Metabolism 2006;2(1):42–52.
- Santoro M, Melillo RM, Fusco A. RET/PTC activation in papillary thyroid carcinoma: European Journal of Endocrinology Prize Lecture. Eur J Endocrinol. 2006;155:645–653.
- Sapkota GP, Cummings L, Newell FS, Armstrong C, Bain J, Frodin M, Grauert M, Hoffmann M, Schnapp G, Steegmaier M, Cohen P, Alessi DR. BI-D1870 is a specific inhibitor of the p90 RSK (ribosomal S6 kinase) isoforms in vitro and in vivo. Biochem J 2007;401(1):29-38.
- Sawai H, Okada Y, Kazanjian K, Kim J, Hasan S, Hines OJ, et al. The G691S RET polymorphism increases glial cell line-derived neurotrophic factor-induced pancreatic cancer cell invasion by amplifying mitogen-activated protein kinase signaling. Cancer Res 2005; 65:11536–11544.
- Schlumberger M., Carlomagno F., Baudin E., Bidart J. M., Santoro M. New therapeutic approaches to treat medullary thyroid carcinoma. Nature Clinical Practice Endocrinology and Metabolism 2008; 4: 22-32.
- Schuchardt A, D'Agati V, Larsson-Blomberg L, Costantini F, Pachnis V. Defects in the kidney and enteric nervous system of mice lacking the tyrosine kinase receptor Ret. Nature. 1994 Jan 27;367(6461):380-3.
- Serra V, Eichhorn PJ, García-García C, Ibrahim YH, Prudkin L, Sánchez G, Rodríguez O, Antón P, Parra JL, Marlow S, Scaltriti M, Pérez-Garcia J, Prat A, Arribas J, Hahn WC, Kim SY, Baselga J. RSK3/4 mediate resistance to PI3K pathway inhibitors in breast cancer. J Clin Invest. 2013 Jun;123(6):2551-63.
- Sierra JR, Cepero V, Giordano S. Molecular mechanisms of acquired resi stance to tyrosine kinase targeted therapy. Mol Cancer. 2010 Apr 12;9:75.
- Smallridge RC, Copland JA. Anaplastic thyroid carcinoma: pathogenesis and emerging therapies. Clinical Oncology (R Coll Radiol) 2010;22(6):486–497.
- Solit DB, Rosen N. Towards a unified model of RAF inhibitor resistance. Cancer Discov. 2014 Jan;4(1):27-30.
- Song M. Progress in Discovery of KIF5B-RET Kinase Inhibitors for the Treatment of Non-Small-Cell Lung Cancer. J Med Chem 2015 Feb 4. [Epub ahead of print]
- Sutherland BW, Kucab J, Wu J, Lee C, Cheang MC, Yorida E, Turbin D, Dedhar S, Nelson C, Pollak M, Leighton Grimes H, Miller K, Badve S, Huntsman D, Blake-Gilks C, Chen M, Pallen CJ, Dunn SE. Akt phosphorylates the Y-box binding protein 1 at Ser102 located in the cold shock domain and affects the anchorage-independent growth of breast cancer cells. Oncogene. 2005 Jun 16;24(26):4281-92.

- Takahashi M, Ritz J, Cooper GM. Activation of a novel human transforming gene, ret, by DNA rearrangement. Cell. 1985 Sep;42(2):581-8.
- Tamburrino A, Molinolo AA, Salerno P, Chernock RD, Raffeld M, Xi L, Gutkind JS, Moley JF, Wells SA Jr, Santoro M. Activation of the mTOR pathway in primary medullary thyroid carcinoma and lymph node metastases. Clin Cancer Res. 2012 Jul 1;18(13):3532-40.
- Tan Y, Ruan H, Demeter MR, Comb MJ. p90(RSK) blocks bad-mediated cell death via a protein kinase C-dependent pathway. J Biol Chem. 1999 Dec 3;274(49):34859-67.
- Thornton K, Kim G, Maher VE, Chattopadhyay S, Tang S, Moon YJ, Song P, Marathe A, Balakrishnan S, Zhu H, Garnett C, Liu Q, Booth B, Gehrke B, Dorsam R, Verbois L, Ghosh D, Wilson W, Duan J, Sarker H, Miksinski SP, Skarupa L, Ibrahim A, Justice R, Murgo A, Pazdur R. Vandetanib for the treatment of symptomatic or progressive medullary thyroid cancer in patients with unresectable locally advanced or metastatic disease: U.S. Food and Drug Administration drug approval summary. Clin Cancer Res. 2012 Jul 15;18(14):3722-30.
- Todaro M, Iovino F, Eterno V, Cammareri P, Gambara G, Espina V, Gulotta G, Dieli F, Giordano S, De Maria R, Stassi G. Tumorigenic and metastatic activity of human thyroid cancer stem cells. Cancer Res. 2010 Nov 1;70(21):8874-85.
- Vasconcelos FC, Silva KL, Souza PS, Silva LF, Moellmann-Coelho A, Klumb CE, Maia RC. Variation of MDR proteins expression and activity levels according to clinical status and evolution of CML patients. Cytometry B Clin Cytom. 2011 May;80(3):158-66.
- Vidal M, Wells S, Ryan A & Cagan R. ZD6474 suppresses oncogenic RET isoforms in a Drosophila model for type 2 multiple endocrine neoplasia syndromes and papillary thyroid carcinoma. Cancer Research 2005;65:3538–3541.
- Viola D, Cappagli V, Elisei R. Cabozantinib (XL184) for the treatment of locally advanced or metastatic progressive medullary thyroid cancer. Future Oncol 2013;9(8):1083-92.
- Volante M, Papotti M. Poorly differentiated thyroid carcinoma: 5 years after the 2004 WHO classification of endocrine tumours. Endocrine Pathology 2010;21(1):1–6.
- Wang R, Hu H, Pan Y, Li Y, Ye T, Li C, Luo X, Wang L, Li H, Zhang Y, Li F, Lu Y, Lu Q, Xu J, Garfield D, Shen L, Ji H, Pao W, Sun Y, Chen H. RET fusions define a unique molecular and clinicopathologic subtype of non-small-cell lung cancer. J Clin Oncol 2012;30(35):4352-9.
- Wedge SR, Ogilvie DJ, Dukes M, Kendrew J, Chester R, Jackson JA, Boffey SJ, Valentine PJ, Curwen JO, Musgrove HL, Graham GA, Hughes GD, Thomas AP, Stokes ES, Curry B, Richmond GH, Wadsworth PF, Bigley AL & Hennequin LF. ZD6474 inhibits vascular

endothelial growth factor signaling, angiogenesis, and tumor growth following oral administration. Cancer Research 2002;62:4645–4655.
- Weinstein IB, Joe A. Oncogene addiction. Cancer Research 2008;68:3077–80.
- Wells SA Jr, Pacini F, Robinson BG, Santoro M. Multiple endocrine neoplasia type 2 and familial medullary thyroid carcinoma: an update. J Clin Endocrinol Metab. 2013 Aug;98(8):3149-64.
- Wells SA Jr, Robinson BG, Gagel RF, Dralle H, Fagin JA, Santoro M, Baudin E, Elisei R, Jarzab B, Vasselli JR, Read J, Langmuir P, Ryan AJ, Schlumberger MJ. Vandetanib in patients with locally advanced or metastatic medullary thyroid cancer: a randomized, double-blind phase III trial. J Clin Oncol. 2012 Jan 10;30(2):134-41.
- Wells SA Jr, Santoro M. Update: the status of clinical trials with kinase inhibitors in thyroid cancer. J Clin Endocrinol Metab. 2014 May;99(5):1543-55.
- Widmann C, Gibson S, Jarpe MB, and Johnson GL.. Mitogen activated protein kinase: conservation of a three-kinase module from yeast to human. Physiol Rev 1999;79:143–180.
- Wiesner T, He J, Yelensky R, Esteve-Puig R, Botton T, Yeh I, Lipson D, Otto G, Brennan K, Murali R, Garrido M, Miller VA, Ross JS, Berger MF, Sparatta A, Palmedo G, Cerroni L, Busam KJ, Kutzner H, Cronin MT, Stephens PJ, Bastian BC. Kinase fusions are frequent in Spitz tumours and spitzoid melanomas. Nat Commun. 2014;5:3116.
- Williams D. Cancer after nuclear fallout: lessons from the Chernobyl accident. Nat Rev Cancer 2002; 2:543–549
- Williams D. Radiation carcinogenesis: lessons from Chernobyl. Oncogene 2008;27 Suppl 2:S9–S18.
- Xing M. Molecular pathogenesis and mechanisms of thyroid cancer Nat Rev Cancer. 2013;13(3):184–199.
- Yang E, Zha J, Jockel J, Boise LH, Thompson CB, Korsmeyer SJ. Bad, a heterodimeric partner for Bcl-XL and Bcl-2, displaces Bax and promotes cell death. Cell. 1995 Jan 27;80(2):285-91.
- Yano S, Wang W, Li Q, Matsumoto K, Sakurama H, Nakamura T, Ogino H, Kakiuchi S, Hanibuchi M, Nishioka Y, Uehara H, Mitsudomi T, Yatabe Y, Nakamura T, Sone S. Hepatocyte growth factor induces gefitinib resistance of lung adenocarcinoma with epidermal growth factor receptor-activating mutations. Cancer Res. 2008 Nov 15;68(22):9479-87.
- Zaru R, Ronkina N, Gaestel M, Arthur JS, Watts C. The MAPK-activated kinase Rsk controls an acute Toll-like receptor signaling response in dendritic cells and is activated through two distinct pathways. Nat Immunol. 2007 Nov;8(11):1227-35.
- Zha J, Harada H, Yang E, Jockel J, Korsmeyer SJ. Serine phosphorylation of death agonist BAD in response to survival factor

results in binding to 14-3-3 not BCL-X(L). Cell. 1996 Nov 15;87(4):619-28.

- Zhang J, Yang PL, Gray NS. Targeting cancer with small molecule kinase inhibitors. Nat Rev Cancer. 2009 Jan;9(1):28-39.

Attached Manuscript

Valentina De Falco, Preziosa Buonocore, Magesh Muthu, Liborio Torregrossa, Fulvio Basolo, Marc Billaud, Joseph M. Gozgit, Francesca Carlomagno, and Massimo Santoro

Ponatinib (AP24534) is a novel potent Inhibitor of oncogenic RET mutants associated with thyroid cancer

J Clin Endocrinol Metab. 2013 May;98(5):E811-9.

Ponatinib (AP24534) Is a Novel Potent Inhibitor of Oncogenic RET Mutants Associated With Thyroid Cancer

Valentina De Falco, Preziosa Buonocore, Magesh Muthu, Liborio Torregrossa, Fulvio Basolo, Marc Billaud, Joseph M. Gozgit, Francesca Carlomagno, and Massimo Santoro

Istituto di Endocrinologia ed Oncologia Sperimentale del Consiglio Nazionale delle Ricerche, Dipartimento di Medicina Molecolare e Biotecnologie Mediche (V.D.F., P.B., M.M., F.C., M.S.), Università di Napoli Federico II, 80131 Naples, Italy; Dipartimento di Chirurgia (L.T., F.B.), Università di Pisa, Pisa, Italy; Institut Albert Bonniot (M.B.), Centre de Recherche Institut National de la Santé et de la Recherche Médicale/Université Joseph Fourier U823, La Tronche, France; and ARIAD Pharmaceuticals, Inc (J.M.G.), Cambridge, Massachusetts 02139

Context: The *RET* tyrosine kinase encoding gene acts as a dominantly transforming oncogene in thyroid carcinoma and other malignancies. Ponatinib (AP24534) is an oral ATP-competitive tyrosine kinase inhibitor that is in advanced clinical experimentation in leukemia.

Objective: We tested whether ponatinib inhibited RET kinase and oncogenic activity.

Methods: Ponatinib activity was studied by an in vitro RET immunocomplex kinase assay and immunoblotting. The effects of ponatinib on proliferation of human TT, MZ-CRC-1, and TPC-1 thyroid carcinoma cells, which harbor endogenous oncogenic *RET* alleles, and of NIH3T3 fibroblasts transfected with oncogenic *RET* mutants were determined. Ponatinib activity on TT cell xenografted tumors in athymic mice was measured.

Results: Ponatinib inhibited immunopurified RET kinase at the IC_{50} of 25.8 nM (95% confidence interval [CI] = 23.15–28.77 nM). It also inhibited (IC_{50} = 33.9 nM; 95% CI = 26.41–43.58 nM) kinase activity of RET/V804M, a RET mutant displaying resistance to other tyrosine kinase inhibitor. Ponatinib blunted phosphorylation of point-mutant and rearranged RET-derived oncoproteins and inhibited proliferation of *RET*-transformed fibroblasts and *RET* mutant thyroid carcinoma cells. Finally, after 3 weeks of treatment with ponatinib (30 mg/kg/d), the volume of TT cell (medullary thyroid carcinoma) xenografts was reduced from 133 mm^3 to an unmeasurable size (difference = 133 mm^3, 95% CI = −83 to 349 mm^3) ($P < .001$). Ponatinib-treated TT cell tumors displayed a reduction in the mitotic index, RET phosphorylation, and signaling.

Conclusions: Ponatinib is a potent inhibitor of RET kinase and has promising preclinical activity in models of RET-driven medullary thyroid carcinoma. **(*J Clin Endocrinol Metab* 98: E811–E819, 2013)**

Oncogenic conversion of the RET (REarranged during Transfection) transmembrane receptor tyrosine kinase (RTK) is associated with several human malignancies (1). Virtually all (98%) cases of multiple endocrine neoplasia (MEN) type 2 (MEN2), featuring medullary thyroid carcinoma (MTC), are caused by germline activating *RET* point mutations and approximately 50% of patients with sporadic MTC bear somatic *RET* mutations, most commonly M918T (1–3). A fraction (5%–40%) of cases of the most common type of thyroid cancer, papillary thyroid

ISSN Print 0021-972X ISSN Online 1945-7197
Printed in U.S.A.

Received July 3, 2012. Accepted March 18, 2013.
First Published Online March 22, 2013

Abbreviations: CI, confidence interval; MEN, multiple endocrine neoplasia; MTC, medullary thyroid carcinoma; PTC, papillary thyroid carcinoma; RTK, receptor tyrosine kinase; TK, tyrosine kinase; TKI, tyrosine kinase inhibitor.

carcinoma (PTC), result from chromosomal inversions or translocations that generate hybrid transforming genes, termed *RET/PTC*. *RET/PTC* genes are composed of the TK-encoding domain of *RET* fused to the promoter and 5′-terminal region of unrelated genes, most commonly *CCDC6* (*RET/PTC1*) and *NCOA4* (*RET/PTC3*) (4). *RET* gene rearrangements have been recently demonstrated to play an important role in a subset of cases of non–small cell lung cancer (5–7) and chronic myelomonocytic leukemia (8), up-regulated *RET* expression is associated with several malignancies, including neuroblastoma (9), pancreatic cancer (10), and breast cancer (11).

Small molecule tyrosine kinase inhibitors (TKIs) of various chemical classes inhibiting RET tyrosine kinase (TK) are in clinical development (12, 13). The clinically most advanced RET TKIs are vandetanib (ZD6474) and cabozantinib (XL184), both recently registered for the treatment of locally advanced or metastatic MTC (14–17). Ponatinib (AP24534) is an oral multitargeted TKI that potently inhibits BCR-ABL and additional protein tyrosine kinases, including SRC-related kinases, and members of the III/IV/V RTK classes, such as FLT3 (fms-related tyrosine kinase 3), KIT, FGFR1 (fibroblast growth factor receptor 1), PDGFRα (platelet-derived growth factor receptor α), and VEGFR-2/KDR (vascular endothelial growth factor [VEGF] receptor-2/kinase insert domain receptor) (18–20). Unlike vandetanib, ponatinib is a class 2 inhibitor, eg, a TKI that preferentially binds the inactive conformation of the kinase (21). Ponatinib inhibits both native and mutant forms of BCR-ABL, including the T315I gatekeeper mutant, which is refractory to imatinib and was highly active in patients with Ph-positive leukemias with resistance to TKIs (Ref. 22 and NCT01207440, www.clinicaltrials.gov).

Here, we provide evidence that ponatinib is a novel potent RET TKI that might be suited for treatment of RET-driven malignancies, such as MTC.

Materials and Methods

Compounds

Ponatinib (AP24534) was provided by ARIAD Pharmaceuticals, Inc (Cambridge, Massachusetts) and dissolved as described in Supplemental Methods published on The Endocrine Society's Journals Online web site at http://jcem.endojournals.org.

Cell cultures

Human embryonic kidney 293 cells were used for transient transfections as described in Supplemental Methods. NIH3T3 and RAT1 fibroblasts stably expressing the oncogenic RET mutants were described previously (14, 23, 24). The TT cell line was derived from a sporadic MTC (25) and harbors a cysteine 634 to tryptophan (C634W) *RET* mutation (26) as well as a tandem duplication of the mutated *RET* allele (27). MZ-CRC-1 cells were derived from a malignant pleural effusion from a patient with metastatic MTC (28) and bear the *RET* substitution of threonine 918 for methionine (M918T) (15). Human TPC-1 cells harbor the *RET/PTC1* rearrangement (14); TPC-1 and BCPAP PTC cells were authenticated by DNA short tandem repeat analysis (29). Nthy-ori 3-1 is a human thyroid follicular epithelial cell line immortalized by the simian virus 40 large T gene. Cell lines were cultured, and cell proliferation assays were performed as described in Supplemental Methods.

Plasmids

Plasmids were described previously (23, 24, 30) as reported in Supplemental Methods.

Protein Studies

Protein studies were performed as described in Supplemental Methods.

In vitro kinase assay

The in vitro RET autophosphorylation assay was performed as described elsewhere (31) and reported in Supplemental Methods.

Tumorigenicity assay

Animal studies were performed according to institution-approved protocols in compliance with the Italian Ministry of Health Guide for the Care and Use of Laboratory Animals. TT cells (5×10^7) were injected sc into the right dorsal portion of female BALB/c nude (*nu/nu*) mice. When tumor volume reached 100 to 150 mm^3 (experiment 1) or 700 to 750 mm^3 (experiment 2) (after approximately 30 or 40 days from injection, respectively), animals were randomly assigned to receive by oral gavage vehicle (9 and 6 mice in experiment 1 and 2, respectively) or ponatinib (30 mg/kg/d) (10 and 6 mice in experiment 1 and 2, respectively) for 21 or 7 days in experiment 1 and 2, respectively. Tumor size was assessed by calipers at regular intervals, and tumor volume was calculated according to the formula $(L \times W^2)/2$, where L is length and W is width of tumor. Tumors from experiment 2 were excised and divided in 2 parts. Half the tissue was snap-frozen in liquid nitrogen and used for protein extraction. The other half was fixed overnight in neutral buffered formalin and processed for histological examination. In another experiment (experiment 3), a lower dose of ponatinib (20 mg/kg/d, 5 doses in 7 days) was administered (for 3 consecutive days, interrupted for 2 days and administered again for 2 consecutive days) to tumor (~400 mm^3)–bearing mice (n = 8); vehicle was used in control mice (n = 7). Finally, for target inhibition experiments (experiment 4), another group of nude mice (n = 6) were injected with 5×10^7 TT cells. After approximately 40 days, when tumors measured ~500 mm^3, animals were randomly assigned to receive per os a single dose of ponatinib (30 mg/kg) (n = 4) or vehicle (n = 2). Then 5 hours after dosing, tumors were excised, and RET protein phosphorylation was determined by immunoblot.

Histological examination and immunohistochemistry

Tumor samples from experiment 2 were fixed in 10% neutral-buffered formalin, embedded in paraffin, and processed for

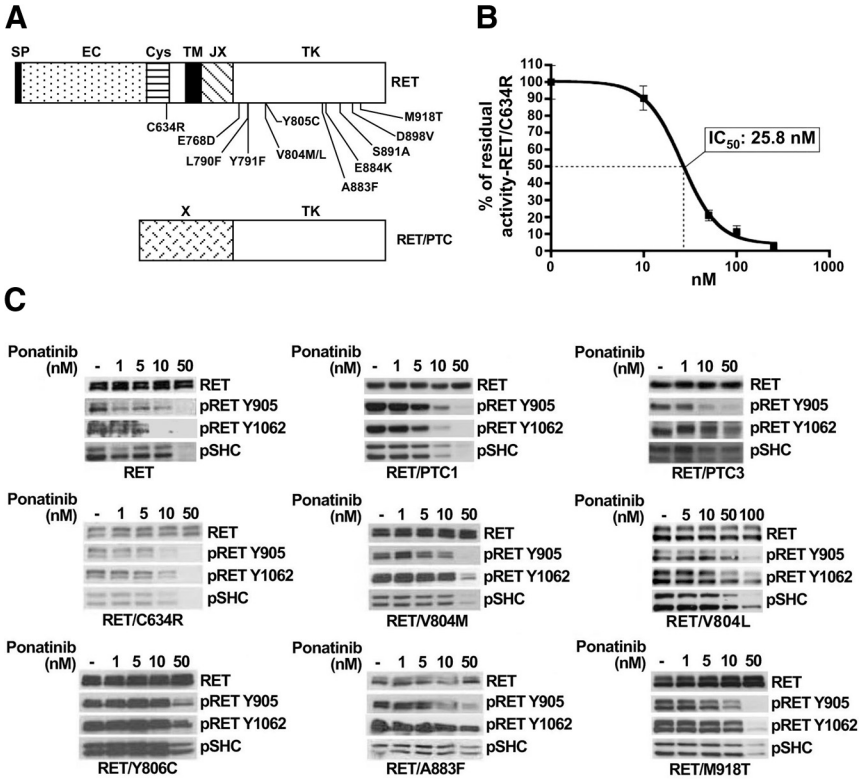

Figure 1. In vitro inhibition of RET kinase by ponatinib. A, Schematic representation of RET protein structure, RET mutants, and rearrangements used in this study. SP, signal peptide; EC, extracellular domain; Cys, cysteine-rich domain; TM, transmembrane domain; JX, juxtamembrane domain TK, tyrosine kinase domain; X, RET fusion partners. B, In vitro RET autophosphorylation assay. Protein extracts from RAT1-RET/C634R cells were immunoprecipitated with anti-RET and subjected to an immunocomplex kinase assay in the presence of [γ-^{32}P]ATP. Ponatinib or vehicle (dimethyl sulfoxide) was added to the reaction mixture to reach the indicated concentrations. Reaction products were separated by SDS-PAGE and autoradiographed. Phosphorimaging was used to quantify the results. Each point represents the mean value for 4 independent determinations and is plotted as a percentage of residual activity; error bars represent 95% CIs. The IC_{50} value is indicated. C, Inhibition of RET and oncogenic RET mutant phosphorylation and signaling by ponatinib. Serum-starved (18-hours) cells, transfected with the indicated RET constructs, were treated with different concentrations of drug for 1 hour; 50 μg of total cell lysates were immunoblotted with antibodies specific for phospho-RET/Y905, phospho-RET/Y1062, or phospho-SHC. Equal gel loading was determined by using an anti-RET antibody. Data are representative of 3 independent experiments.

hematoxylin and eosin staining and immunohistochemical analysis as described in Supplemental Methods.

Statistical analysis

Statistical analysis was performed as described in Supplemental Methods.

Results

Ponatinib inhibits RET kinase and RET phosphorylation in intact cells

We studied whether ponatinib (AP24534) was able to inhibit in vitro RET enzymatic activity. To this aim, RET/C634R (Figure 1A), the oncogenic RET mutant most frequently found in MEN2A, was used (1). RET/C634R protein was immunoprecipitated and incubated in kinase buffer containing [γ-^{32}P]ATP in the presence of different concentrations of the drug. Samples were separated by SDS-PAGE; gels were dried and exposed to phosphorimaging to measure the extent of RET protein autophosphorylation. The average results of 3 independent assays showed that ponatinib was a potent RET TKI, inhibiting RET kinase with an IC_{50} of 25.8 nM (95% confidence interval [CI] = 23.15–28.77) (Figure 1B).

We tested whether ponatinib activity against RET enzyme in vitro translated into a reduction of phosphorylation and signaling of oncogenic RET proteins in intact cells. *RET* point mutants depicted in Figure 1A and Supplemental Figure 1 were selected from *RET* mutation databases (www.arup.utah.edu/database/MEN2/MEN2_welcome.php and www.sanger.ac.uk/genetics/CGP/cosmic/). All these mutants have been associated to familial or sporadic MTC (2, 3). C634R has been described above; M918T is the *RET* mutant most frequently found in MEN2B and sporadic MTC. A883F is associated with cases of MEN2B that are negative for M918T. V804 and Y806 mutants were reported previously to be refractory to vandetanib and other TKIs (24, 30). We also tested ponatinib activity against most common *RET*-derived fusion oncogenes associated with PTC (Figure 1A). Human embryonic kidney 293 cells were transiently transfected with the various *RET* constructs, and, after 48 h, treated for 60 minutes with ponatinib at the indicated doses and harvested. Immunoblotting with phospho-specific antibodies was applied to detect RET protein phosphorylation at 2 sites: Y905, located in the kinase activation loop, and Y1062, a multidocking site involved in RET downstream signaling. Phosphorylation of SHC, a RET TK substrate, was studied as well (32, 33). Ponatinib efficiently inhibited phosphorylation of the RET mutants tested and SHC with an IC_{50} of 5 to 100 nM (Figure 1C and Supplemental Figure 1). RET/L790F and RET/Y791F (Supplemental Figure 1) were slightly more sensitive to ponatinib than the other mutants, whereas

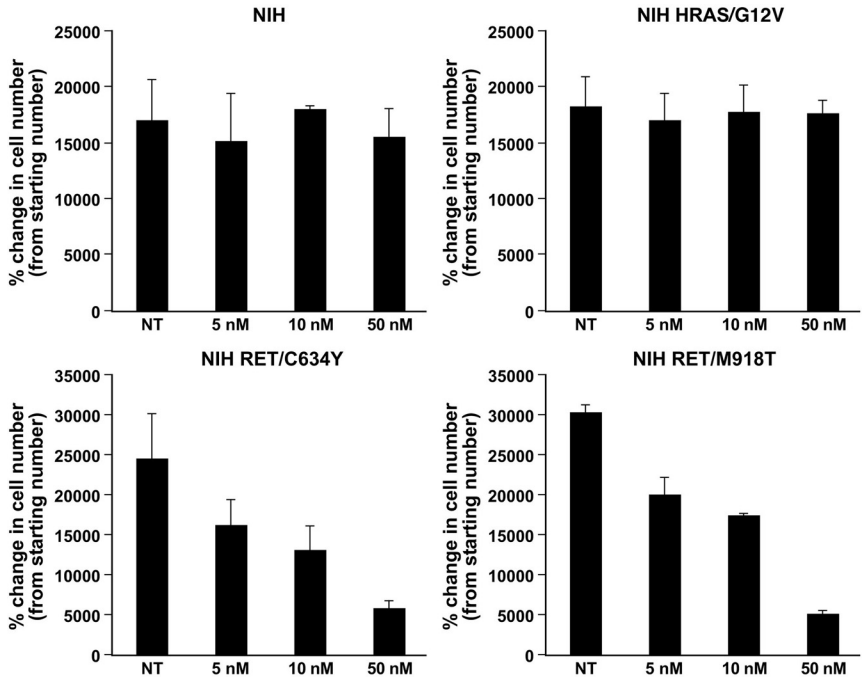

Figure 2. Inhibition of RET-mediated proliferation by ponatinib. NIH3T3-derived cell lines were incubated with vehicle or the indicated ponatinib doses in 5% and 2.5% calf serum (parental and transfected cells, respectively) and counted at 6 days. Cell proliferation was calculated as percent change with respect to the initial cell number: each point represents the mean value for 3 dishes, and error bars represent 95% CIs. Statistical significance was determined by 1-way ANOVA with the Bonferroni multiple comparison test.

RET/V804M, RET/V804L, RET/Y806C, RET/A883F (Figure 1C), and RET/E768D and RET/D898V (Supplemental Figure S1) were less sensitive but were still inhibited at 50 to 100 nM. Accordingly, an immunocomplex kinase assay showed that IC_{50} of ponatinib for RET/V804M in vitro kinase activity was 33.9 nM (95% CI = 26.41–43.58) (Supplemental Figure 2). Wild-type RET protein undergoes autophosphorylation when overexpressed, and such phosphorylation was inhibited by ponatinib (Figure 1C).

Ponatinib efficiently inhibits RET-mediated cancer cell proliferation

We asked whether ponatinib affected RET-driven cell proliferation. To this aim, proliferation assays were performed by using different doses of compound on NIH3T3 cells transformed by *RET*/C634Y or *RET*/M918T mutants. As controls, cells transformed by the unrelated *HRAS*/G12V oncogene or parental NIH3T3 cells were used. Oncogene (*RET* and *HRAS*) expression renders NIH3T3 cells serum-independent for growth. At 6 days, 5 nM ponatinib strongly reduced cell proliferation driven by *RET*/C634Y (from 24×10^3% [95% CI = 19×10^3%–29×10^3%] to 16×10^3% [95% CI = 13×10^3%–19×10^3%]) and RET/M918T (from 30×10^3% [95% CI = 29×10^3%–31×10^3%] to 19.5×10^3% [95% CI = 17.5×10^3%–21.5×10^3%]) ($P < .001$). Conversely, up to 50 nM ponatinib exerted no significant ($P > .05$) growth inhibition of parental and HRAS-transformed cells (Figure 2 and Supplemental Results).

We measured the antiproliferative effects of ponatinib in human thyroid cancer cells endogenously expressing oncogenic *RET* mutants. For this experiment, we selected TT (MTC cells harboring the *RET*/C634W mutation), MZ-CRC-1 (MTC cells harboring the *RET*/M918T mutation), and TPC-1 (PTC cells harboring the *RET/PTC1* rearrangement) cells. As controls, we used BCPAP cells (PTC cells harboring the *BRAF*/V600E mutation and no *RET* mutation) and Nthy-ori 3-1 cells (nontransformed thyrocytes immortalized by the simian virus 40 large T gene). Figure 3A shows that ponatinib had potent effects in RET-positive but not in RET-negative cells. At 4 days, 5 nM ponatinib reduced proliferation of TT cells (from 91% [95% CI = 68%–114%] to 9% [95% CI = −14%–32%]) ($P < .05$) and TPC-1 cells (from 2900% [95% CI = 2487%–3313%] to 1644% [95% CI = 1592%–1696%]) ($P < .001$) (Figure 3A). Moreover, 5 nM ponatinib (4 days) reduced the number of MZ-CRC-1 cells with respect to the vehicle control (from 33% [95% CI = 13%–53%) to −10% [95% CI = −2% to −18%]) ($P < .05$), therefore not only blocking cell growth but also exerting slight cytotoxicity (Figure 3A). Notably, at 4 days, up to 50 nM (BCPAP) or 10 nM (Nthy-ori 3-1) ponatinib did not exert significant ($P > .05$) growth inhibition in RET-negative cells. At 50 nM, ponatinib reduced Nthy-ori 3-1 proliferation by approximately 36% ($P < .01$) (Figure 3A).

MTC cells show a slow proliferation rate in culture. Thus, we performed additional growth curve experiments by extending exposure to the drug up to 2 weeks. In these conditions, a ponatinib dose as small as 1 nM exerted significant growth inhibition. Indeed, TT cells treated (15 days) with vehicle or with 1 nM ponatinib numbered 1635×10^3 (95% CI = 1472×10^3–1797×10^3) and 103.5×10^3 (95% CI = 84.8×10^3–122.2×10^3), respectively ($P < .001$), and MZ-CRC-1 cells treated (16 days) with vehicle or with 1 nM ponatinib numbered 1362×10^3 (95% CI = 1192×10^3–1531×10^3) and 160.8×10^3 (95% CI = 114.2×10^3–207.5×10^3), respectively ($P < .001$) (Figure 3B).

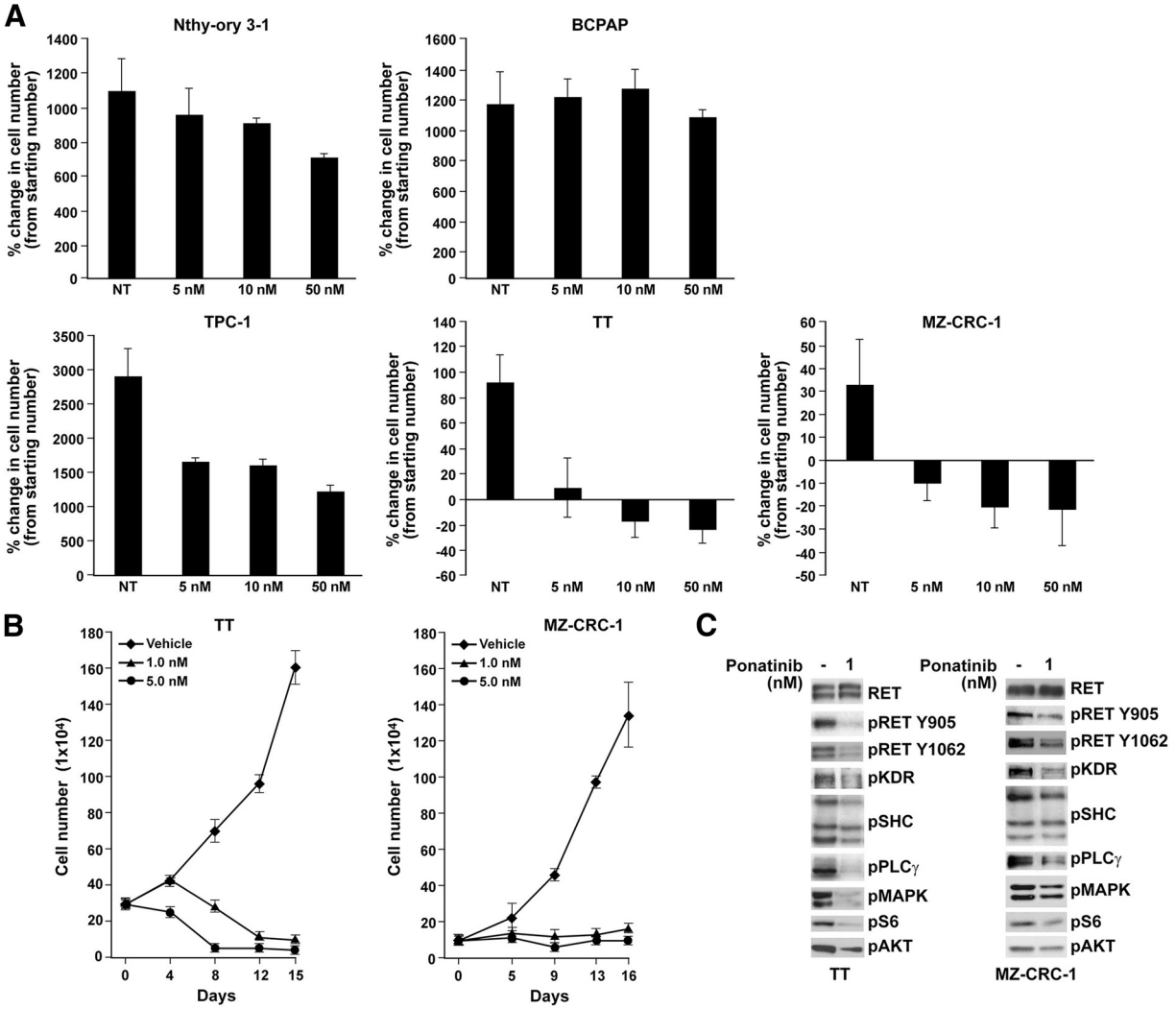

Figure 3. Inhibition of RET-mediated growth and signaling by ponatinib in human thyroid cancer cells. A, The indicated cell lines were incubated with vehicle or different doses of ponatinib in 2.5% (BCPAP, Nthy-ory 3-1, TPC-1, or MZ-CRC-1) or 4% (TT) serum and counted at 4 days. Cell proliferation was calculated as percent change with respect to initial cell number: each point represents the mean value for 3 dishes, and error bars represent 95% confidence intervals. B, MZ-CRC-1 (2.5% serum) or TT (4% serum) were incubated with the indicated doses of ponatinib or vehicle and counted at different time points. Each point represents the mean value for 3 dishes, and error bars represent 95% confidence intervals. C, TT and MZ-CRC-1 cells were treated with vehicle or ponatinib for 13 or 14 days, respectively. Cell lysates (50 μg) were immunoblotted with the antibodies indicated. Data are representative of 3 independent experiments.

Proteins were harvested, and RET phosphorylation was determined by immunoblot at 13 (TT) or 14 (MZ-CRC-1) days of ponatinib treatment. Consistent with growth inhibition, RET phosphorylation clearly decreased at ponatinib doses as small as 1 nM (Figure 3C). In parallel, ponatinib also decreased phosphorylation of several proteins that function in the RET signaling cascade, such as SHC, PLCγ (phospholipase Cγ), MAPK (mitogen-activated protein kinase; extracellular signal-regulated kinase [ERK]), AKT, and ribosomal S6 protein (Figure 3C). The ponatinib dose (1 nM) is smaller that that able to achieve an efficient reduction of RET phosphorylation after 1 hour of treatment (Figure 1C) and to inhibit RET kinase in vitro (Figure 1B). This result might be explained by the fact that ponatinib is a type 2 kinase inhibitor that preferentially binds to the inactive conformation of the kinase, a conformation that, in intact cells, might be fostered by chronic exposure to the drug (21).

Ponatinib is a multitargeted agent and its growth inhibitory effects can be mediated by the concurrent inhibition of additional tyrosine kinases other than RET. Among the additional ponatinib targets (18), TT cells did not show detectable phosphorylation of ABL (Y245) (Supplemental Figure 3B), Lyn (Y397), Lck (Y394), Fyn (Y420), and Yes (Y426) kinases (data not shown). Instead, pp60SRC (Y416) showed detectable phosphorylation in TT cells; however, at 1 hour of treatment, phospho-Y416-SRC was not inhibited by 10 nM ponatinib (Supplemental Figure 3B) but only by 50 nM ponatinib (data not shown). To explore additional ponatinib targets, we tested levels of

phosphorylation of 42 different RTKs in TT and MZ-CRC-1 cells. Besides RET, both cell lines expressed detectable phosphorylation of additional RTKs such as EGFR (epidermal growth factor receptor), VEGFR-2/KDR (VEGF receptor 2), InsR (insulin receptor), IGF1R (insulin-like growth factor 1 receptor) and DTK (TYRO3) (Supplemental Figure 3A). Among them, VEGFR-2/KDR is a known ponatinib target (18). Accordingly, we observed by immunoblot that ponatinib (10 nM) decreased VEGFR-2/KDR (but not EGFR) phosphorylation (Supplemental Figure 3B). At 2 weeks of treatment, ponatinib inhibited VEGFR-2/KDR phosphorylation in TT and MZ-CRC-1 cells even at a dose as small as 1 nM (Figure 3C). Thus, it is possible that ponatinib growth inhibitory effects in MTC cells are due to combined inhibition of RET and VEGFR-2/KDR.

Ponatinib inhibits RET-mediated tumor growth in mouse xenografts

We sought to determine whether ponatinib had inhibitory effects in vivo against RET-dependent tumor growth. In previous studies using BCR-ABL^{T315I} transduced Ba/F3 cells, daily oral ponatinib dosing of 10 and 30 mg/kg caused suppression of tumor growth and 50 mg/kg caused tumor regression (18). At a dose of 30 mg/kg, plasma ponatinib levels in mice were reported to reach 782 nM at 2 hours and then decline to 561 nM at 6 hours and 8 nM at 24 hours postdose (18). Therefore, plasma levels exceeding the in vitro IC_{50} values for RET can be sustained in mice for at least >6 hours with a 30 mg/kg oral dose. Thus, we selected a 30 mg/kg dose to obtain proof of the concept that ponatinib can obstruct in vivo RET-mediated tumor growth. We injected nude mice with 5×10^7 TT cells. After approximately 30 days, when tumors measured ~100 to 150 mm^3, animals were randomly assigned to receive by oral gavage ponatinib (30 mg/kg/d) (n = 10) or vehicle (n = 9) 5 days/wk for 3 weeks. Tumor diameter was monitored with calipers. Treatment with ponatinib strongly reduced tumor growth ($P < .001$) (Figure 4A). After 3 weeks of ponatinib treatment, the volume of TT cell xenografts was reduced from 133 mm^3 (95% CI = 93–173 mm^3) to unmeasurable size, whereas in vehicle-treated mice, mean tumor volume increased from 136 mm^3 (95% CI = 90–181 mm^3) to 541 mm^3 (95% CI = 377–704 mm^3). Effects were very rapid and reduced tumor burden was statistically significant ($P < .05$) as early as at day 8 of treatment. According to previous reports (18), we noted no signs of overt toxicity in mice with a maximal decrease in body weight <10% (untreated vs treated, $P > .05$) (Supplemental Figure 4A), no change in animal behavior, and, only occasionally, a modest skin rash on the back and scalp.

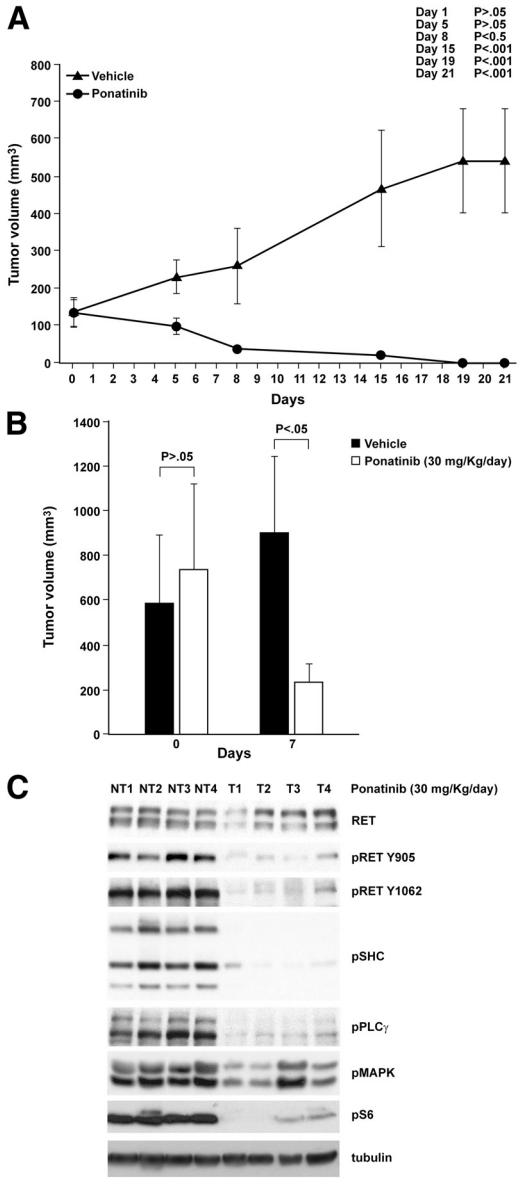

Figure 4. Antitumorigenic effects of ponatinib in TT cell xenografts. A, TT cells (5×10^7/mouse) were inoculated sc into the right dorsal portion of BALB/c nude mice. When tumors measured ~100 to 150 mm^3, animals were randomly assigned to receive ponatinib (30 mg/kg/day; n = 10) or vehicle (n = 9) by oral gavage. Treatment was administered for 5 consecutive days/wk for 3 weeks (day 0 is the treatment starting day). Tumor diameters were measured with calipers, and tumor volumes were calculated. Error bars represent 95% CIs. *P* values for the comparisons (at the different time points) between compound and vehicle are reported. Statistical significance was determined by 1-way ANOVA with the Tukey-Kramer multiple comparison test. B, TT cells (5×10^7/mouse) were inoculated as described in A. When tumors measured ~650 to 700 mm^3, animals were randomly assigned to receive ponatinib (30 mg/kg/day; n = 6) or vehicle (n = 6) by oral gavage. Treatment was administered for 3 consecutive days, interrupted for 2 days, and administered again for another 2 consecutive days (day 0 is the treatment starting day). Tumor diameters were measured with calipers, and tumor volumes were calculated. Error bars represent 95% CIs. *P* values for the comparisons (at the different time points) between compound and vehicle are reported. Statistical significance was determined by 1-way ANOVA with the Tukey-Kramer multiple comparison test. C, Protein lysates (50 μg) of the 7-day vehicle-treated (NT) or ponatinib-treated (T) xenografts were subjected to immunoblotting with the indicated antibodies.

To perform biochemical and histological studies, we treated a set of TT cell-induced large tumors (~650–700 mm^3) for a short time period (7 days). After 7 days of ponatinib (30 mg/kg/d) treatment, the average volume of xenografts (n = 6) was reduced from 736 mm^3 (95% CI = 335–1138 mm^3) to 237 mm^3 (95% CI = 155–320 mm^3), whereas in vehicle-treated mice (n = 6) mean tumor volume increased from 587 mm^3 (95% CI = 268–906 mm^3) to 901 mm^3 (95% CI = 545–1257 mm^3) ($P < .05$) (Figure 4B). In addition, no significant reduction in the weight of the mice (untreated vs treated, $P > .05$) was observed in these mice (Supplemental Figure 4B). At 7 days, tumors were excised, and proteins were harvested from ponatinib-treated and vehicle-treated tumors. RET and RET-signaling component (SHC, PLCγ, and ribosomal S6) phosphorylation was decreased upon ponatinib treatment; MAPK phosphorylation was decreased in all but 1 sample (Figure 4C). On histological examination, ponatinib-treated tumors featured a reduction in tumor cell density and diffuse fibrosis ($P < .001$) (Figure 5 and Supplemental Table 1). No significant change in the extent of necrosis (Supplemental Table 1) and in the density of microvessels (data not shown) was observed. Moreover, ponatinib treatment caused a reduction in the proliferative index, with a strong reduction in Ki-67 reactive cells (Figure 5 and Supplemental Table 1) and mitotic index (Supplemental Table 1). Treated tumors showed also a small, albeit significant ($P < .001$), increase in tumor cell death with an increased fraction of cells immunoreactive for cleaved caspase 3 (Supplemental Table 1).

Finally, for target inhibition experiments, we injected another group of nude mice (n = 6) with 5×10^7 TT cells. After approximately 40 days, when tumors measured ~500 mm^3, animals were randomly assigned to receive by oral gavage a single dose of ponatinib (30 mg/kg) (n = 4) or vehicle (n = 2). As early as 5 hours after dosing, RET protein phosphorylation was clearly decreased (Supplemental Figure 5).

Furthermore, a lower (66%) dose of ponatinib (20 mg/kg/d, 5 doses in 7 days) was also able to cause a significant reduction ($P < .05$) of TT cell-induced tumor volume (in treated mice [n = 8] average volume was reduced from 440 mm^3 [95% CI = 244–636 mm^3] to 88 mm^3 [95% CI = 51–127 mm^l, whereas in vehicle-treated mice [n = 7], mean tumor volume increased from 382 mm^3 [95% CI = 183–580 mm^3] to 635 mm^3 [95% CI = 305–964 mm^3]) ($P < .05$) (Supplemental Figure 6A). In parallel, RET protein phosphorylation was decreased (Supplemental Figure 6B).

Discussion

RET genetic alteration is involved in several human malignancies, including PTC (*RET/PTC* gene rearrangements) (4), MTC (*RET* point mutations) (1–3), lung adenocarcinoma (*KIF5B/RET* and *RET/PTC1*) (5–7), and chronic myelomonocytic leukemia (*BCR-RET* and *FGFR1OP-RET*) (8). Thus, RET kinase is an appealing molecular target for cancer therapy. Several RET TKIs

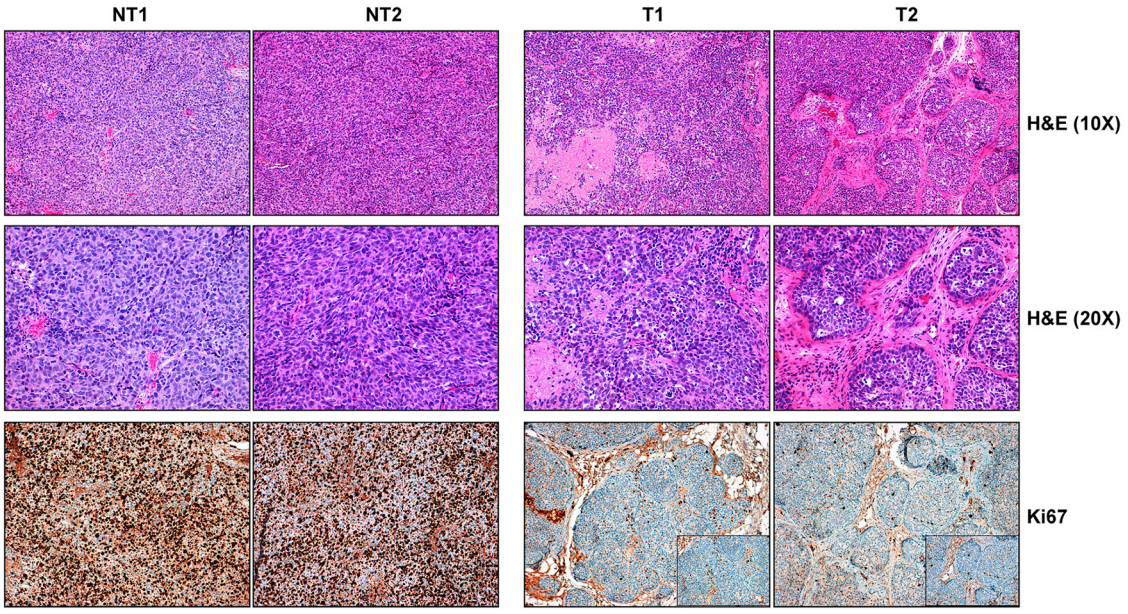

Figure 5. Histopathologic examination of ponatinib effects in TT cells xenografts. Top, Hematoxylin and eosin (H&E) staining was performed on vehicle- and ponatinib-treated xenografts of B. Representative images of 4 independent samples are shown. In ponatinib-treated samples (T), the presence of diffuse fibrosis as fibrous bands around nests of neoplastic cells was observed (×10 and ×20 magnification). Bottom, Ki-67 immunohistochemical staining of vehicle-treated xenografts (NT) compared with ponatinib-treated xenografts (T) (×10 magnification). Insets: ×20 magnification.

have been identified, and their efficacy has been studied in preclinical models and, in some cases, in clinical trials. The most advanced drugs, vandetanib (ZD6474) and cabozantinib (XL184), target RET as well as other receptors including VEGFR-2/KDR (in the case of both) and EGFR (in the case of vandetanib) (12, 13). A lesson learned from other neoplasia is that it is important to have available alternative and more potent TKIs if the first inhibitor fails or patients develop resistance. In some instances, resistance can be mediated by mutations in the target kinase that impair drug binding, as in the case of mutations targeting the "gatekeeper" residue, positioned at the gate of the ATP binding pocket (22).

Here, we show that ponatinib (AP24534) is a potent RET kinase inhibitor at clinically achievable drug levels. The IC_{50} of ponatinib for the isolated RET kinase was 25.8 nM and in intact MTC cells, when the treatment was prolonged for approximately 2 weeks, strong inhibition of RET phosphorylation and cell proliferation was detected at a ponatinib concentration of 1 nM. Plasma levels exceeding the in vitro IC_{50} values for RET were previously reported to be sustained in mice for at least >6 hours with 30 mg/kg oral dosing, declining to 8 nM at 24 hours postdose (18). Here we show that 30 mg/kg ($P < .001$) or 20 mg/kg ($P < .05$) ponatinib doses reduced growth of TT cell xenografts in nude mice as well as RET phosphorylation. In TT cell xenografts, RET target inhibition was observed as early as 5 hours after 30 mg/kg ponatinib dosing. A limitation of our study is that a dose-response experiment was not performed to determine the minimal ponatinib dose effective in the mouse TT cell xenograft. However, it is important to note that at doses of 30 mg, the trough blood ponatinib concentration surpassed 40 nM in human patients with leukemia (34).

Ponatinib is a multitargeted agent and its effects in MTC cells can result from the inhibition of other targets besides RET. At variance from other known ponatinib targets, VEGFR-2/KDR is expressed and phosphorylated in both MTC samples (35) and cell lines (15), and ponatinib efficiently blocked VEGFR-2/KDR phosphorylation in MTC cells. Thus, it is possible that VEGFR-2/KDR inhibition may cooperate with RET inhibition in mediating ponatinib effects in MTC cells.

RET mutants in the gatekeeper (V804) or the adjacent Y806 residue are resistant to both vandetanib and pyrazolopirimidines (PP1 and PP2) (24, 30). Ponatinib inhibited V804M/L and Y806C RET protein mutants, although at doses higher than those required to inhibit the other RET mutants. This result is consistent with the notion that ponatinib inhibits efficiently the T315I gatekeeper mutant of *BCR-ABL* (18), as well as multiresistant *FLT3-ITD* F691I mutant (36). Mutations targeting the *RET* residue Y806 are exceedingly rare; V804, instead, is quite commonly mutated in both familial (from 5% to 32%) and sporadic cases of MTC, particularly in some geographic regions (37).

MTC is commonly associated with RET oncogenic conversion and 2 multitarget agents with RET inhibitory activity, vandetanib and cabozantinib, have been recently approved for MTC treatment (16, 17). Given the potent anti-RET activity of ponatinib, our data suggest that it may be worth testing in patients affected by MTC and possibly other *RET*-driven neoplasms.

Acknowledgments

We thank R. F. Gagel (Department of Endocrine Neoplasia and Hormonal Disorders, The University of Texas MD Anderson Cancer Center, Houston, Texas) for MZ-CRC-1, N. Fabien (Department of Immunology, Centre Hospitalier Lyon-Sud, Hospices Civils de Lyon, Inserm U851, Pierre-Benite) for BCPAP, and M. Nagao (Carcinogenesis Division, National Cancer Center Research Institute, Tokyo, Japan) for TPC1 cells. We thank Salvatore Sequino (Dipartimento di Medicina Molecolare e Biotecnologie Mediche, Università di Napoli, Federico II, Naples, Italy) for animal care.

Address all correspondence and requests for reprints to: Massimo Santoro, MD, PhD, Dipartimento di Biologia e Patologia Cellulare e Molecolare, Università di Napoli Federico II, via S. Pansini 5, 80131 Naples, Italy. E-mail: masantor@unina.it.

This work was supported by the Associazione Italiana per la Ricerca sul Cancro (Grant IG11822) and the Italian Ministero dell'Università e della Ricerca (Grants MERIT-RBNE08YFN3 and 2009X23L78_002) from Italian Ministero dell'Università e della Ricerca.

Disclosure Summary: J.M.G. is a full-time employee of ARIAD Pharmaceuticals, Inc, and has equity interests in ARIAD Pharmaceuticals, Inc. The other authors have nothing to disclose.

References

1. **Wells SA Jr, Santoro M.** Targeting the RET pathway in thyroid cancer. *Clin Cancer Res*. 2009;15:7119–7123.
2. **Eng C.** Common alleles of predisposition in endocrine neoplasia. *Curr Opin Genet Dev*. 2010;20:251–256.
3. **de Groot JW, Links TP, Plukker JT, Lips CJ, Hofstra RM.** RET as a diagnostic and therapeutic target in sporadic and hereditary endocrine tumors. *Endocr Rev*. 2006;27:535–560.
4. **Nikiforov YE, Nikiforova MN.** Molecular genetics and diagnosis of thyroid cancer. *Nat Rev Endocrinol*. 2011;7:569–580.
5. **Lipson D, Capelletti M, Yelensky R, et al.** Identification of new ALK and RET gene fusions from colorectal and lung cancer biopsies. *Nat Med*. 2012;18:382–384.
6. **Takeuchi K, Soda M, Togashi Y, et al.** RET, ROS1 and ALK fusions in lung cancer. *Nat Med*. 2012;18:378–381.
7. **Kohno T, Ichikawa H, Totoki Y, et al.** KIF5B-RET fusions in lung adenocarcinoma. *Nat Med*. 2012;18:375–377.

8. **Ballerini P, Struski S, Cresson C, et al.** RET fusion genes are associated with chronic myelomonocytic leukemia and enhance monocytic differentiation. *Leukemia*. 2012;26:2384–2389.
9. **Beaudry P, Nilsson M, Rioth M, et al.** Potent antitumor effects of ZD6474 on neuroblastoma via dual targeting of tumor cells and tumor endothelium. *Mol Cancer Ther*. 2008;7:418–424.
10. **Gil Z, Cavel O, Kelly K, et al.** Paracrine regulation of pancreatic cancer cell invasion by peripheral nerves. *J Natl Cancer Inst*. 2010; 102:107–118.
11. **Morandi A, Plaza-Menacho I, Isacke CM.** RET in breast cancer: functional and therapeutic implications. *Trends Mol Med*. 2011; 17:149–157.
12. **Schlumberger M, Carlomagno F, Baudin E, Bidart JM, Santoro M.** New therapeutic approaches to treat medullary thyroid carcinoma. *Nat Clin Pract Endocrinol Metab*. 2008;4:22–32.
13. **Sherman SI.** Targeted therapies for thyroid tumors. *Mod Pathol*. 2011;24(Suppl 2):S44–S52.
14. **Carlomagno F, Vitagliano D, Guida T, et al.** ZD6474, an orally available inhibitor of KDR tyrosine kinase activity, efficiently blocks oncogenic RET kinases. *Cancer Res*. 2002;62:7284–7290.
15. **Vitagliano D, De Falco V, Tamburrino A, et al.** The tyrosine kinase inhibitor ZD6474 blocks proliferation of RET mutant medullary thyroid carcinoma cells. *Endocr Relat Cancer*. 2010;18:1–11.
16. **Wells SA Jr, Robinson BG, Gagel RF, et al.** Vandetanib in patients with locally advanced or metastatic medullary thyroid cancer: a randomized, double-blind phase III trial. *J Clin Oncol*. 2012;30: 134–141.
17. **Kurzrock R, Sherman SI, Ball DW, et al.** Activity of XL184 (Cabozantinib), an oral tyrosine kinase inhibitor, in patients with medullary thyroid cancer. *J Clin Oncol*. 2011;29:2660–2666.
18. **O'Hare T, Shakespeare WC, Zhu X, et al.** AP24534, a pan-BCR-ABL inhibitor for chronic myeloid leukemia, potently inhibits the T315I mutant and overcomes mutation-based resistance. *Cancer Cell*. 2009;16:401–412.
19. **Gozgit JM, Wong MJ, Wardwell S, et al.** Potent activity of ponatinib (AP24534) in models of FLT3-driven acute myeloid leukemia and other hematologic malignancies. *Mol Cancer Ther*. 2011;10:1028–1035.
20. **Gozgit JM, Wong MJ, Moran L, et al.** Ponatinib (AP24534), a multitargeted pan-FGFR inhibitor with activity in multiple FGFR-amplified or mutated cancer models. *Mol Cancer Ther*. 2012;11:690–699.
21. **Zhou T, Commodore L, Huang WS, et al.** Structural mechanism of the Pan-BCR-ABL inhibitor ponatinib (AP24534): lessons for overcoming kinase inhibitor resistance. *Chem Biol Drug Des*. 2011;77: 1–11.
22. **Cortes JE, Kantarjian H, Shah NP, et al.** Ponatinib in refractory Philadelphia chromosome-positive leukemias. *N Engl J Med*. 2012; 367:2075–2088.
23. **Pasini A, Geneste O, Legrand P, et al.** Oncogenic activation of RET by two distinct FMTC mutations affecting the tyrosine kinase domain. *Oncogene*. 1997;15:393–402.
24. **Carlomagno F, Guida T, Anaganti S, et al.** Disease associated mutations at valine 804 in the RET receptor tyrosine kinase confer resistance to selective kinase inhibitors. *Oncogene*. 2004;23:6056–6063.
25. **Berger CL, de Bustros A, Roos BA, et al.** Human medullary thyroid carcinoma in culture provides a model relating growth dynamics, endocrine cell differentiation, and tumor progression. *J Clin Endocrinol Metab*. 1984;59:338–343.
26. **Carlomagno F, Salvatore D, Santoro M, et al.** Point mutation of the RET proto-oncogene in the TT human medullary thyroid carcinoma cell line. *Biochem Biophys Res Commun*. 1995;207:1022–1028.
27. **Huang SC, Torres-Cruz J, Pack SD, et al.** Amplification and overexpression of mutant RET in multiple endocrine neoplasia type 2-associated medullary thyroid carcinoma. *J Clin Endocrinol Metab*. 2003;88:459–463.
28. **Cooley LD, Elder FF, Knuth A, Gagel RF.** Cytogenetic characterization of three human and three rat medullary thyroid carcinoma cell lines. *Cancer Genet Cytogenet*. 1995;80:138–149.
29. **Salerno P, De Falco V, Tamburrino A, et al.** Cytostatic activity of adenosine triphosphate-competitive kinase inhibitors in BRAF mutant thyroid carcinoma cells. *J Clin Endocrinol Metab*. 2010;95: 450–455.
30. **Carlomagno F, Guida T, Anaganti S, et al.** Identification of tyrosine 806 as a molecular determinant of RET kinase sensitivity to ZD6474. *Endocr Relat Cancer*. 2009;16:233–241.
31. **Carlomagno F, Anaganti S, Guida T, et al.** BAY 43–9006 inhibition of oncogenic RET mutants. *J Natl Cancer Inst*. 2006;98:326–334.
32. **Borrello MG, Pelicci G, Arighi E, et al.** The oncogenic versions of the Ret and Trk tyrosine kinases bind Shc and Grb2 adaptor proteins. *Oncogene*. 1994;9:1661–1668.
33. **Asai N, Murakami H, Iwashita T, Takahashi M.** A mutation at tyrosine 1062 in MEN2A-Ret and MEN2B-Ret impairs their transforming activity and association with shc adaptor proteins. *J Biol Chem*. 1996;271:17644–17649.
34. **Cortes J, Talpaz M, Bixby D, et al.** A phase 1 trial of oral ponatinib (AP24534) in patients with refractory chronic myelogenous leukemia (CML) and other hematologic malignancies: emerging safety and clinical response findings. *Blood* 2010;116:210.
35. **Rodríguez-Antona C, Pallares J, Montero-Conde C, et al.** Overexpression and activation of EGFR and VEGFR2 in medullary thyroid carcinomas is related to metastasis. *Endocr Relat Cancer*. 2010;17: 7–16.
36. **Zirm E, Spies-Weisshart B, Heidel F, et al.** Ponatinib may overcome resistance of FLT3-ITD harbouring additional point mutations, notably the previously refractory F691I mutation. *Br J Haematol*. 2012;157:483–492.
37. **Romei C, Mariotti S, Fugazzola L, et al.** Multiple endocrine neoplasia type 2 syndromes (MEN 2): results from the ItaMEN network analysis on the prevalence of different genotypes and phenotypes. *Eur J Endocrinol*. 2010;163:301–308.

Ponatinib (AP24534) is a novel potent inhibitor of oncogenic RET mutants associated to thyroid cancer

Valentina De Falco, et al.

Supplemental informations

Inventory:
-Supplemental Methods
-Supplemental Results
-Supplemental Figures and Legends
-Supplemental Table

Supplemental Methods

Compounds — For *in vitro* experiments, ponatinib was dissolved in dimethyl sulfoxide (DMSO) at a concentration of 10 mM and stored at –80°C. For *in vivo* experiments, it was dissolved in sodium citrate, pH 2.7, and stored at room temperature.

Cell Cultures — HEK293 cells were from American Type Culture Collection (ATCC, Rockville, MD) and were grown in Dulbecco's Modified Eagle Medium (DMEM) supplemented with 10% fetal calf serum (Invitrogen, Carlsbad, CA, USA). Transient transfections were carried out with the FuGENE HD reagent according to manufacturer's instructions (Roche, Mannheim, Germany). NIH3T3 and RAT1 fibroblasts were grown in DMEM supplemented with 5% calf serum. TT cell line was obtained in 2002 from ATCC and authenticated by *RET* genotyping. TT cells were grown in RPMI 1640 supplemented with 16% fetal calf serum (Invitrogen). MZ-CRC-1 cells were kindly provided in 2009 by Robert F. Gagel (MD Anderson, Houston, TX) and authenticated by *RET* genotyping. MZ-CRC-1 cells were grown in DMEM supplemented with 10% fetal calf serum (Invitrogen). Human papillary thyroid cancer BCPAP cells were obtained in 1994 from N. Fabien (CNRS, Oullins, France) and TPC-1 cells were obtained in 1990 from M. Nagao (National Cancer Center Research Institute, Tokyo, Japan). These cell lines were grown in DMEM with 10% fetal calf

serum (Invitrogen). Nthy-ori 3-1 cells were obtained from European Collection of Cell Cultures (ECACC) (Wiltshire, UK) in 2010 and were grown in RPMI supplemented with 10% fetal calf serum (Invitrogen). All media were supplemented with 2 mM L-glutamine and 100 units/ml penicillin-streptomycin (Invitrogen). All cells were passaged for fewer than 2 months after resuscitation.

For cell proliferation assays, $1x10^4$ (NIH3T3, NIH RET/C634Y, NIH RET/M918T), $5x10^3$ (NIH HRAS/G12V), $3x10^4$ (Nthy-ori 3-1, BCPAP), $7x10^4$ (TPC-1), $3x10^5$ (TT), or $1x10^5$ (MZ-CRC-1) cells were plated in 35-mm dishes. The day after plating, the cells were counted and the compound or vehicle were added. Cells were counted in triplicate at the indicated time points and the number of cells at the last day of the experiment was used to calculate growth inhibition.

Plasmids — Plasmids encoding wild type RET, oncogenic RET point mutants (C634R, E768D, L790F, Y791F, V804M, Y806C, A883F, E884K, S891A, D898V, M918T) and RET rearrangements (RET/PTC1, RET/PTC3) were cloned in the pBABE expression vector.

Protein Studies — Immunoblotting experiments were performed according to standard procedures. Briefly, cells were harvested in lysis buffer (50 mM Hepes, pH 7.5, 150 mM NaCl, 10% glycerol, 1% Triton X-100, 1 mM EGTA, 1.5 mM $MgCl_2$, 10 mM NaF, 10 mM sodium pyrophosphate, 1 mM Na_3VO_4, 10 µg of aprotinin/ml, 10 µg of leupeptin/ml) and clarified by centrifugation at 10,000 x *g*. Protein concentration was estimated with a modified Bradford assay (Bio-Rad Laboratories, Berkeley, CA, USA). Antigens were revealed by an enhanced chemiluminescence detection kit (ECL, Amersham Pharmacia Biotech). Signal intensity was quantified with the Phosphorimager (Typhoon 8600, Amersham Pharmacia Biotech) interfaced with the ImageQuant software. Anti-phospho-SHC, which recognizes SHC proteins when phosphorylated at Y317 (#07-206), was from Upstate Biotechnology Inc. (Lake Placid, NY, USA). Anti-phospho-PLCγ (Y783) (#2821), -VEGFR-2/KDR (Y1175) (#2478), -MAPK (ERK) (T302/Y304) (#9102), -AKT (S473) (#9271), -S6 (S240/S244) (#2215), -ABL (#2861), and -SRC (#2101) were from Cell Signaling Technologies (Danvers, MA, USA). Anti-phospho-EGFR (#44788G) was from Invitrogen (Carlsbad, CA, USA). Monoclonal anti-

α-tubulin was from Sigma Aldrich (St Louis, MO, USA). Anti-RET is a polyclonal antibody raised against the tyrosine kinase protein fragment of human RET. Anti-pY905 and anti-pY1062 are phospho-specific affinity-purified polyclonal antibodies that recognize RET proteins phosphorylated at Y905 and Y1062, respectively. Monoclonal anti-α-tubulin was from Sigma Aldrich (St Louis, MO, USA). Secondary antibodies coupled to horseradish peroxidase were from Amersham Pharmacia Biotech.

***In vitro* kinase assay —** Subconfluent cells were solubilized in lysis buffer without phosphatase inhibitors. Then, 50 μg of proteins were immunoprecipitated with anti-RET; immunocomplexes were recovered with protein A sepharose beads, washed 5 times with kinase buffer, and incubated 20 min at room temperature in kinase buffer containing 2.5 μCi [γ-^{32}P] ATP and unlabelled ATP to a final concentration of 20 μM. Samples were separated by SDS-PAGE. Gels were dried and exposed to autoradiography. Signal intensity was analyzed by the Phosphorimager (Typhoon 8600) interfaced with the ImageQuant software. Half maximal kinase inhibitory concentration (IC_{50}) value was calculated by using PRISM (GraphPad software).

Phospho-RTK Array — The relative levels of tyrosine phosphorylation of 42 receptor tyrosine kinases (RTKs) were evaluated with a Human Phospho-RTK array (R&D Systems, Inc. Minneapolis, MN, USA). Each array contained 42 different anti-RTK antibodies and six controls printed in duplicate. Briefly, cells were lysed in NP-40 lysis buffer (1% NP-40, 20 mM Tris-HCl pH 8.0, 137 mM NaCl, 10% Glycerol, 2 mM EDTA, 1 mM Sodium Orthovanadate, 10 μg/ml Aprotinin, 10 μg/ml Leupeptin) and centrifuged at 14,000 *g* for 30 minutes at 4°C. Non-specific binding was blocked for 1 hour at room temperature on a rocking platform. For each filter, 500 μg of protein lysate was used. The lysates were diluted in Array Buffer 1 (provided with the kit), added to each array, and incubated overnight at 4°C. Freshly diluted detection antibody was added to the arrays for 2 hours of room temperature. Phosphorylation levels were detected by chemiluminescence (ECL; Amersham Pharmacia Biotech).

Histological examination and immunohistochemistry — Tumor samples were fixed in 10% neutral-buffered formalin, embedded in paraffin, and 5 μm sections were stained with haematoxylin-eosin according to standard procedures. Extent of tumor necrosis or fibrosis was assessed as percentage of the total tumor area. Mitotic Index (MI) was assessed by counting mitotic figures in the cell dense areas at the periphery of the sample in 5 high-power (40 × objective, area of single field 0.166 mm^2) fields. Ki-67 expression was detected by incubating the slides with the rabbit monoclonal primary antibody (clone 30-9) (Ventana Medical System, ready to use for the Ventana automated slide stainer). Ki-67 staining was expressed as the percentage of cancer cells with positively-stained nuclei, counting at least 1,000 cells at 40 × magnification. Caspase 3 cleavage was assessed by immunostain with anti-cleaved caspase-3 (Asp175) antibody (Cell Signaling, #9664) and expressed as the number of cleaved caspase-3 immunoreactive cells out of ~2,000 neoplastic cells at in fields distant from necrotic areas (40 × magnification). Immunoreactions were displayed by the avidin–biotin–peroxidase complex (ABC) method by a Benchmark immunostainer (Ventana, Tucson, AZ). Counterstaining was performed with haematoxylin. Negative controls were carried out by omitting the primary antibodies. Immunohistochemical evaluation was determined by 2 pathologists (LT and FB) blinded to the treatment code. Microvascular count (MVC) was determined using anti-FVIII polyclonal antibody (Ventana Medical System, ready to use for the Ventana automated slide stainer). A single microvessel was defined as any brown immunostained endothelial cell separated from adjacent microvessel, tumor cells and other connective tissue elements. Areas with most intense vascularization (hot spot) under low microscopic power were scanned at 20 × magnification and the number of stained blood vessels was counted in 5 fields. Large vessels with thick, muscular walls were excluded from the counts. The sections were observed under a light microscope and photographed by digital camera (Olympus, Tokyo, Japan).

Statistical Analysis — Kinase activity curves were graphed using the curve-fitting PRISM (GraphPad software). To compare cell growth, we used the One-way ANOVA with standard parametric methods

and the Bonferroni Multiple Comparison Test (InStat program, GraphPad software). To compare tumor growth, we used the One-way ANOVA with standard parametric methods and the Tukey-Kramer Multiple Comparison Test (InStat program, GraphPad software). P values were statistically significant at $P < .05$.

Supplemental Results

Growth curves

NIH3T3-derived cell lines were incubated with vehicle or the indicated ponatinib doses in 5% and 2.5% calf serum (parental and transfected cells, respectively), and counted at 6 days. % change with respect to initial cell number is reported in Figure 2. In details: RET/C634Y cells treated (6 days) with vehicle numbered 2,155 x 10^3 (95% CI=1,771 x 10^3 to 2,539 x 10^3) and those treated with 5 nM ponatinib numbered 1,435 x 10^3 (95% CI=1,162 x 10^3 to 1,708 x 10^3) (P < .001); RET/M918T cells treated (6 days) with vehicle numbered 3,357 x 10^3 (95% CI=3,261 x 10^3 to 3,453 x 10^3) while those treated with 5 nM ponatinib numbered 2,170 x 10^3 (95% CI=1,944 x 10^3 to 2,396 x 10^3), respectively (P <.001); NIH cells treated (6 days) with vehicle numbered 2,201 x 10^3 (95% CI=1,649 x 10^3 to 2,753 x 10^3) while those treated with 5 nM ponatinib numbered 1,953 x 10^3 (95% CI=1,397 x 10^3 to 2,508 x 10^3) (P >.05); HRAS/G12V cells treated (6 days) with vehicle numbered 917.0 x 10^3 (95% CI=786.6 x 10^3 to 1,047 x 10^3) while those treated with 5 nM of ponatinib numbered 855.8 x 10^3 (95% CI=741.2 x 10^3 to 970.4 x 10^3) (P >.05).

Human thyroid cell lines were incubated with vehicle or different doses of ponatinib in 2.5% (BCPAP, Nthy-ory 3-1, TPC-1, MZ-CRC-1) or 4% (TT) serum and counted at 4 days. % change with respect to initial cell number is reported in Figure 3. In details: Nthy-ory 3-1 cells treated with vehicle numbered 389.9 x 10^3 (95% CI=254.8 x 10^3 to 525.0 x 10^3), those treated with 5 nM ponatinib numbered 345.6 x 10^3 (95% CI=237.1 x 10^3 to 454.0 x 10^3) (P >.05), and those treated with 50 nM ponatinib numbered 262.0 x 10^3 (95% CI=245.9 x 10^3 to 278.2 x 10^3) (P <.01); BCPAP cells treated with vehicle numbered 398.2 x 10^3 (95% CI=331.1 x 10^3 to 465.2 x 10^3), those treated with 5 nM ponatinib numbered 443.5 x 10^3 (95% CI=386.8 x 10^3 to 500.2 x 10^3) (P >.05) and those treated with 50 nM ponatinib numbered 370.5 x 10^3 (95% CI=354.6 x 10^3 to 386.4 x 10^3) (P >.05); TPC-1 cells treated with vehicle numbered 212.3 x 10^4 (95% CI=148.0 x 10^4 to 276.6 x 10^4) while those treated with 5 nM ponatinib numbered 121.1 x 10^4 (95% CI=110.5 x 10^4 to 131.6 x 10^4) (P <.001); TT cells treated with vehicle numbered 109.3 x 10^3 (95% CI=80.2 x 10^3 to 138.5 x 10^3) while those treated with 5 nM ponatinib numbered 62.5 x 10^3 (95% CI=33.1 x 10^3 to 91.9 x 10^3) (P <.05); MZ-CRC-1

cells treated with vehicle numbered 73.6 x 10^3 (95% CI=49.3 x 10^3 to 97.9 x 10^3) while those treated with 5 nM of ponatinib numbered 50.1 x 10^3 (95% CI=40.1 x 10^3 to 60.1 x 10^3) ($P < .05$)

Supplemental Figures and Legends

Fig. 1

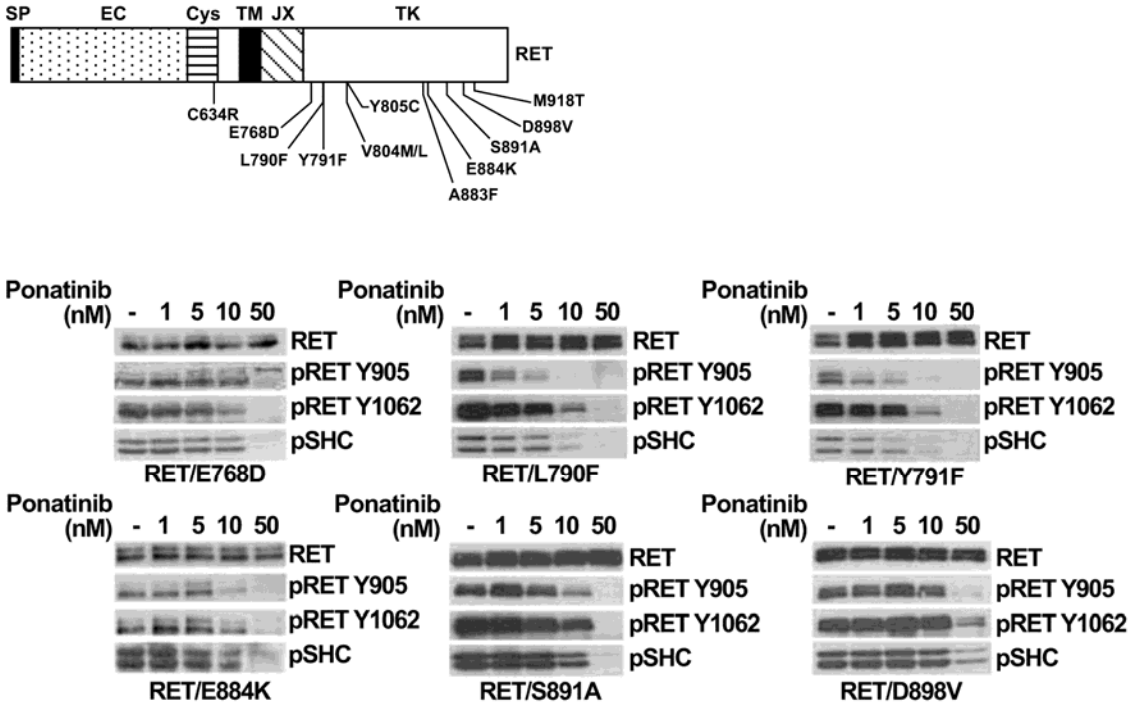

Fig. 1. *In vitro* inhibition of RET mutants by ponatinib. **Upper)** Schematic representation of RET mutants used in this study: SP: signal peptide; EC: extracellular domain; Cys: cysteine rich domain; TM: transmembrane domain; JX: juxtamembrane domain TK: tyrosine kinase domain; X: RET fusion partners. **Bottom)** Inhibition of oncogenic RET mutants phosphorylation and signaling by ponatinib. Serum-starved (18 hours) cells, transfected with the indicated RET constructs, were treated with different concentrations of drug for 1 hour; 50 μg of total cell lysates were subjected to immunoblotting with antibodies specific for phospho-RET/Y905 or -RET/Y1062. SHC protein phosphorylation was measured by a phospho-specific antibody. Equal gel loading was determined by anti-RET antibody. Data are representative of 3 independent experiments.

Fig. 2

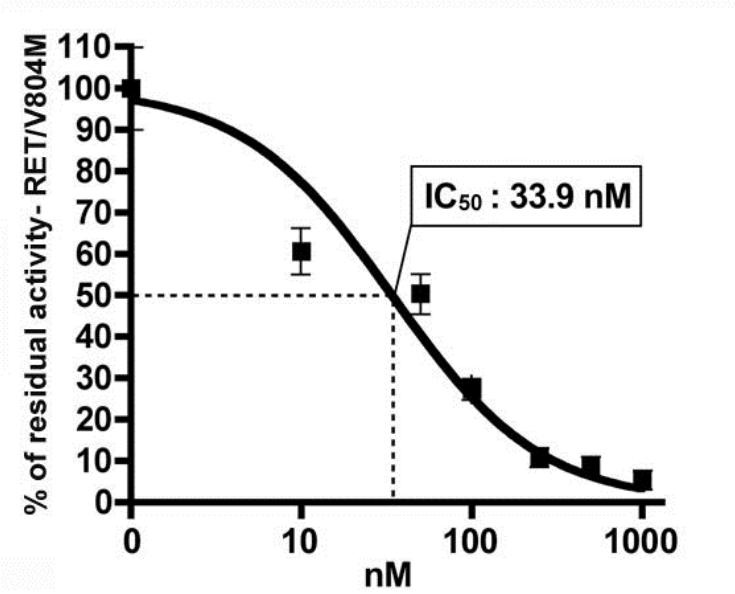

Fig. 2. *In vitro* RET auto-phosphorylation assay. Protein extracts from RAT1-RET/V804M cells were immunoprecipitated with anti-RET and subjected to an immunocomplex kinase assay in the presence of [γ-^{32}P] ATP. Ponatinib or vehicle alone (DMSO) were added to the reaction mixture to reach the indicated concentrations. Reaction products were separated by SDS-PAGE and autoradiographed. Phosphor-imaging was used to quantify the results. Each point represents the mean value for 4 independent determinations and is plotted as percentage of residual activity; error bars represent 95% confidence intervals. IC_{50} value (PRISM, GraphPad Software) was indicated.

Fig. 3

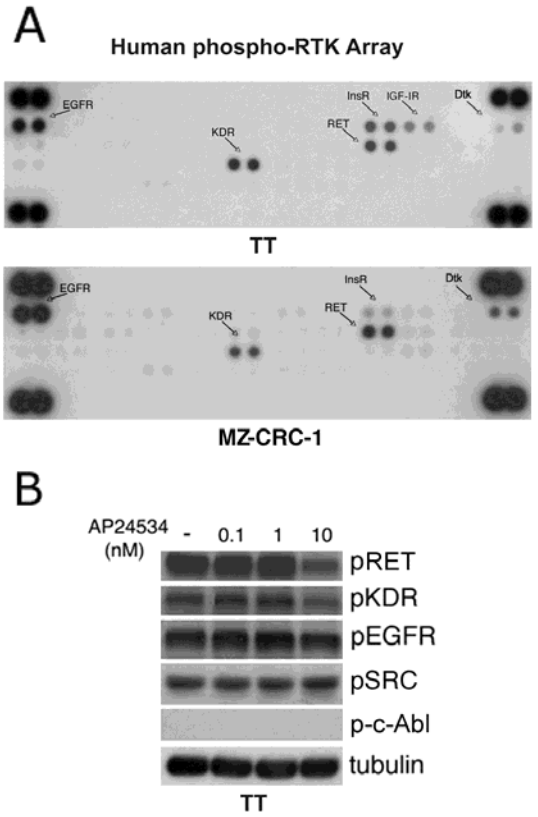

Fig. 3. RTK inhibition by ponatinib in TT and MZ-CRC-1 cells **A)** Protein lysates (500 μg) from TT or MZ-CRC-1 cells were added to each array, and incubated overnight at 4°C. Detection antibody was added to the arrays for 2 hours of room temperature and phosphorylation levels of 42 different RTK as duplicated spots were detected by chemiluminescence. **B)** TT cells were treated with different concentrations of ponatinib (AP24534) for 1 hour; 50 μg of total cell lysates were subjected to immunoblotting with antibody specific for phospho-RET/Y905, phospho-KDR/Y1175, phospho-EGFR/Y1068, phospho-SRC/Y416, or phospho-ABL/Y245. Equal gel loading was determined by anti-tubulin antibody. The signal was analyzed at the Phosphorimager. Data are representative of 3 independent experiments.

Fig. 4

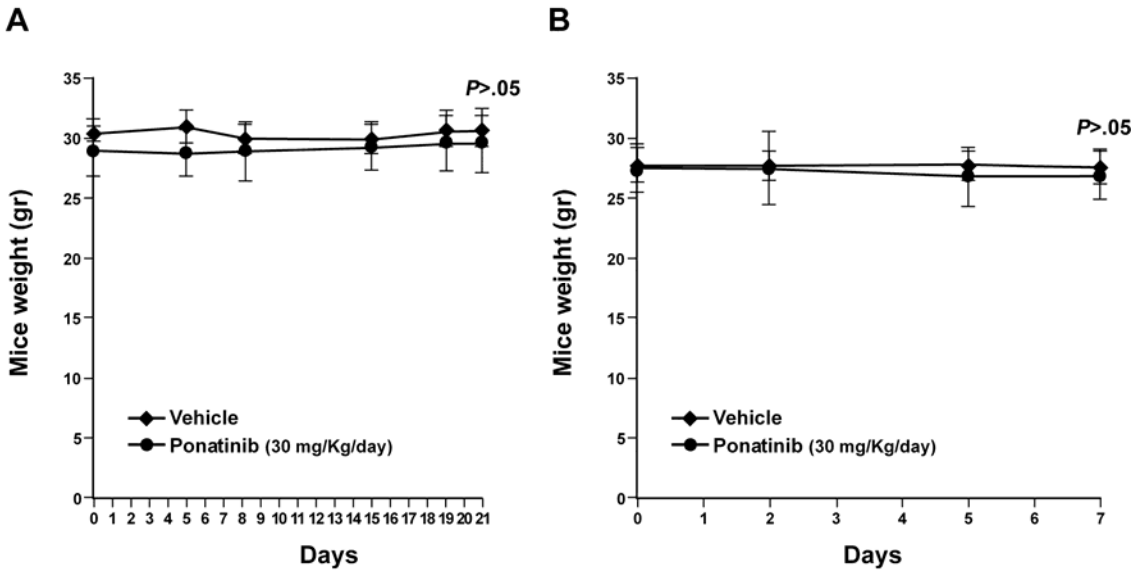

Fig. 4. Effects on mice weight by ponatinib in mice xenografted with TT cells. **A)** TT cells ($5x10^7$/mouse) were inoculated as described in Fig.4A. When tumors measured ~100-150 mm^3, animals were randomly assigned to receive ponatinib (30 mg/kg/day) (n. 10) or vehicle (n. 9) by oral gavage. Treatment was administered for 5 consecutive days/week for three weeks (day 0 is the treatment starting day). Mice weights were measured. Error bars represent 95% confidence intervals. *P* value for the comparisons at 21 days between compound and vehicle is indicated. Statistical significance was determined by the one-way ANOVA with the Tukey-Kramer Multiple Comparison Test. **B)** TT cells ($5x10^7$/mouse) were inoculated as described in Fig.4B. When tumors measured ~650-700 mm^3, animals were randomly assigned to receive ponatinib (30 mg/kg/day) (n. 6) or vehicle (n. 6) by oral gavage. Treatment was administered for 3 consecutive days, interrupted for 2 days and administered again for 2 consecutive days (day 0 is the treatment starting day). Mice weights were measured. Error bars represent 95% confidence intervals. *P* value for the comparisons at 7 days between compound and vehicle is indicated. Statistical significance was determined by the one-way ANOVA with the Tukey-Kramer Multiple Comparison Test.

Fig. 5

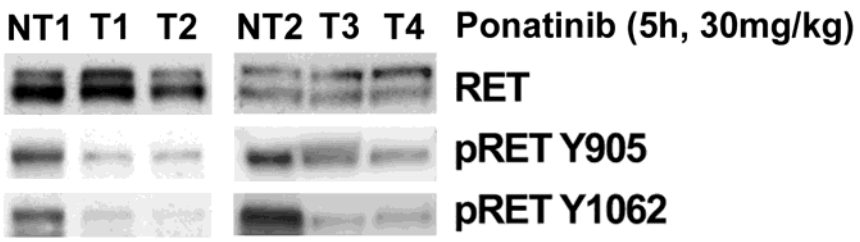

Fig. 5 *In vivo* inhibition of RET by ponatinib in mice xenografted with TT cells. TT cells ($5x10^7$/mouse) were inoculated subcutaneously into the right dorsal portion of BALB/c nude mice. When tumors measured ~500 mm^3, animals were randomly assigned to receive *per os* a single dose of ponatinib (30 mg/kg) (T1, T2, T3, T4) or vehicle (NT1, NT2) for 5 hours. 50 μg of total cell lysates were subjected to immunoblotting with antibody specific for phospho-RET/Y905 or -RET/Y1062. Equal gel loading was determined by anti-RET antibody. The signal was analyzed at the Phosphorimager.

Fig. 6

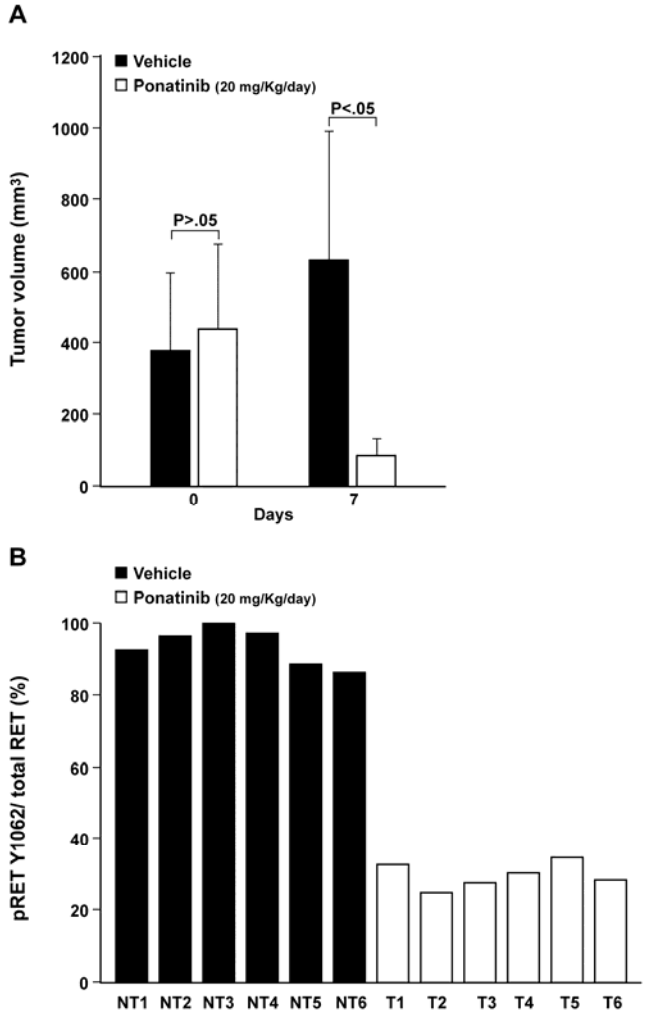

Fig. 6 Anti-tumorigenic effects of ponatinib (20 mg/kg/day) in TT cells xenografts. **A)** TT cells ($5x10^7$/mouse) were inoculated as described in Fig. 4. When tumors measured ~400 mm^3, animals were randomly assigned to receive ponatinib (20 mg/kg/day) (n. 8) or vehicle (n. 7) by oral gavage. Treatment was administered for 3 consecutive days, interrupted for 2 days and administered again for 2 consecutive days (day 0 is the treatment starting day). Tumor diameters were measured with calipers and tumor volumes were calculated. Error bars represent 95% confidence intervals. *P* values for the comparisons between compound and vehicle are reported. Statistical significance was determined by the one-way ANOVA with the Tukey-Kramer Multiple Comparison Test. B) Protein lysates (50 μg) were subjected to immunoblotting with antibody specific for RET or phospho-RET/Y1062. The signal was analyzed at the Phosphorimager and expressed as pRET/RET fraction.

Table 1. Histopathologic examination of ponatinib effects in TT cell xenografts

ID	Ki-67 (%)[1]	Mitotic index[2] (n° mitosis per 5 HPF) T vs NT P<.001	Apoptotic index[3] (n° of cleaved caspase-3 positive apoptotic cells) T vs NT P<.001	Necrosis (%)[4] T vs NT P>.05	Fibrosis (%)[5] T vs NT P<.001
1 NT	TMTM	26	15	10	0
2 NT	TMTM	25	16	5	0
3 NT	TMTM	28	16	5	0
4 NT	TMTM	24	17	5	0
5 NT	TMTM	22	17	5	0
6 NT	TMTM	23	22	2	0
7 NT	TMTM	28	18	5	0
8 NT	TMTM	25	16	10	0
1 T	5	1	56	20	5
2 T	5	1	37	5	30
3 T	5	0	50	10	20
4 T	5	0	34	5	30
5 T	2	1	38	5	30
6 T	5	1	34	10	30
7 T	5	0	27	5	5

[1]Ki-67 immunostaining was expressed as the percentage of cancer cells with positively-stained nuclei, counting at least 1,000 cells at 40 × magnification. TMTM: too many to count
[2] Mitotic Index (MI) was assessed by counting mitotic figures in the cell dense areas at the periphery of the sample in 5 high-power (40 × objective, area of single field 0.166 mm^2) fields.
[3] The apoptotic index was calculated as the number of cleaved caspase-3 immunoreactive cells counting ~2,000 neoplastic cells at 40 × magnification, in fields distant from necrotic areas.
[4, 5] Extent of tumor necrosis or fibrosis was assessed as percentage of the total tumor area.
[2-5]*P* values for the comparisons between compound (NT) and vehicle (T) are indicated. Statistical significance was determined by the Mann-Whitney Test.